JAERI-M
83-079

SYSTEM PRESSURE EFFECTS ON REFLOODING PHENOMENA OBSERVED IN THE SCTF CORE-I FORCED FLOODING TESTS

June 1983

Hiromichi ADACHI, Yukio SUDO, Makoto SOBAJIMA,
Takamichi IWAMURA, Masahiro OSAKABE, Akira OHNUKI
and Yutaka ABE

日本原子力研究所
Japan Atomic Energy Research Institute

JAERI-M レポートは，日本原子力研究所が不定期に公刊している研究報告書です。

入手の問合わせは，日本原子力研究所技術情報部情報資料課（〒319—11 茨城県那珂郡東海村）あて，お申しこしください。なお，このほかに財団法人原子力弘済会資料センター（〒319—11 茨城県那珂郡東海村日本原子力研究所内）で複写による実費頒布をおこなっております。

JAERI-M reports are issued irregularly.

Inquiries about availability of the reports should be addressed to Information Section, Division of Technical Information, Japan Atomic Energy Research Institute, Tokai-mura, Naka-gun, Ibaraki-ken 319—11, Japan.

編集兼発行　日本原子力研究所
印　　刷　日立高速印刷株式会社

JAERI-M 83-079

System Pressure Effects on Reflooding Phenomena Observed in the SCTF Core-I Forced Flooding Tests

Hiromichi ADACHI, Yukio SUDO, Makoto SOBAJIMA,
Takamichi IWAMURA, Masahiro OSAKABE, Akira OHNUKI
and Yutaka ABE
Department of Nuclear Safety Research,
Tokai Research Establishment, JAERI

(Received May 11, 1983)

The Slab Core Test Facility was constructed to investigate two-dimensional thermo-hydrodynamics in the core and the interaction in fluid behavior between the core and the upper plenum during the last part of blowdown, refill and reflood phases of a posturated loss-of-coolant accident (LOCA) of a pressurized water reactor (PWR).

The present report described the analytical results on the effects of system pressure on reflooding phenomena observed in Tests S1-SH2, S1-01 and S1-02 which are belonging to the SCTF Core-I forced-feed reflooding test series. Nominal system pressures in these tests are 0.4, 0.2 and 0.15 MPa, respectively. By comparison among the data of these three tests, the effects of system pressure on thermo-hydrodynamic behavior in the pressure vessel including the core and the primary coolant loops of the SCTF can be clarified under the forced flooding condition. Major items investigated in the present report are (1) overall temperature behaviors in the core, (2) change of heat transfer coefficient and heat flux at the rod surface before the quench, (3) two-dimensional thermo-hydrodynamic behaviors in the core and upper plenum and (4) hot leg carryover.

Keyword: Reactor Safety, LOCA, PWR, Blowdown, Refill, Reflood, Core Cooling, ECCS, System Pressure, Thermo-hydraulics

---

The work was performed under contract with the Atomic Energy Bureau of Science and Technology Agency of Japan.

平板炉心再冠水試験・第1次模擬炉心強制冠水試験で観察された系圧力の再冠水現象に及ぼす影響について

日本原子力研究所東海研究所安全工学部
安達　公道・数土　幸夫・傍島　　真・岩村　公道
刑部　真弘・大貫　　晃・阿部　　豊

（１９８３年５月11日受理）

平板炉心試験装置（ＳＣＴＦ）試験計画は、加圧水型原子炉（ＰＷＲ）の冷却材喪失事故（ＬＯＣＡ）時のブローダウン過程末期から，リフィル，再冠水過程における炉心を解明することを主目的としている。

本報告書では，平板炉心再冠水試験・第1次模擬炉心強制冠水試験シリーズのうち，試験Ｓ１－ＳＨ２，Ｓ１－０１およびＳ１－０２において観察された，系圧力の再冠水現象に及ぼす影響についての解析結果を報告する。これらの試験における公称系圧力は，それぞれ0.4，0.2および0.１５ＭＰａである。これらの３つの試験の結果を比較することによって，系圧力が炉心を含む圧力容器や，一次冷却系ループ内の熱水力現象に及ぼす影響を解明することができる。本報告書における主な検討項目は，(1)炉心の全体的な温度挙動，(2)クエンチに到る発熱棒表面の熱伝達率及び熱流束の変化，(3)炉心や上部プレナムの二次元的な熱水力挙動，(4)ホットレグキャリオーバの４つである。

本報告書は，電源開発促進対策特別会計法に基づき，科学技術庁からの受託によって行なった研究の成果である。

Contents

目　　次

List of Tables

List of Figures

List of Tables in Appendix A

List of Figures in Appendix A

List of Figures in Appendixes B through D

Test Identification Character TID = B : Test S1-SH2
= C : Test S1-01
= D : Test S1-02

1. Introduction

The Slab Core Test Facility (SCTF) Test Program[1][2][3] is a part of the Large Scale Reflood Test Program as well as the Cylindrical Core Test Facility (CCTF) Test Program. Principal purposes of both the test programs are to clarify the thermo-hydrodynamic behaviors in the primary coolant system of a pressurized water reactor (PWR) during the last part of blowdown, refill and reflood phases of a large break loss-of-coolant accident (LOCA) and to demonstrate and quantify the safety margin of the effect of emergency core cooling system (ECCS) against the accident. Various experimental and analytical efforts are being made for these purposes.

In the CCTF test program, primary concern is paid on system simulation. On the other hand, the SCTF test is a kind of separate effect test and the major objectives are to clarify the following items:

(1) Two-dimensional thermo-hydrodynamics in a wide core (chimney effect, sputtering effect, blockage effect, etc.),

(2) Flow interaction between core and upper plenum (fall back of water, water carryover from core, etc.), and

(3) Hot leg carryover characteristics (upper plenum entrainment/de-entrainment, counter-current flow in hot leg, etc.).

To meet these objectives, the SCTF is designed and fabricated so as to simulate the extracted slab cut from an 1,100 MWe class PWR pressure vessel with full height, full radius and one bundle width as illustrated in Fig. 1.1.

In the first half of the SCTF Core-I test series, effects of the various test parameters on reflood phenomena were studied by applying so-called the forced-feed reflooding method. That is, the downcomer was isolated from the lower plenum by inserting a blocking plate and emergency core cooling (ECC) water was directly injected into the lower plenum. By this method, correct and reliable test data can be accumulated because core inlet water flow rate can be given as a test parameter and be measured accurately at the ECC water injection piping.

In the present report, system pressure effects on reflood phenomena are discussed by using the test data from the three forced-feed reflooding tests, Tests S1-SH2, S1-01 and S1-02. In these tests, nominal system pressure was changed as a test parameter between 0.15 and 0.4 MPa. This pressure range is reasonably expected in the refill and reflood phases of LOCA. Major test conditions and chronology of events for each test are

given in Tables 1.1 and 1.2, respectively. Only difference in test condition among these three test is the system pressure and the other conditions are essentially the same.

Overall temperature behavior in the core, change of heat transfer coefficient and heat flux at the rod surface before the quench, some information on two-dimensional thermo-hydrodynamic behaviors in the core and upper plenum and hot leg carryover characteristics are discussed in this report from the view point of system pressure effect.

For better understanding of the test results, a short description about the test facility is given in Appendix A. Some selected test data are also given in Appendixes B through D. Data identification method for the data is given at the first part of Appendix B.

Table 1.1 Test conditions for SCTF Core-I Forced-Feed Reflooding Tests under Various System Pressures

Test No.	Date	Objective	Test conditions							
			Max. core temperature at BOCREC (K)	Initial pressure at containment tank-II (MPa)	ECC water injection rate (kg/s)		Max. core inlet water subcooling (K)	Extraction from upper plenum	Radial power profile	Power decay curve
					Acc max.	LPCI				
S1-SH2	May.14/81	High pressure	965	0.397	20	11.1	14.7	*	*	*
S1-01	May.22/81	Base case	970	0.195	22	11.4	15.5	*	*	*
S1-02	Jun.2/81	Low pressure	970	0.15	21.4	10.6	19.0	*	*	*
Nominal test conditions for base case			973	0.2	22.4	11.1	as low as possible	None	Westinghouse initial core	ANS+Actinides +D.N.

Note: * = the same as the base case

Table 1.2 Chronology of Events in SCTF Core-I Forced-Feed Reflooding Tests under Various System Pressures

Event No.	Events
1	Core power "ON"
2	Acc injection initiation
3	Core power decay initiation
4	BOCREC (Bottom-of-Core Recovery)
5	Switch Acc to LPCI
6	Maximum ECC injection rate
7	Maximum containment tank-II pressure
8	Maximum core temperature
9	Maximum core pressure
10	Maximum core inlet water subcooling
11	Whole core quenched

Test S1-SH2		
Event No.	Time after core power "ON"	Time after BOCREC
1	0 sec	-105sec
2	96	-9
3	101	-4
4	105	0
5	116	11
7(0.425MPa)	118	13
6(22kg/s)	119	14
9(0.475MPa)	120	15
8(1000K)	137	32
11	308	203
10(14.7K)	320	215

Test S1-01		
Event No.	Time after core power "ON"	Time after BOCREC
1	0 sec	-107 sec
2	97	-10
3	102	-5
4	107	0
5	117	10
6(23kg/s)	118	11
7(0.218MPa)	127	20
8(1012K)	140	33
9(0.233MPa)	155	48
10(15.5K)	160	53
11	399	292

Table 1.2 Chronology of Events in SCTF Core-I Forced-Feed Reflooding Tests under Various System Pressures

Test S1-02		
Event No.	Time after core power "ON"	Time after BOCREC
1	0 sec	-106 sec
2	95	-11
3	100	-6
4	106	0
5	115	9
6(21.7kg/s)	115	9
7(0.169MPa)	124	18
8(1016K)	153	47
9(0.214MPa)	173	67
10(19.0K)	173	67
11	452	346

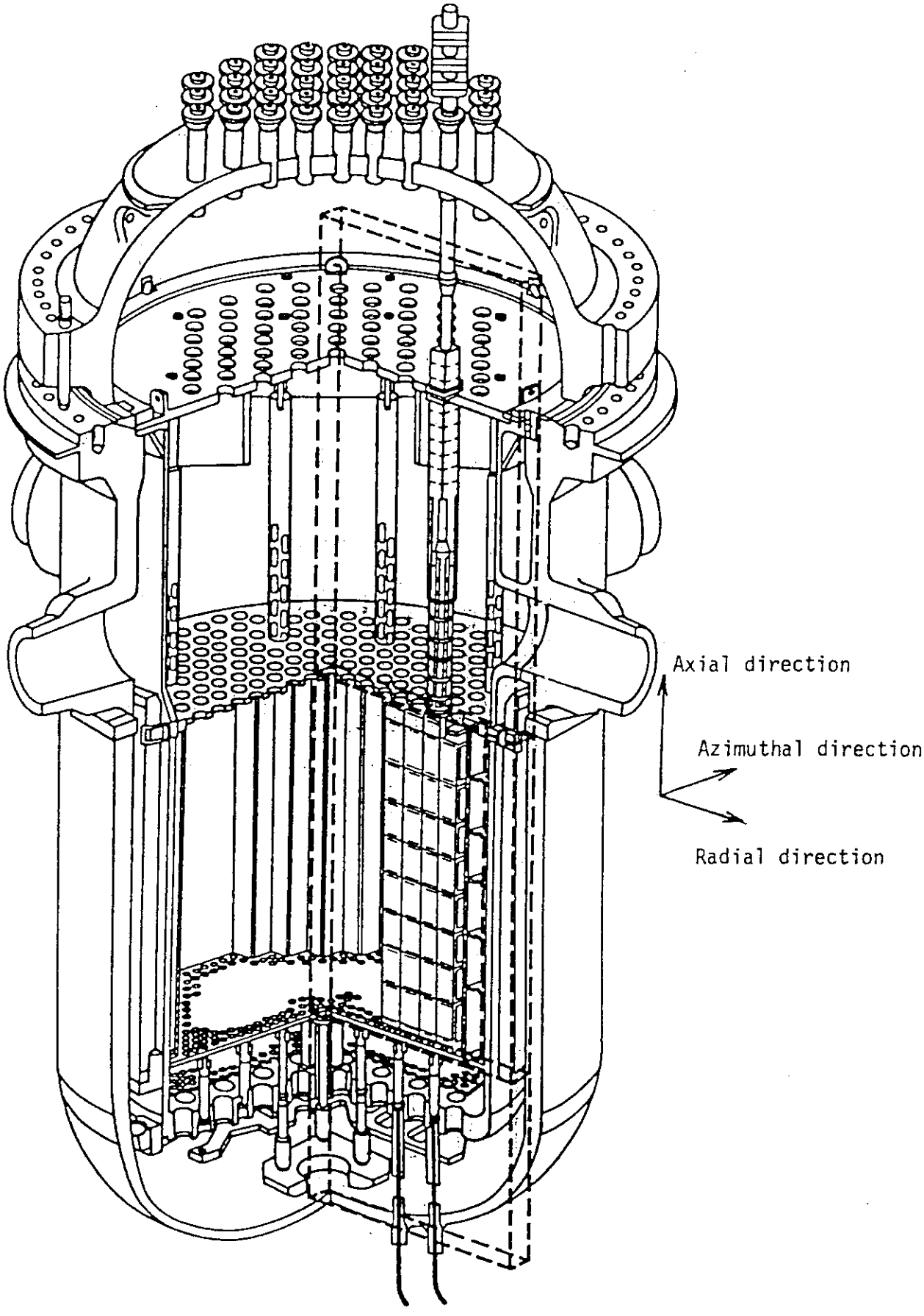

Fig. 1.1 Simulated Part of PWR Pressure Vessel with Slab Core Test Facility (SCTF)

2. Overall Core Thermal Behaviors

Figure 2.1 illustrates the typical cladding temperature history during the reflood phase. Technical terms on core thermal behaviors used in this report are defined in this figure. In this chapter, system pressure effects on temperature rise from the bottom-of-core recovery (BOCREC) time to the turnaround time, quench time and propagation velocity of the quench front are discussed.

(1) Temperature Rise

In Fig. 2.2 temperature rise of rod from the BOCREC time to the turnaround time for Tests S1-SH2 (high system pressure, 0.4 MPa) and S1-02 (low system pressure, 0.15 MPa) is compared with that for Test S1-01 (base case, 0.2 MPa). Here, thermocouple elevation number identifies the vertical location of thermocouples and each thermocouple elevation number represents all the thermocouples in the core attached at the same elevation. Since cooling behaviors in the top one quarter of the core are affected by the fall back water from the top of core and the upper plenum, each figure is separately given for the part below the 2330 mm above the bottom of heated length and that above the 2760 mm above the bottom of heated length.

This figure shows the slightly smaller temperature rise at the higher system pressure in the bottom three quarters of the core. This may be caused by the higher heat transfer coefficient for the given time after BOCREC.

(2) Quench Time

Figure 2.3 shows the similar comparison on quench time. The quench time is clearly shorter when the system pressure is higher. Of course the higher water accumulation rate in the core may be one of the reasons of the earlier quench at the higher system pressure, and the higher Leidenfrost temperature is also a candidate of the cause. Figure 2.4 shows examples of cladding temperature histories at the various elevations of the bundle 4 with the highest bundle power. The measurement locations are shown in the right side of the figure. According to this figure, the higher system pressure gives the more rapid cooling down and quench from the higher temperature. The former is considered to be caused by the larger rod surface superheat which will be discussed in the next chapter, and the latter by the higher Leidenfrost temperature.

(3) Quench Velocity

The shorter quench time at each measuring point means the more rapid quench front propagation. Figure 2.5 shows the comparison of quench velocity data among the three tests at different system pressures. Here, quench velocity at a given temperature measurement location is defined as the average quench velocity between the two adjacent thermocouples above and below the location. The higher system pressure clearly results in the higher quench velocity.

The relationship between quench velocity and quench temperature is shown in Fig. 2.6 for the three different system pressures. Murao's[4] and Thompson's[5] correlations are also shown in this figure for reference.

The SCTF data show remarkable scattering. The cause should be studied in the future but seems to be the co-existence of bottom-up quenching and top-down quenching especially in the upper part of the core.

The SCTF data also show the different tendency from the corrections, i.e. the experimental quench velocity seems to increase with increase of quench temperature, though the correlations show decrease of quench velocity with increase of quench temperature. This oposite tendency is supposed to be resulted from the more sensitive system pressure effect than the correlations and the remarkable scattering of data due to random occurrence of the top-down quench.

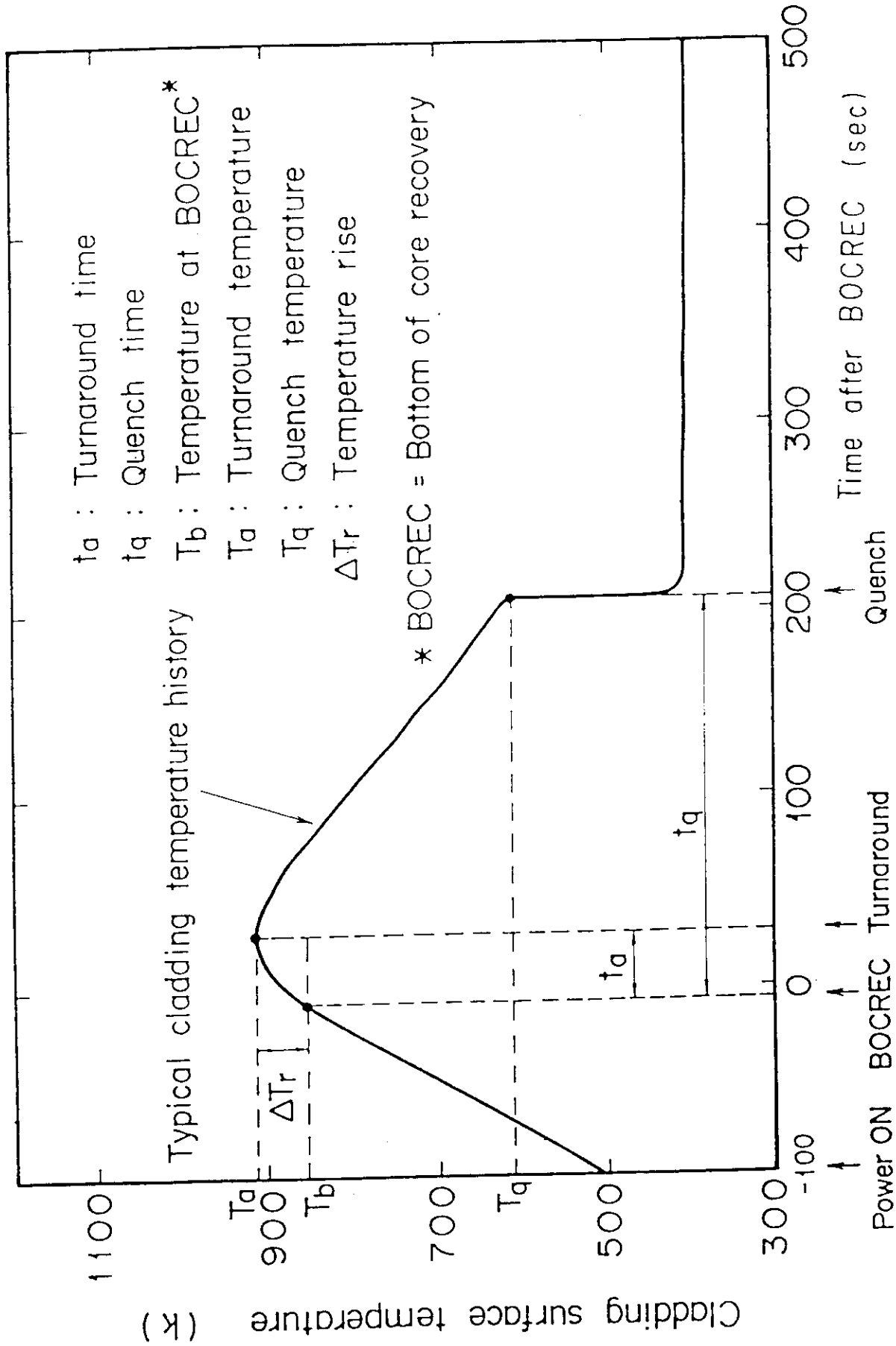

Fig. 2.1 Typical Cladding Temperature History

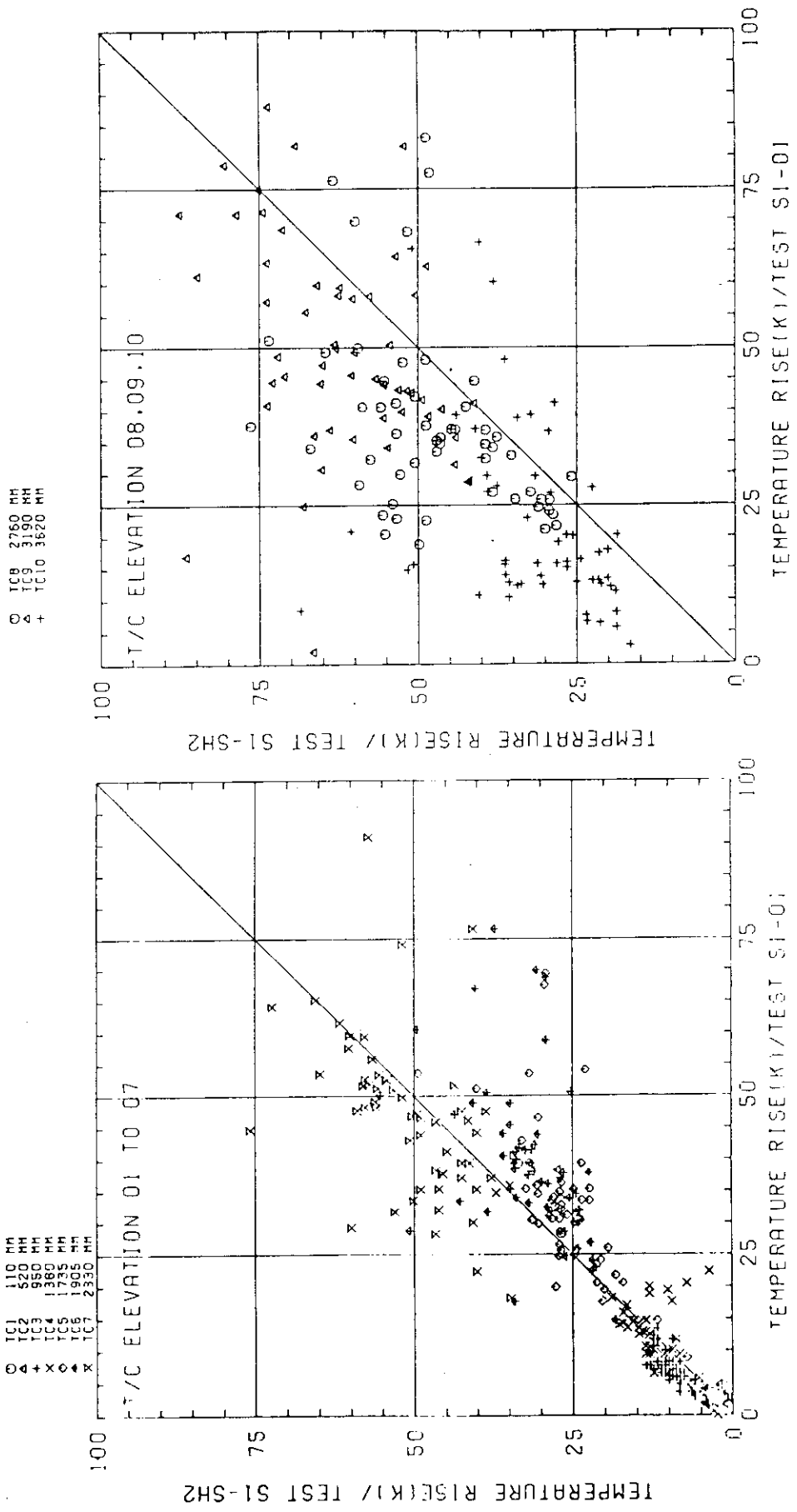

Fig. 2.2(1) Effect of System Pressure on Temperature Rise
(Comparison of Test S1-SH2 with Test S1-01)

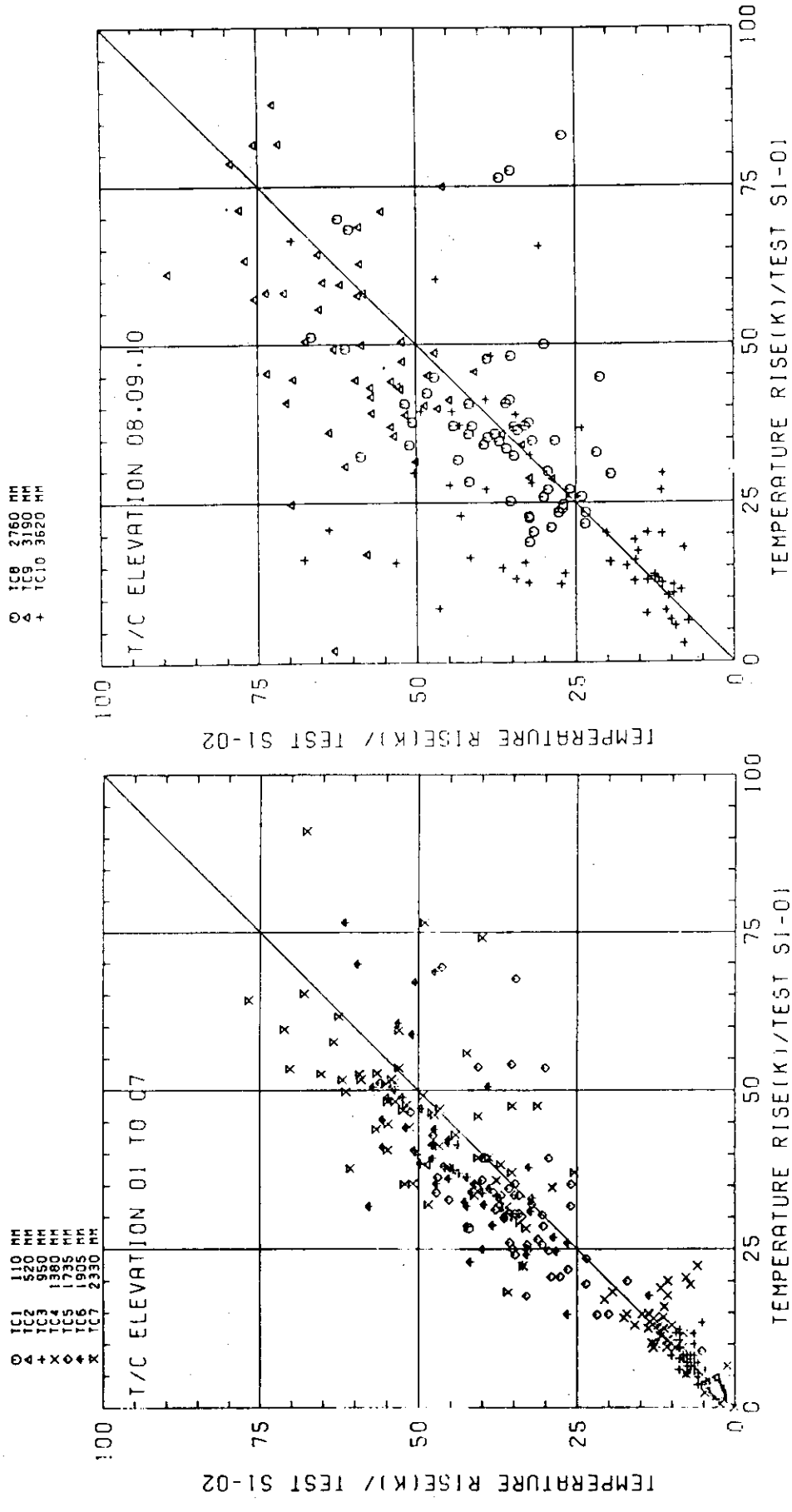

Fig.2.2(2) Effect of System Pressure on Temperature Rise
(Comparison of Test S1-02 with Test S1-01)

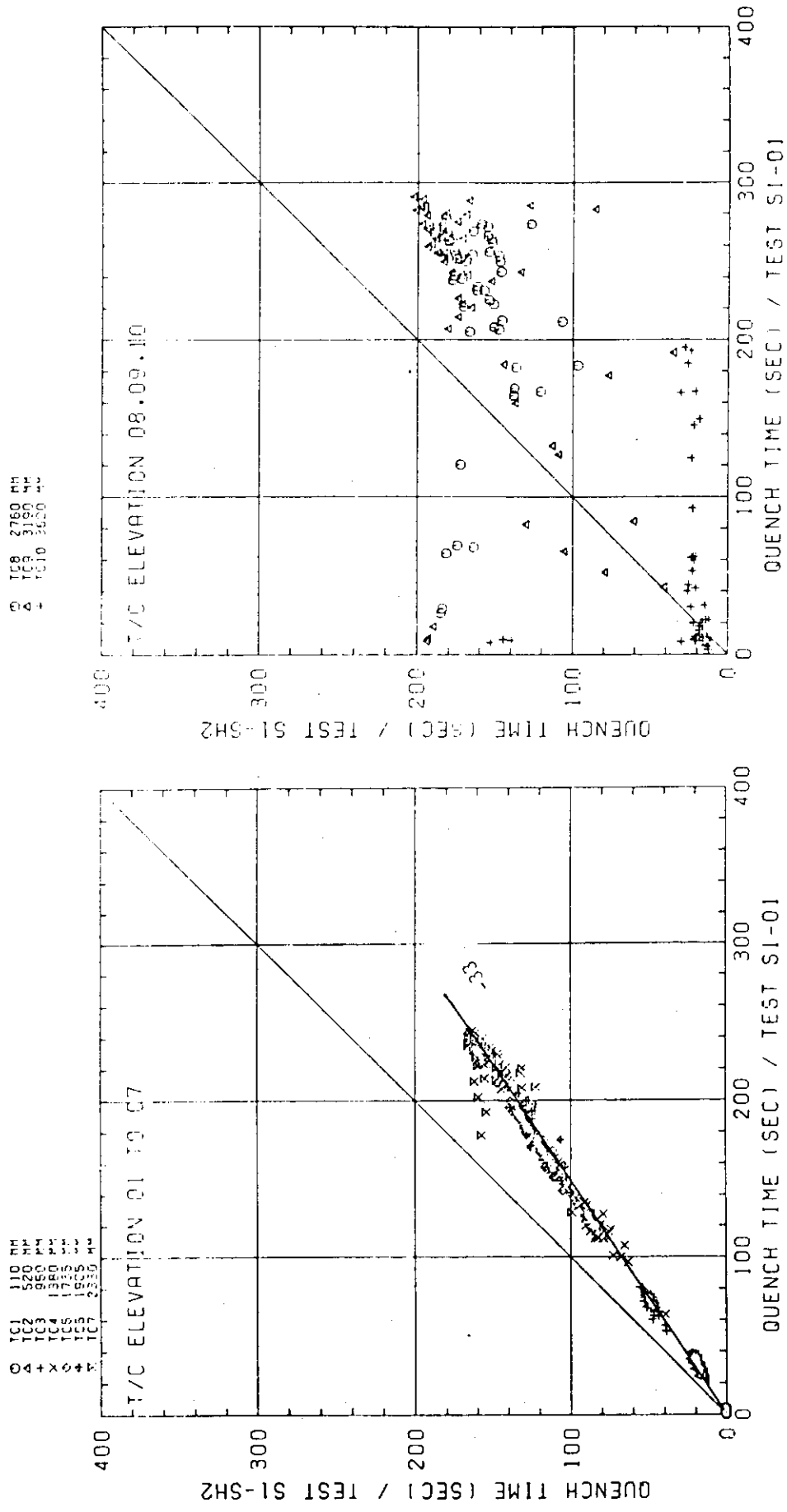

Fig. 2.3(1) Effect of System Pressure on Quench Time
(Comparison of Test S1-SH2 with Test S1-01)

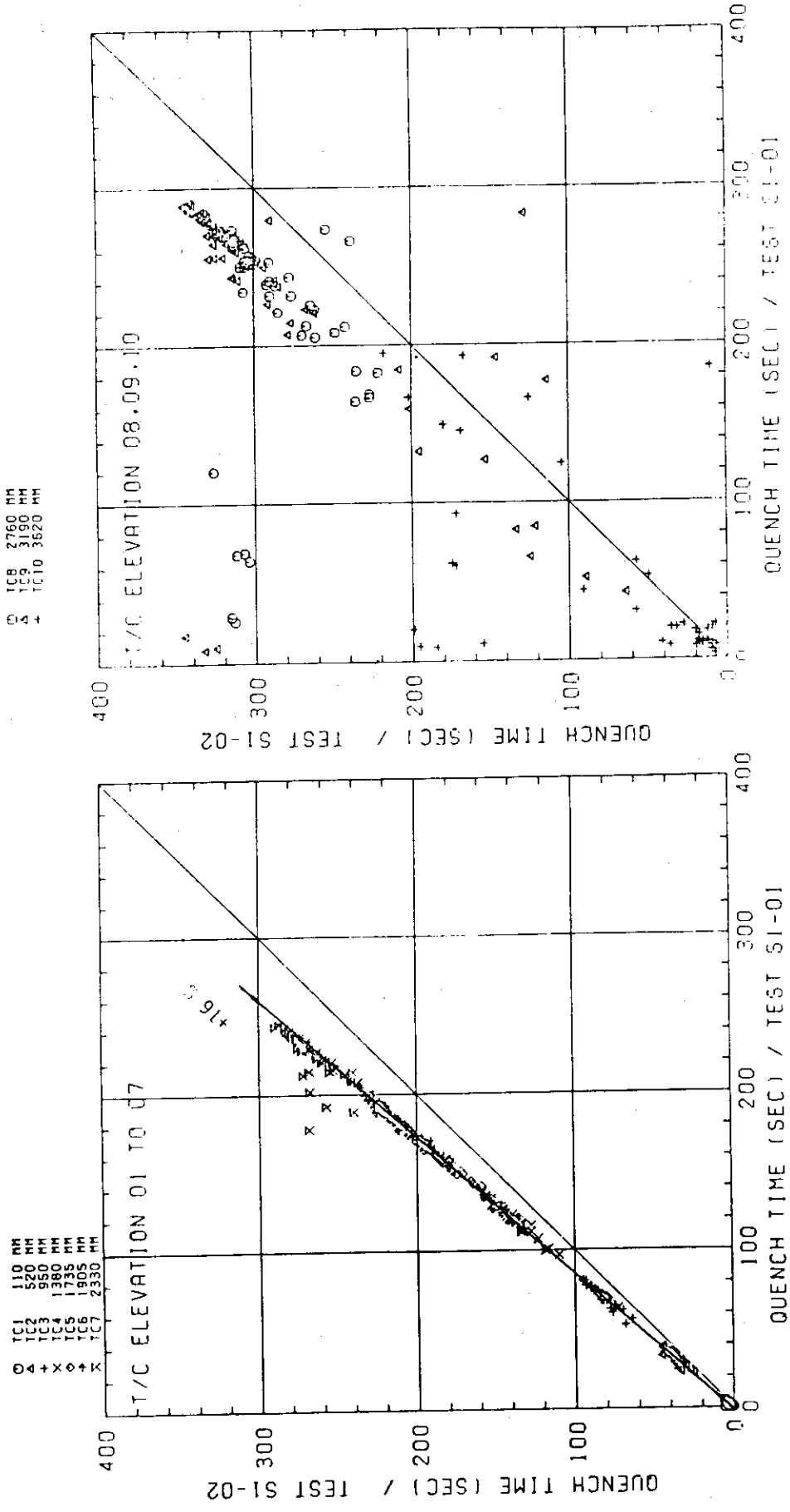

Fig. 2.3(2) Effect of System Pressure on Quench Time
(Comparison of Test S1-02 with Test S1-01)

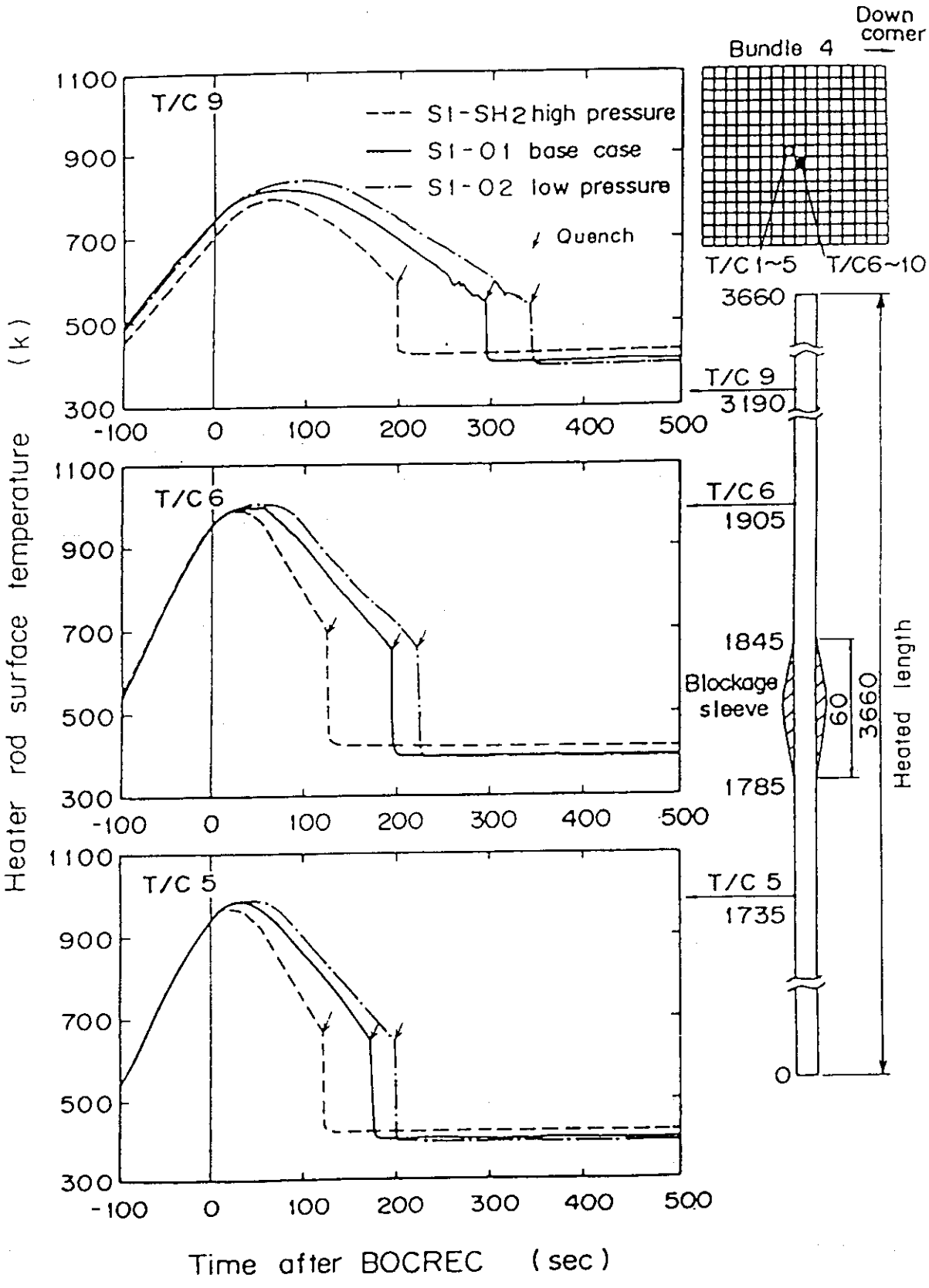

Fig. 2.4 Examples of Cladding Temperature History

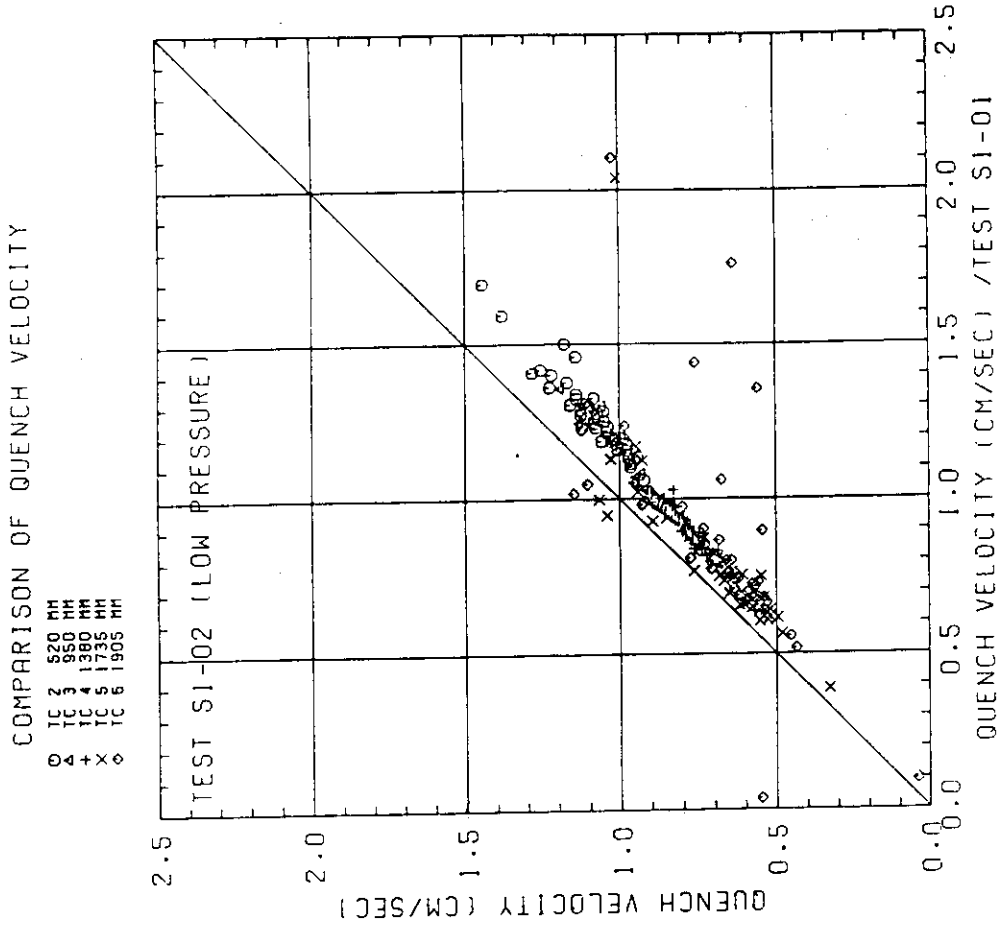

Fig. 2.5(2) Effect of System Pressure on Quench Velocity (Comparison of Test S1-02 with Test S1-01)

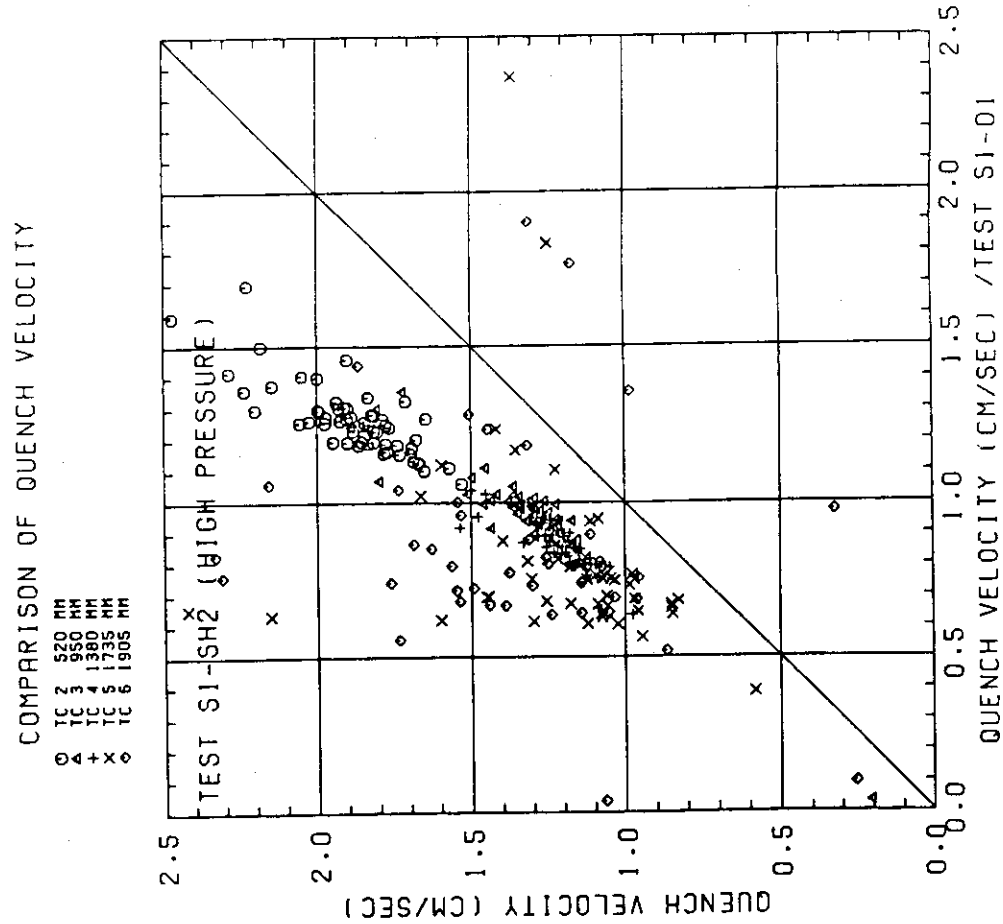

Fig. 2.5(1) Effect of System Pressure on Quench Velocity (Comparison of Test S1-SH2 with Test S1-01)

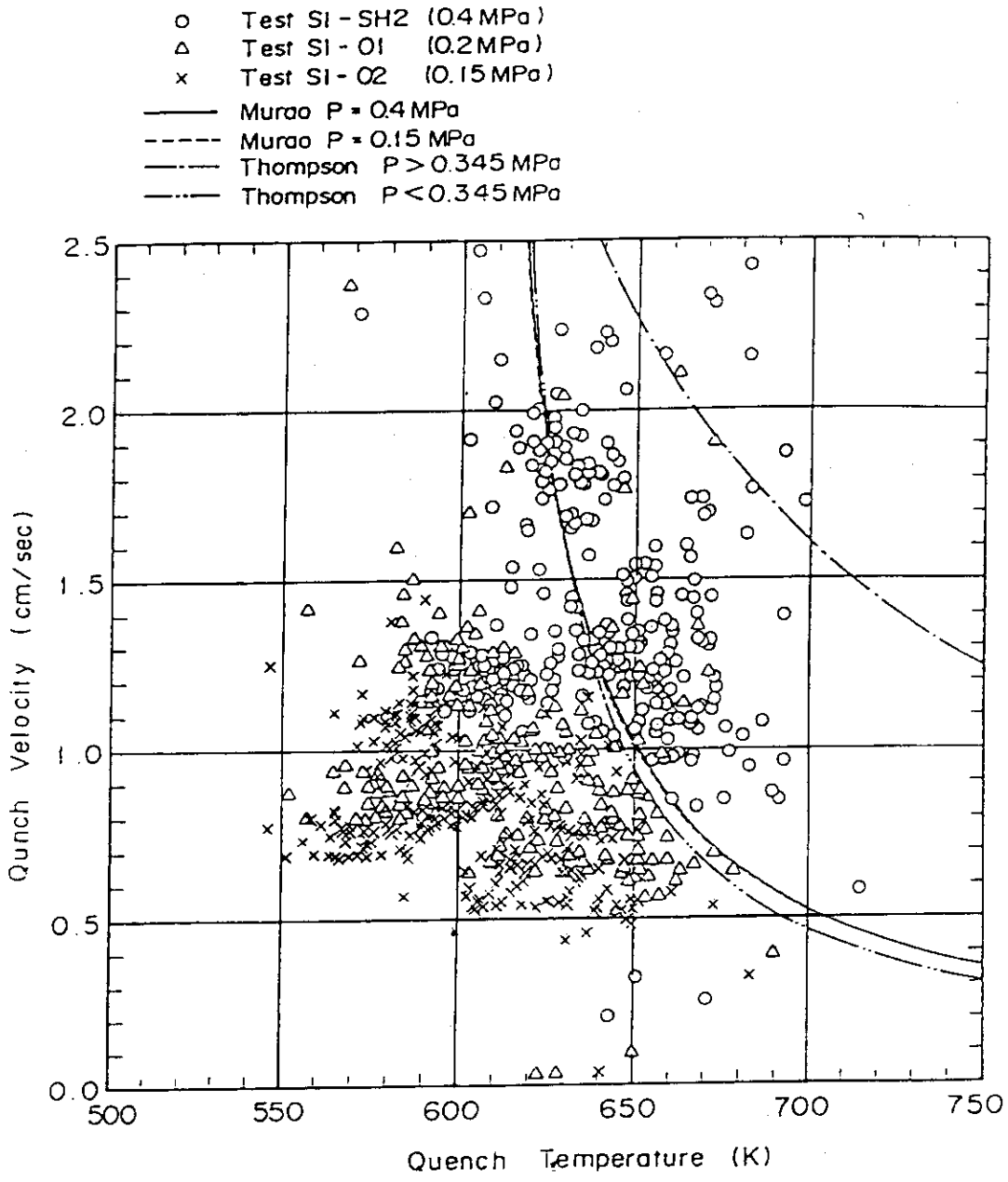

Fig. 2.6 Comparison of Quench Velocity Data with Murao's and Thompson's Correlations

3. Heat Transfer Characteristics

Figure 3.1 shows examples of the change of heat transfer coefficient till the quench at 1735 mm above the bottom of heated length of the bundle 1 corresponding to the center bundle of an actual PWR in the tests under various system pressures. The values are calculated based on the rod surface temperature data. The figure also shows the calculated values with the Sudo's[6] and the Yeh's[7] correlations for reference. The higher system pressure gives the higher heat transfer coefficient for the given time point but the heat transfer coefficient just before the quench is not so affected by the system pressure. This suggests that the relationship between heat trnasfer coefficient and distance above the approaching quench front is not so much affected by the system pressure but the quench front progresses more rapidly when the system pressure is higher. The differential pressure data across core full height shows the more rapid water accumulation in the core when the system pressure is higher as shown in Fig. 3.2. This may be caused by the lower water carryover rate due to the lower steam velocity in the core which is resulted from the higher steam density.

According to Fig. 3.1, heat transfer coefficient before the quench falls between the Sudo's and the Yeh's correlations. This suggests that the heat transfer mode is the neutral between film flow cooling and dispersed flow cooling. Further study is required on this item.

Figure 3.3 shows examples of the change of heat flux in the three tests under various system pressures. The higher system pressure gives the higher heat flux before the quench. Since the heat transfer coefficient before the quench is almost the same among the tests, the difference in heat flux is considered to be caused by the difference in rod surface super heat. Typical temperature transients of the three tests can be illustrated against the time before and after quench as shown in Fig. 3.4. This figure suggests that the rod surface temperature before the quench is much higher when the system pressure is higher. Therefore, in spite of the higher saturation temperature the rod surface super heat is larger when the system pressure is higher. This results in the higher heat flux before the quench in spite of the almost same heat transfer coefficient.

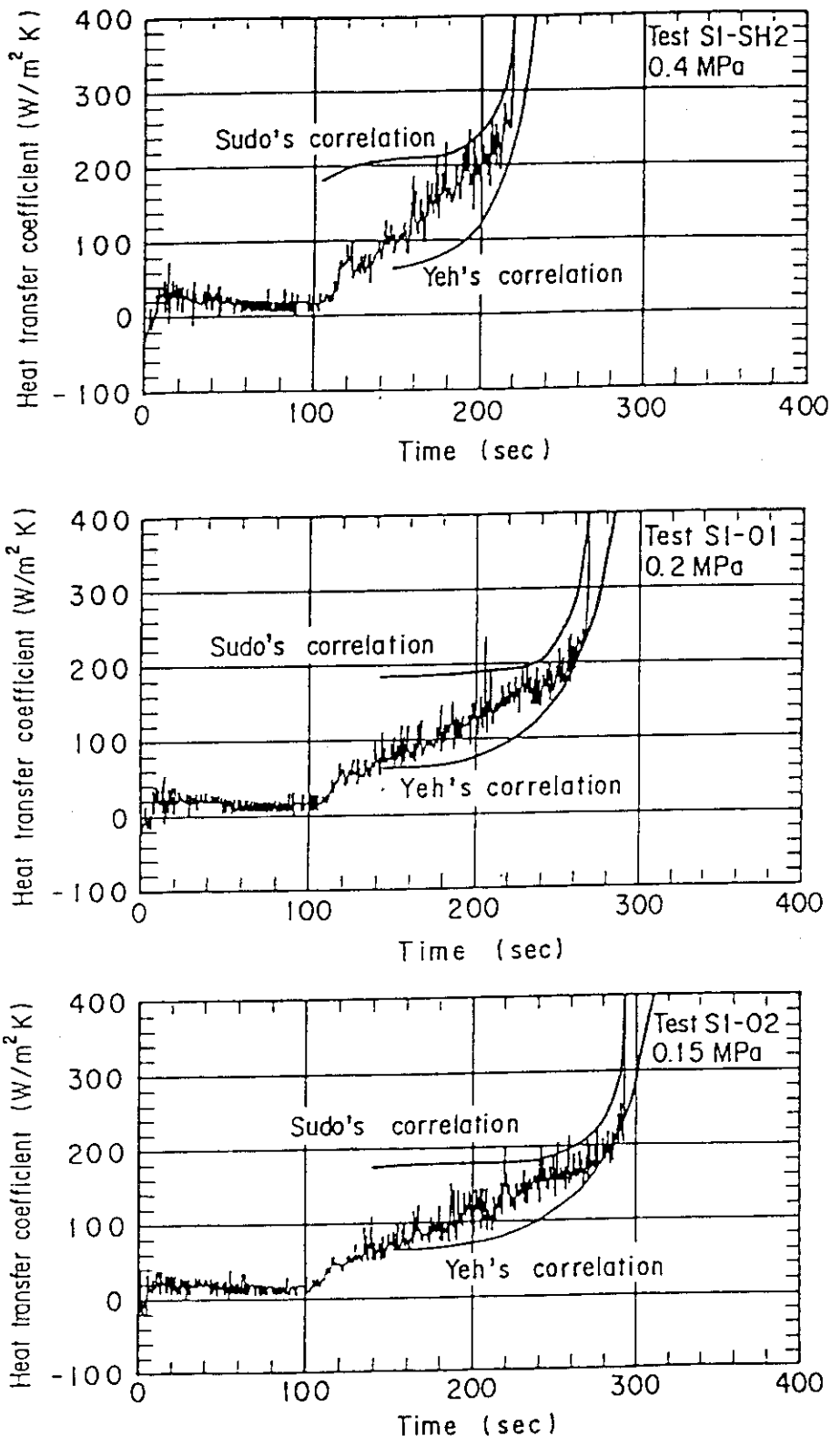

Fig. 3.1 Change of Core Heat Transfer Coefficient at 1735 mm above the bottom of Heated Length of the Bundle 1

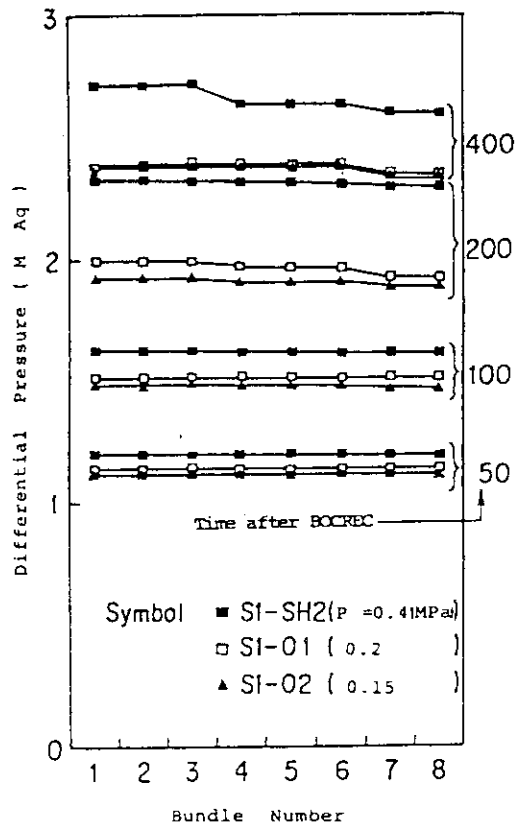

Fig. 3.2 Effect of System Pressure on Core Water Accumulation

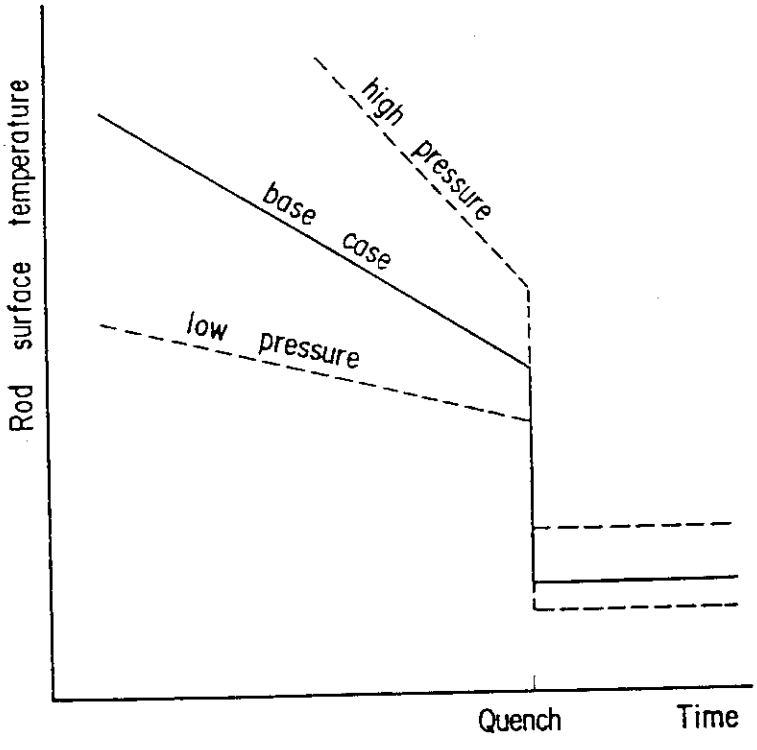

Fig. 3.4 Effect of System Pressure on Rod Surface Temperature before the Quench

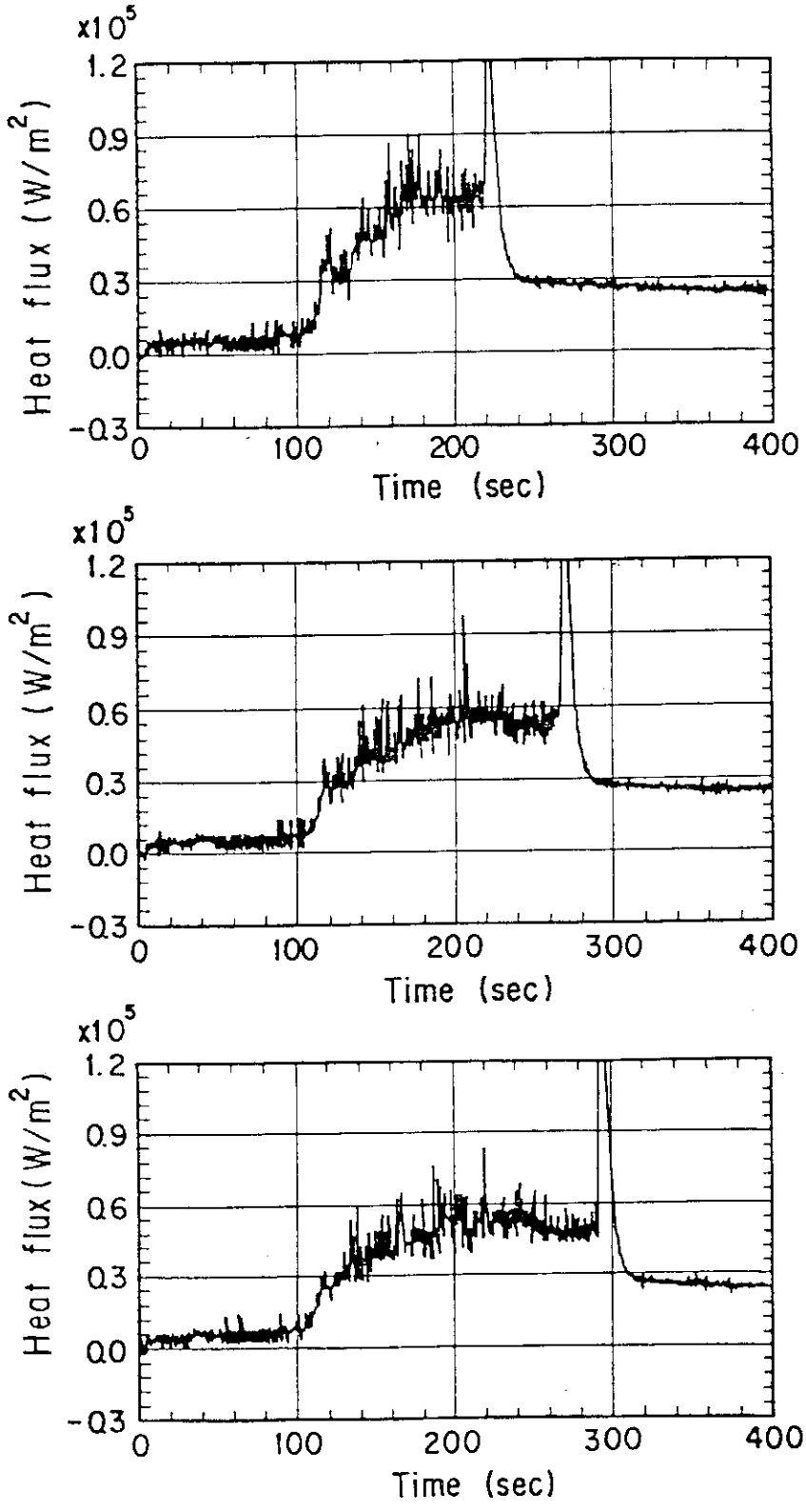

Fig. 3.3 Change of Rod Surface HEAT Flux at 1735 mm above the Bottom of Heated Length of the Bundle 1

4. Two-Dimensional Thermo-Hydrodynamics in the Pressure Vessel

In a wide core such as the SCTF, various thermo-hydrodynamic variables have a distribution not only vertically but also horizontally showing two-dimensional behaviors in the core. Fluid behaviors in the upper plenum and at the interface between the core and the upper plenum have also a horizontal distribution. In this chapter, system pressure effects on such two-dimensional phenomena are discussed.

(1) Horizontal Differential Pressure

Figure 4.1 shows the comparison of horizontal differential pressure across core radius at 1905 mm above the bottom of heated length between Tests S1-SH2 and S1-02. The higher system pressure gives the more significant horizontal differential pressure suggesting the stronger cross flow effect in the core. The remarkable negative differential pressure from about 240 sec after the BOCREC seen in Test S1-SH2 is considered to be resulted from the fall buck water flow to the peripheral region of the core (the bundle 8 side).

(2) Density Distribution in the Core

Figures 4.2(1) through 4.2(3) shows examples of horizontal fluid density distribution in the core at 2570 mm above the bottom of heated length in the three tests under different system pressures. Fluid density seems to be higher at the higher system pressure. This may be caused by the lower void fraction due to the higher steam density. Horizontal density change also seems slightly more remarkable when the system pressure is higher but the behavior is very complex and time dependent.

(3) Water Level in the End Boxes

Figure 4.3 shows the water level data in the end boxes in the three tests. In each the test, remarkable water accumulation in the bundle 8 side is found. The amount of water in the end box above the bundle 8 is more and the ratio of the water level in the end box above the bundle 8 to the others is larger when the system pressure is higher.

(4) Water Level in the Upper Plenum

Figure 4.4 shows the water level distribution on the upper core support plate (UCSP) in the three tests. The higher system pressure results in the

more water accumulation on the UCSP because of the lower void fraction below the mixture level due to the higher steam density. The bundle 8 side shows the higher water level than the bundle 1 side but system pressure effects on the water level distribution is unclear.

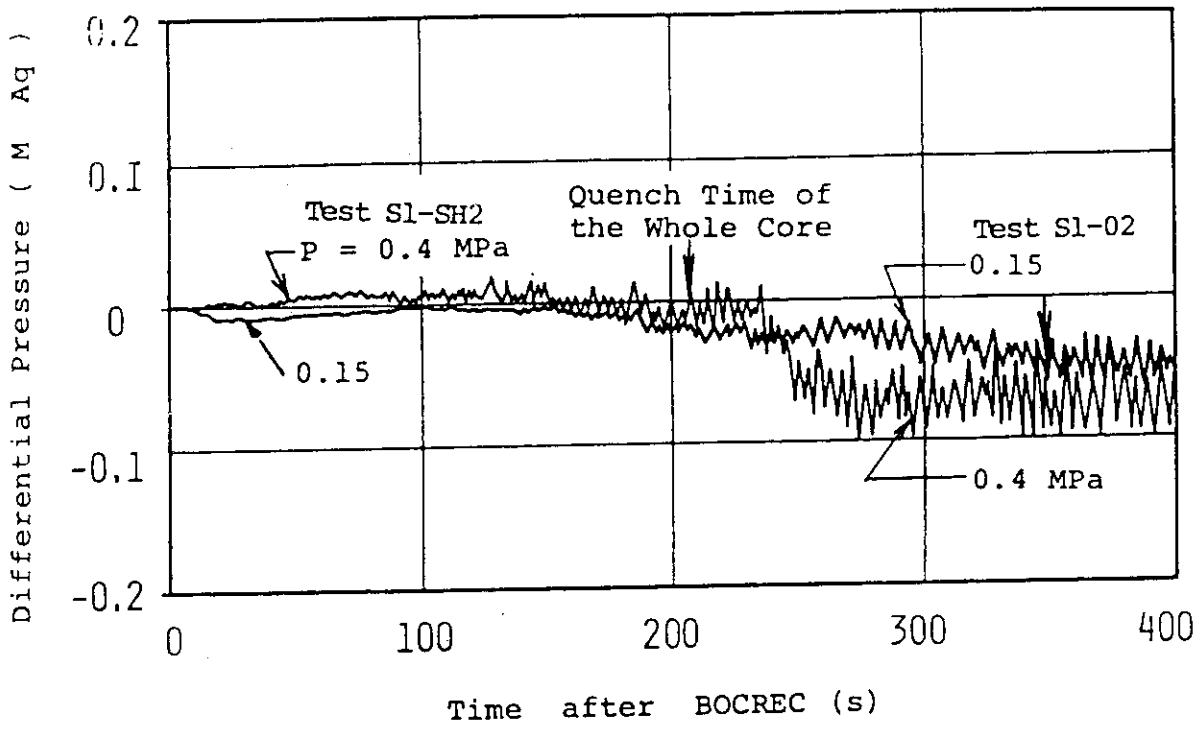

Fig. 4.1 Horizontal Differential Pressure at 1905 mm above the Bottom of Heated Length between the Bundle 1 (Designated Center Bundle) and the Bundle 8 (Peripheral Bundle)

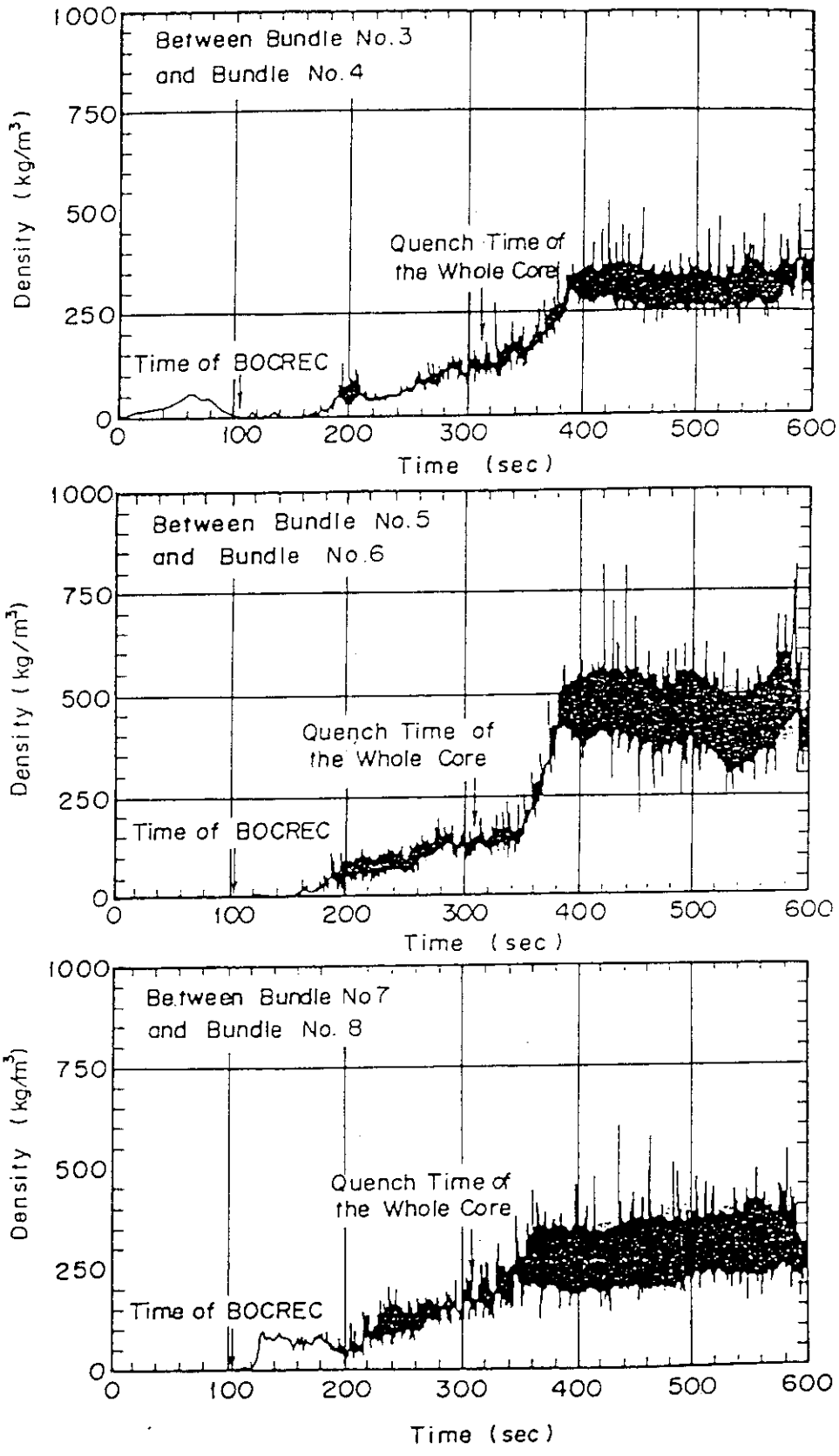

Fig. 4.2 Transients of Fluid Density at 2570 mm above the Bottom of Heated Length

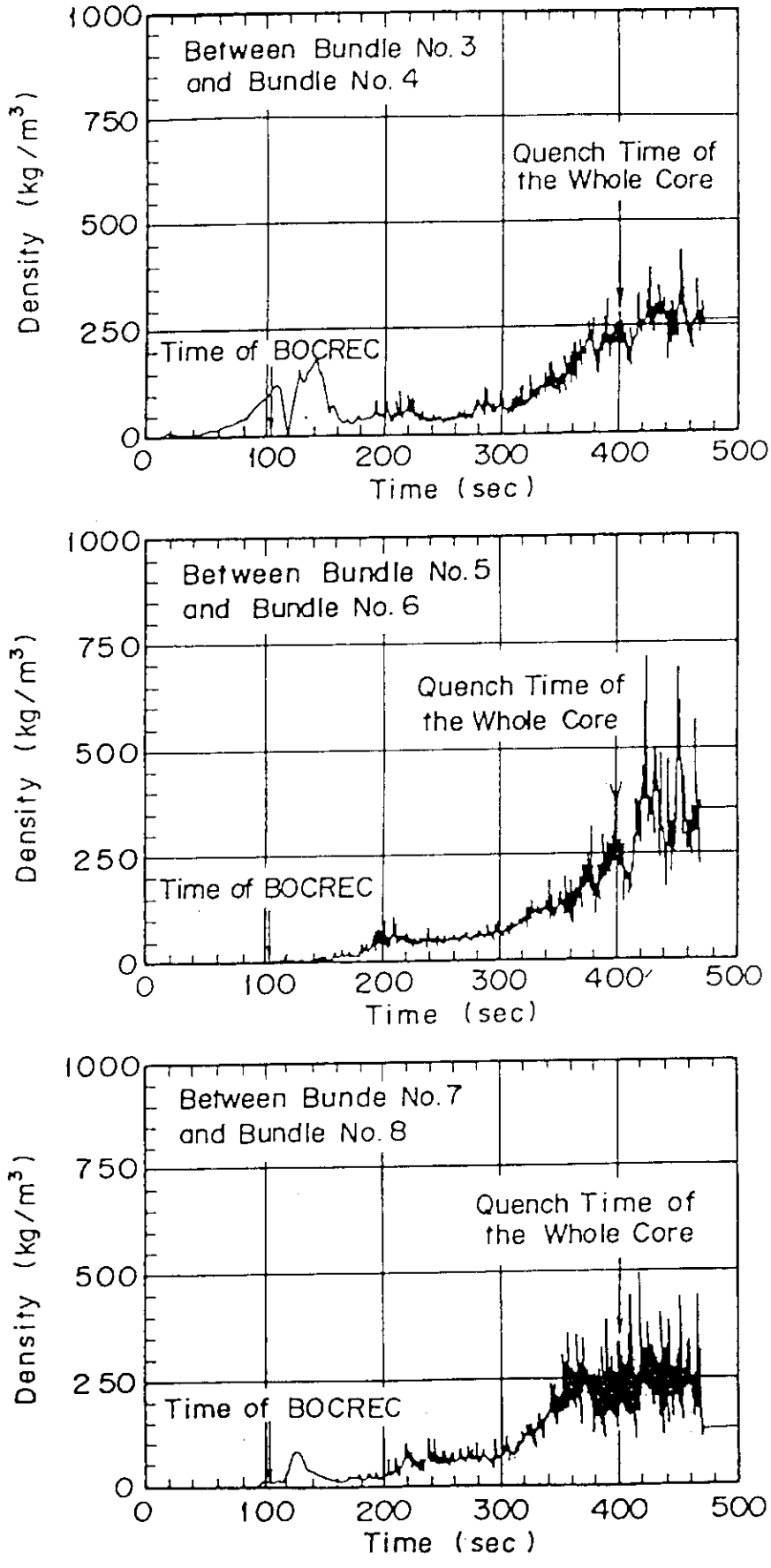

Fig. 4.2 Transients of Fluid Density at 2570 mm above the Bottom of Heated Length

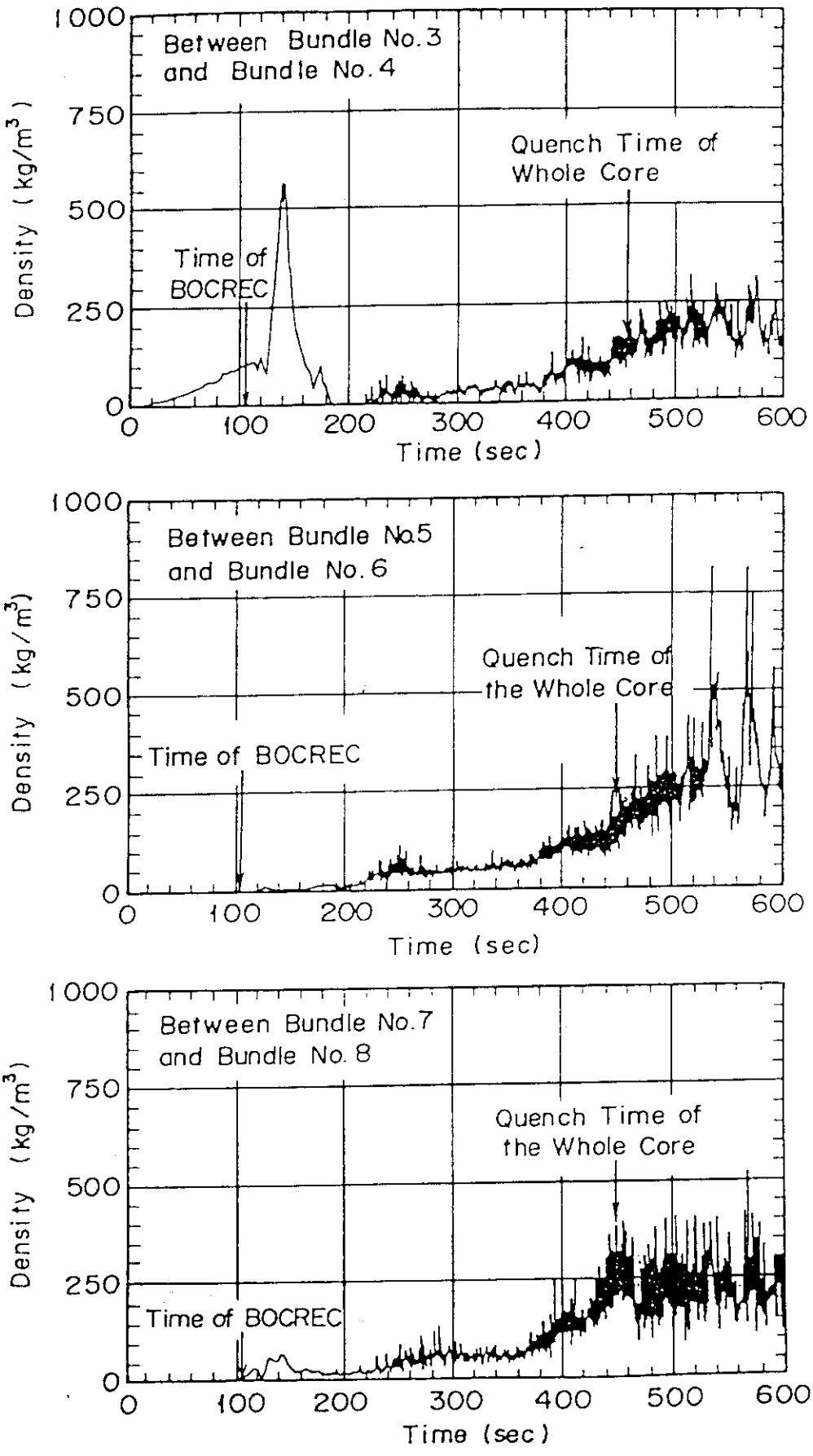

Fig. 4.2 Transients of Fluid Density at 2570 mm above the Bottom of Heated Length

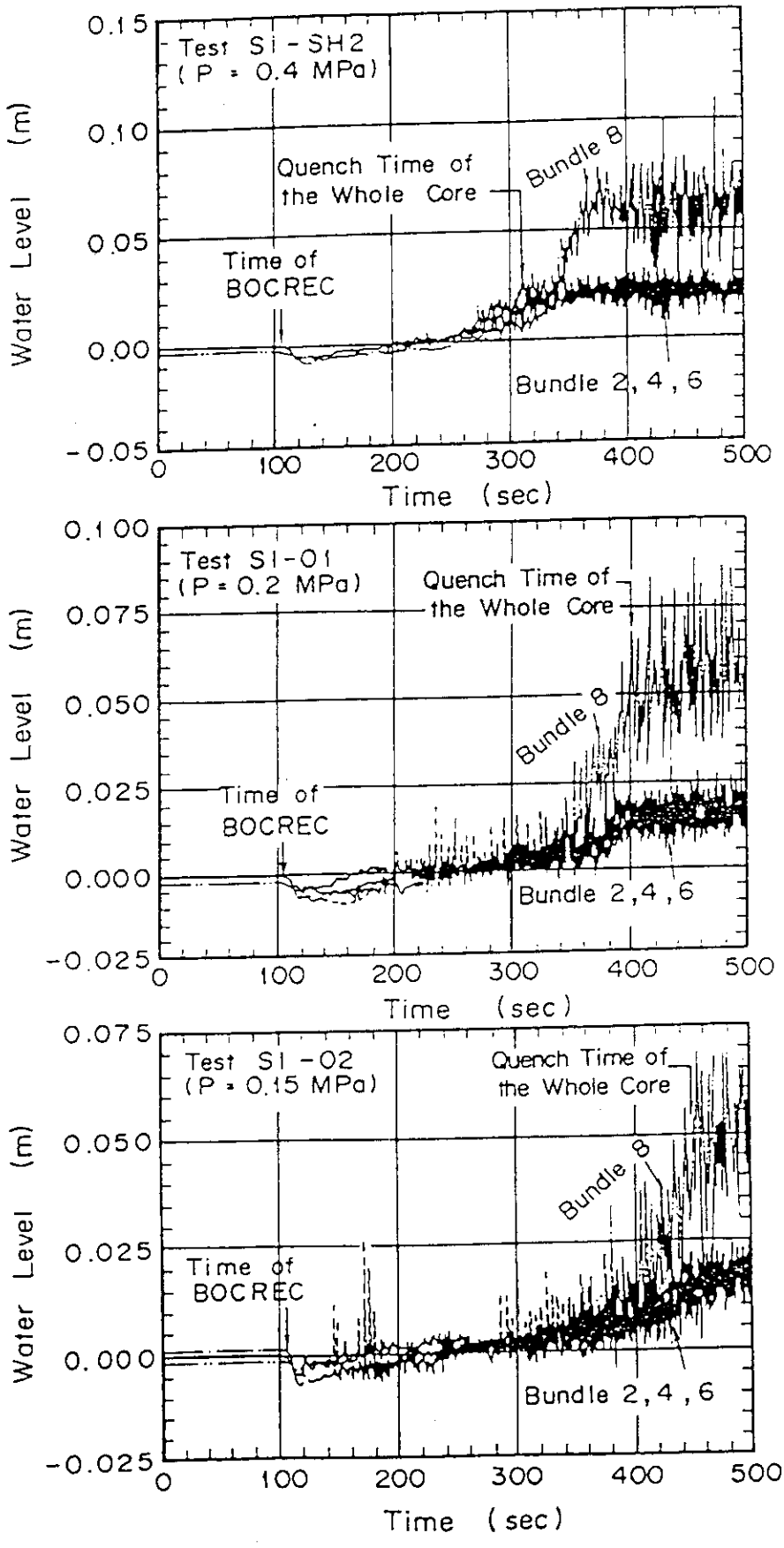

Fig. 4.3 Transients of Water Level in End Boxes above the Bundles 2, 4, 6 and 8

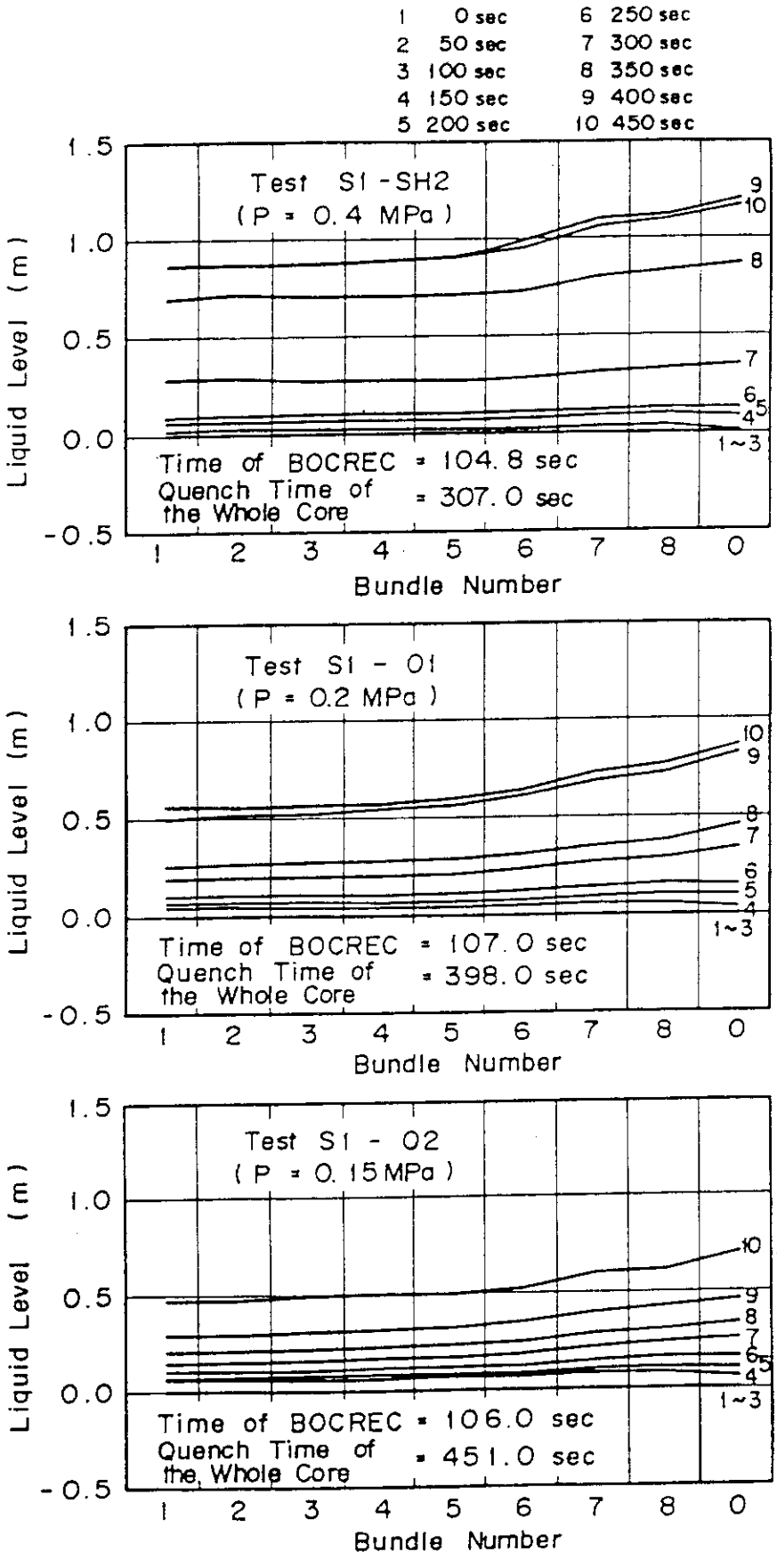

Fig. 4.4 Horizontal Water Level Distribution on UCSP

5. Hot Leg Carryover

Figure 5.1 shows the integrated carryover water mass through the hot leg in the three tests with different system pressures, which is calculated as the total water mass accumulation in the steam-water separator with the inlet plenum simulator, and the containment tanks-II. Both the components are considered to be the receiver of the carryover water through the hot leg. This figure shows that the higher system pressure gives the smaller charryover water mass. This can be explained as follows: That is, the larger steam density due to the higher system pressure results in the lower steam velocities in the core, upper plenum and hot leg, and thus entrainment decreases and de-entrainment increases.

Figure 5.2 gives steam velocity in the hot leg in the three tests. The solid lines are calculated based on the steam flow rate measurement at the intact and broken cold legs and water level measurement at the hot leg, and the broken lines are obtained with the hot leg spool piece. Both data show that the higher system pressure results in the lower steam velocity in the hot leg.

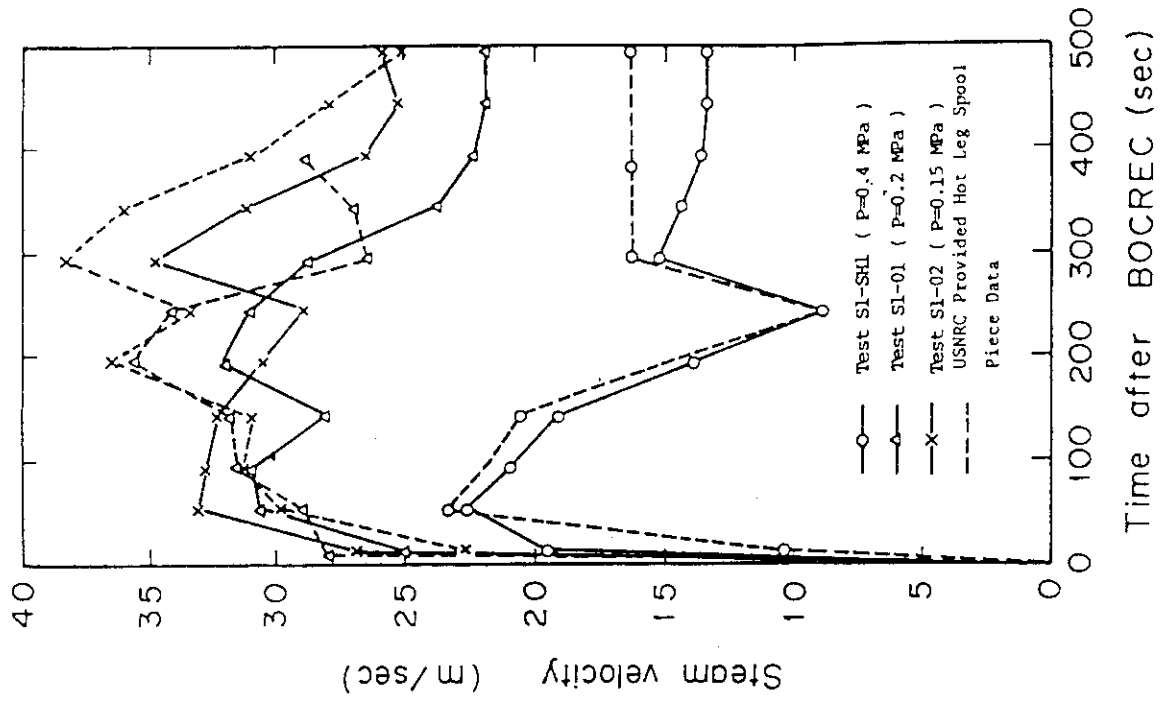

Fig. 5.2 Steam Velocity in Hot Leg

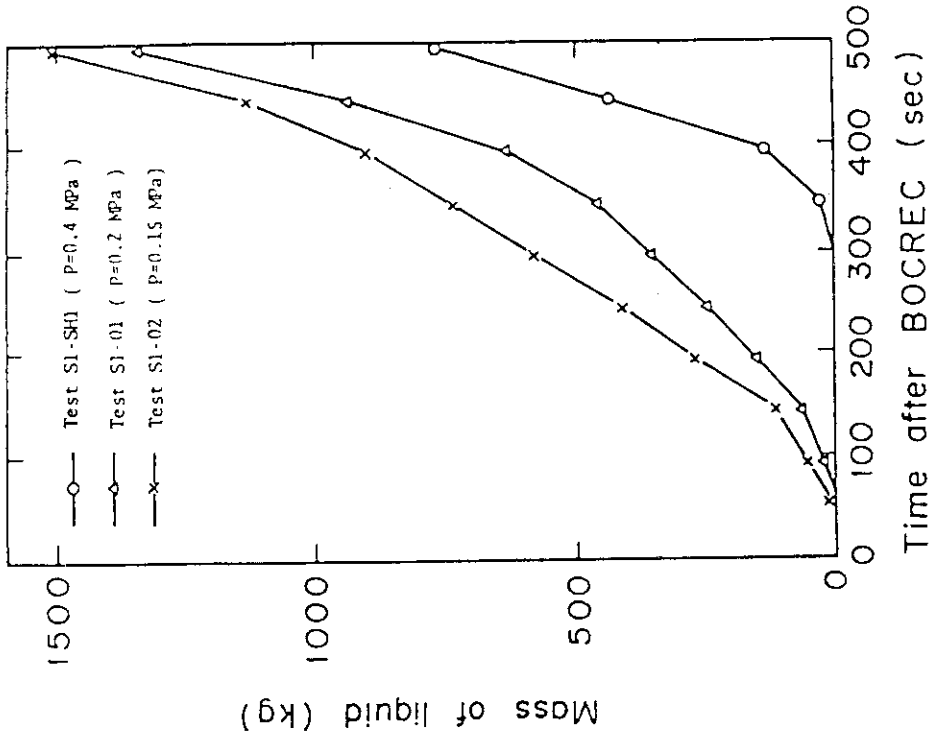

Fig. 5.1 Integrated Carryover Water Mass through Hot Leg

6. Conclusions

Through the three SCTF Core-I forced-feed reflood tests, Tests S1-SH2, S1-01 and S1-02, at the different system pressures, the following conclusions are obtained:

(1) When the system pressure is higher, the temperature rise from the BOCREC time to the turnaround time is slightly smaller, the quench time is shorter and the quench front propagation velocity is higher in comparison with the case under lower system pressure.

(2) Heat trnasfer coefficient before the quench is almost the same with regardless of system pressure.

(3) In spite of the above conclusion (2), heat flux before the quench is higher when the system pressure is higher because of the higher rod surface super heat resulted from the more rapid cooling down of the rods.

(4) Non-uniform horizontal distribution is seen in core pressure, core fluid density, and water levels in the end boxes and in the upper plenum. Water mass in the various portions of the pressure vessel increases with system pressure. Two dimensionality of the fluid behavior in the pressure vessel becomes, generally speaking, more significant with the increase of system pressure.

(5) Hot leg carryover water mass decreases with the increase of system pressure, because of decrease of steam velocities in the core, upper plenum and hot leg pipe resulting in the smaller entrainment rate and larger de-entrainment rate.

Acknowledgement

The authors are much indebted to Dr. M. Nozawa, and Dr. S. Katsuragi, the former and present Center Directors of the Nuclear Safety Research Center, JAERI, respectively, and Dr. M. Ishikawa and Dr. K. Hirano, the former and present Deputy Heads of Dep. Nuclear Safety Research, respectively, for their guidance and encouragement for this program.

They would like to express their appreciation to Messrs. Y. Murao, T. Iguchi, T. Sudoh, J. Sugimoto and H. Akomoto for their useful discussions, Messrs. Y. Niitsuma and T. Wakabayashi for their contribution in instrumentation, to Messrs. Y. Fukaya, N. Suzuki, T. Oyama, J. Matsumoto, T. Nishikizawa, K. Komori and H. Sonobe of Safety Facility Engineering Service Section for their excellent operation of the test facility, and to Messrs. R. K. Fujita and D. H. Miyasaki, the former and present resident engineers from USNRC, respectively, for their devoted help.

References

(1) K. Hirano and Y. Murao : Large Scale Reflood Test, J. At. Energy Soc. Japan, Vol. 22, No. 10, pp. 681∿686 (1980).
(2) H. Adachi, et al. : SCTF Core I Test Results (System pressure effects on reflooding phenomena), JAERI-M 82-075 (1982).
(3) H. Adachi, et al. : SCTF Core I Reflooding Test Results, NUREG/CP-0041, Vol. 1, pp.287∿306 (1983).
(4) Y. Murao, J. Nucl. Sci. Technol., Vol. 15, No. 12, pp.875∿885 (1978).
(5) T. S. Thompson, Rewetting of Hot Surface, AECL-5060 (1975).
(6) Y. Sudo, J. Nucl. Sci. Technol., Vol. 17, NO. 7, pp.516∿530 (1980).
(7) H. C. Yeh, et. al., Nucl. Technol., 46(MID-DEC), pp.473∿481 (1979).

Acknowledgement

The authors are much indebted to Dr. M. Nozawa, and Dr. S. Katsuragi, the former and present Center Directors of the Nuclear Safety Research Center, JAERI, respectively, and Dr. M. Ishikawa and Dr. K. Hirano, the former and present Deputy Heads of Dep. Nuclear Safety Research, respectively, for their guidance and encouragement for this program.

They would like to express their appreciation to Messrs. Y. Murao, T. Iguchi, T. Sudoh, J. Sugimoto and H. Akomoto for their useful discussions, Messrs. Y. Niitsuma and T. Wakabayashi for their contribution in instrumentation, to Messrs. Y. Fukaya, N. Suzuki, T. Oyama, J. Matsumoto, T. Nishikizawa, K. Komori and H. Sonobe of Safety Facility Engineering Service Section for their excellent operation of the test facility, and to Messrs. R. K. Fujita and D. H. Miyasaki, the former and present resident engineers from USNRC, respectively, for their devoted help.

References

(1) K. Hirano and Y. Murao : Large Scale Reflood Test, J. At. Energy Soc. Japan, Vol. 22, No. 10, pp. 681∿686 (1980).
(2) H. Adachi, et al. : SCTF Core I Test Results (System pressure effects on reflooding phenomena), JAERI-M 82-075 (1982).
(3) H. Adachi, et al. : SCTF Core I Reflooding Test Results, NUREG/CP-0041, Vol. 1, pp.287∿306 (1983).
(4) Y. Murao, J. Nucl. Sci. Technol., Vol. 15, No. 12, pp.875∿885 (1978).
(5) T. S. Thompson, Rewetting of Hot Surface, AECL-5060 (1975).
(6) Y. Sudo, J. Nucl. Sci. Technol., Vol. 17, NO. 7, pp.516∿530 (1980).
(7) H. C. Yeh, et. al., Nucl. Technol., 46(MID-DEC), pp.473∿481 (1979).

Appendix A Slab Core Test Facility (SCTF) Core-I

A.1 Test Facility

The Slab Core Test Facility was designed under the following design phylosophy and design criteria:

a. Design Philosophy

(1) The facility should provide the capability to study the two-dimensional, thermohydraulic behavior and core flow within the reactor vessel especially due to the radial power distribution during the end of blowdown, refill and reflood phases of a simulated LOCA for a pressurized water reactor.

(2) To properly simulate the core heat transfer and hydrodynamics, a special emphasis is put on the proper simulation of the components in the pressure vessel. As the components in the pressure vessels are provided a simulated core, downcomer, core baffle region, lower plenum, upper plenum and upper head. On the other hand, simplified primary coolant loops are provided. As the primary coolant loops are provided a hot leg, an intact cold leg, broken cold legs and a steam water separator. The object of the steam/water separator is to measure the flow rate of carryover water coming out of the upper plenum.

b. Design Criteria

(1) The reference reactor for simulation to the SCTF is the Trojan reactor in the United States which is a four loop 3300 MWt PWR. The Ooi reactor in Japan is also referred which is of the similar type to the Trojan reactor.

(2) A full scale radial and axial section of a pressurized water reactor is provided as a simulated core of the SCTF with single bundle width.

(3) The simulated core consists of 8 bundles arranged in a row. Each bundle has electrically heated rods simulating fuel rods and non-heated rod with 16×16 array.

(4) The flow area and fluid volume of components are scaled down based on the core flow area scaling.

(5) To properly simulate the flow behavior of carryover water and entrainment, the elevations of hot leg and cold legs are designed to be the same as the PWRs as much as possible.

(6) The honeycomb structure is used as the side walls which accomodate the slab core, upper plenum and the upper part of lower plenum, so

as to minimize the effect of walls on the disturbance of the core heat transfer and hydrodynamics.

(7) To investigate the effect of flow resistance in the primary loops are provided the orifices of which dimension is changeable.

(8) The maximum allowable temperature of the simulated fuel rods is 1900°C and the maximum allowable pressure of the facility is 6 kg/cm^2 absolute.

(9) The facility is equipped with a hot leg equivalent to four actual hot legs connecting the upper plenum and the steam water separator, an intact cold leg equivalent to three actual intact cold legs connecting the steam water separator and the downcomer and two broken cold legs, one is for the steam water separator side and the other for the pressure vessel side.

(10) The ECCS consists of an Acc., a LPCI and a combined injection systems.

(11) ECC water injection ports are the cold leg, hot leg, upper plenum, downcomer, lower plenum and above the upper core support plate. These portions are to be chosen according to the object of the test.

(12) For better simulation of lower plenum flow resistance, simulated fuel rods do not penetrate through the bottom plate of the lower plenum but terminate below the bottom of the core.

(13) For measurements in the pressure vessel including core measurements, the feature of the slab geometry of the pressure vessel is utilized as much as possible. Design and arrangement of the instruments are done so as to be able to carry out installation calibration and removal of the instruments.

(14) View windows are provided where flow pattern recognition is important. The locations are, the interface between the core and the upper plenum, hot leg, pressure vessel side broken cold leg and the downcomer.

(15) The blocked bundle test is carried out in Core-I in order to investigate the effect of the ballooned fuel rods and the unblocked normal bundle test for the Core-II and -III.

(16) Simulated types of break are cold leg break and hot leg break.

(17) The components and systems such as the containment tanks and ECC water supply system in the CCTF are shared with the SCTF to the maximum extent.

The overall schematic diagram of the SCTF is shown in Fig.A-1. The principal dimensions of the facility is shown in Table A-1, and the

comparison of dimensions between the SCTF and the referred PWR is shown in Fig.A-2.

A.1.1 Pressure Vessel and Internals

The pressure vessel is of slab geometry as shown in Fig.A-3. The height of the components in the pressure vessel is almost the same as the reference reactor's, and the flow area and the fluid volume of each component are scaled down based on the nominal core flow area scaling.

The core consists of 8 bundles in a row and each bundles include simulated fuel rods and non-heated rods with 16 × 16 array. The core arrangement for the SCTF Core-I is shown in Fig.A-4, which includes 6 normal bundles and 2 blocked bundles. The core is enveloped by the honeycomb thermal insulator which is attached on the barrel.

The downcomer is located at one end of the pressure vessel which corresponds to the periphery of the actual reactor. The core baffle region is, on the other hand, located between the core and the downcomer. For better understanding, the cross section of the pressure vessel at the elevation of midplane of the core is shown in Fig.A-5.

The design of upper plenum internals is based on that of the new Westinghouse 17 × 17 array fuel assemblies. The internals consist of control rod guide tubes, support columns, orifice plates and open holes and those arrangements is shown in Fig.A-6. The radius of each internal is scaled down by factor 8/15 from that of an actual reactor. Flow resistance baffles are inserted into the guide tubes. The elevation and the configuration of baffles plates are shown in Fig.A-7 and A-8.

The height of the hot leg and cold legs are designed as close to the actual PWR as possible. However, in order to avoid the interference of the nozzles in the downcomer, the height of nozzles for the broken cold leg and the intact cold leg are shifted down compared to that of the hot leg as shown in Fig.A-3.

A.1.2 Heater Rod Assembly

The heater rod assembly for the SCTF Core-I consists of 8 bundles arranged in a row. These bundles are composed of 6 normal unblocked bundles which are located at the 1st, 2nd and 5th to 8th bundles and 2 blocked bundles which are 3rd and 4th bundles as shown in Fig.A-4. Each bundle has 234 electrically heated rods and 22 non-heated rods. The dimensions of the heater rods are based on a 15 × 15 fuel rod bundle,

and the heated length and the outer diameter of each heater rod are 3.66 m and 10.7 mm, respectively. A heater rod consists of a nichrome heater element, magnesium oxide (MgO) and Nichrofer-7216 sheath (equialent to Inconel 600). The sheath wall thickness is about 1.0 mm and is thicker than the actual fuel cladding because of the requirements for thermocouple installation. The heating element is a helical coil and has a 17 step chopped cosine axial power profile as shown in Fig.A-9. The peaking factor is 1.4.

Non-heated rods are either stainless steel pipes or solid rods of 13.8 mm O.D. The heater rods and non-heated rods are fixed at the top of the core allowing the rods to move downward when the thermal expansion occurs. In Fig.A-10 the axial position where blockage sleeves for simulating the balooned fuel rod are equipped is shown. The blockage sleeves consist of three types of sleeve, one is used for the rods at the corner adjacent to the next blocked bundle, another for the rods adjacent to the side walls and the third for the rods except for the periphery of the blocked bundle. These are named A, B and C respectively in the Fig.A-11 and these configurations for these are shown in Fig.A-12.

For better simulation for flow resistance in the lower plenum the simulated rods do not penetrate through the bottom plate of the lower plenum as shown in Fig.A-10.

A.1.3 Primary Loops and ECCS.

Primary loops consist of a hot leg equivalent to the four actual hot legs, a steam/water separator for measuring the flow rate of carry over water, an intact cold leg equivalent to the three actual intact loops, a broken cold leg on the pressure vessel side and a broken cold leg on the steam water separator side. These two broken cold legs are connected to two containment tanks through break valves, respectively. The arrangement of the primary loops is shown in Fig.A-13. The flow area of each loop is scaled down based on the core flow area scaling. It should be emphasized that the cross section of the hot leg is a elongated circle to realize the proper flow pattern in the hot leg. The steam/water separator has a steam generator inlet plenum simulator to realize the flow characteristics of carryover water. The cross section of the hot leg and the configuration of the steam generator inlet plenum simulator are shown in Fig.A-14.

A pump simulator and a loop seal part are provided for the intact cold leg. The arrangement of the intact cold leg is shown in Fig.A-15.

The pump simulator consists of the casing and duct simulators and an orifice plate as shown in Fig.A-16. The loop resistance is adjusted with the orifice plate.

In principle, ECCS consists of an accumulator and a low pressure injection system. The injection port is located as already described in the design criteria. Besides, the UCSP extraction system is provided and the UCSP water injection and extraction systems will be used for combined injection tests.

A.1.4 Containment Tanks and Auxiliary System

Two containment tanks are provided to the SCTF. The containment tank-I is connected with the downcomer through the pressure vessel side broken cold leg and the containment tank-II is connected with the steam/water separator through the steam/water separator side broken cold leg. Especially in the containment tank-I, carryover water from the downcomer is measured by phase separation. These containment tanks and auxiliary system such as a pressurizer for injecting water from the Acc. tank, etc. are shared with the CCTF.

A.2 Instrumentation

The instrumentation in the SCTF has been provided both by JAERI and USNRC. The JAERI-provided instrumentation includes the measurement of temperatures, pressures, differential pressures, liquid levels, flow velocities, and heating powers. USNRC has provided film probes, impedance probes, string probes, liquid level detectors (LLDs), fluid distribution grids (FDGs), turbine meters, drag disks, γ-densitometers, spool pieces and video optical probes. The measurement items of the JAERI- and USNRC-provided instruments are listed in Tables A-2 and A-3, respectively.

Table A-1 Principal Dimensions of Test Facility

1. Core Dimension	
(1) Quantity of Bundle	8 Bundles
(2) Bundle Array	1 × 8
(3) Bundle Pitch	230 mm
(4) Rod Array in a Bundle	16 × 16
(5) Rod Pitch in a Bundle	14.3 mm
(6) Quantity of Heater Rod in a Bundle	234 rods
(7) Quantity of Non-Heated Rod in a Bundle	22 rods
(8) Total Quantity of Heater Rods	234 × 8 = 1872 rods
(9) Total Quantity of Non-Heated Rods	22 × 8 = 176 rods
(10) Effective Heated Length of Heater Rod	3660 mm
(11) Diameter of Heater Rod	10.7 mm
(12) Diameter of Non-Heateed Rod	13.8 mm
2. Flow Area & Fluid Volume	
(1) Core Flow Area* (nominal)	0.227 m^2
(2) Core Fluid Volume	0.92 m^3
(3) Baffle Region Flow Area	0.10 m^2
(4) Baffle Region Fluid Volume	0.36 m^3
(5) Downcomer Flow Area	0.121 m^2
(6) Upper Annulus Flow Area	0.158 m^2
(7) Upper Plenum Horizontal Flow Area	0.525 m^2
(8) Upper Plenum Fluid Volume	1.16 m^2
(9) Upper Head Fluid Volume	0.86 m^3
(10) Lower Plenum Fluid Volume	1.38 m^3
(11) Steam Generator Inlet Plenum Simulator Flow Area	0.626 m^2
(12) Steam Generator Inlet Plenum Simulator Fluid Volume	0.931 m^3
(13) Steam Water Separator Fluid Volume	5.3 m^3
(14) Flow Area at the Top Plate of Steam Generator Inlet Plenum Simulator	0.195 m^2
(15) Hot Leg Flow Area	0.0826 m^2
(16) Intact Cold Leg Flow Area (Diameter = 297.9 mm)	0.0697 m^2
(17) Broken Cold Leg Flow Area (Diameter = 151.0 mm)	0.0179 m^2

* Flow area in the core is 0.35 m^2, including the excess flow area of gaps between the bundle and the surface of thermal insulator and between the core barrel and the pressure vessel wall.

Table A-1 Principal Dimensions of Test Facility

(18) Containment Tank I Fluid Volume	30 m^3
(19) Containment Tank II Fluid Volume	50 m^3
3. Elevation & Height	
(1) Top Surface of Upper Core Support Plate (UCSP)	0 mm
(2) Bottom Surface of UCSP	-76 mm
(3) Top of the Effective Heated Length of Heater Rod	-393 mm
(4) Bottom of the Skirt in the Lower Plenum	-5270 mm
(5) Bottom of Intact Cold Leg	+724 mm
(6) Bottom of Hot Leg	+1050 mm
(7) Top of Upper Plenum	+2200 mm
(8) Bottom of Steam Generator Inlet Plenum Simulator	+1933 mm
(9) Centerline of Loop Seal Bottom	-2281 mm
(10) Bottom Surface of End Box	- 185.1 mm
(11) Top of the Upper Annulus	+2234 mm
(12) Height of Steam Generator Inlet Plenum Simulator	1595 mm
(13) Height of Loop Seal	3140 mm
(14) Inner Height of Hot Leg Pipe	737 mm
(15) Bottom of Lower Plenum	-5770 mm
(16) Top of Upper Head	+2887 mm

Table A-2 Measurement Items of SCTF (JAERI-provided instruments)

LOCATION	ITEM	PROBE	QUANTITY
1. CORE			
center	pressure	DP cell	1
short range of core	diff. press.	DP cell	22
half length of core	diff. press.	DP cell	16
full length of core	diff. press.	DP cell	8
across spacers	diff. press.	DP cell	7
across end box	diff. press.	DP cell	8
across 4 assemblies	diff. press.	DP cell	3
across 8 assemblies	diff. press.	DP cell	3
below and above end box	steam velocity	Pitot-tube	3
sub channel	steam velocity	Pitot-tube	13
below end box hole	fluid temp.	T/C	16
above end box hole	fluid temp.	T/C	16
core baffle	fluid temp.	T/C	6
non-heating rods	fluid temp.	T/C	96
	steam temp.	SSP	16
	clad temp.	T/C	108
heater rods	clad temp.	T/C	640
side walls	wall temp.	T/C	36
core baffle	wall temp.	T/C	6
core baffle	liquid level	DP cell	1
short range of core baffle	liquid level	DP cell	6
heated rod	power		8 sum(1039)
2. UPPER PLENUM			
centre	pressure	DP cell	1
across end box tie plate	diff. press.	DP cell	8
core outlet-hot leg inlet	diff. press.	DP cell	4
periphery of UCSP hole	fluid temp.	T/C	8
centre of UCSP hole	fluid temp.	T/C	8
250mm & 1000mm above UCSP	fluid temp.	T/C	8
surface of UCSP	fluid temp.	T/C	8
above UCSP hole	steam temp.	SSP	8

Table A-2 Measurement Items of SCTF (JAERI-provided instruments)
(Continued)

LOCATION	ITEM	PROBE	QUANTITY
surface of structure	wall temp.	T/C	15
side walls	wall temp.	T/C	8
above end box tie plate	liquid level	DP cell	8
above UCSP	liquid level	DP cell	9
above UCSP (v.)	steam velocity	Pitot-tube	2
inter-structures (h.)	steam velocity	Pitot-tube	2
			sum(97)
3. LOWER PLENUM			
below bottom spacer	pressure	DP cell	1
lower plenum - upper plenum	diff. press.	DP cell	1
core inlet	fluid temp.	T/C	8
inlet from downcomer	fluid temp.	T/C	2
side & bottom walls	wall temp.	T/C	4
below bottom spacer	liquid level	DP cell	1
			sum(17)
4. DOWNCOMER			
upper position	pressure	DP cell	1
horizontal direction	diff. press.	DP cell	1
four levels	fluid temp.	T/C	8
side wall	wall temp.	T/C	2
inner wall	wall temp.	T/C	2
below cold leg level	liquid level	DP cell	1
above cold leg level	liquid level	DP cell	1
below core inlet level	liquid level	DP cell	1
bottom	momentum flux	Drag disk	2
			sum(19)
5. HOT LEG			
full length	diff. press.	DP cell	1
multiple points	fluid temp.	T/C	3
	steam temp.	SSP	3
	wall temp.	T/C	1
	liquid level	DP cell	2
			sum(10)

Table A-2 Measurement Items of SCTF (JAERI-provided instruments)

(Continued)

LOCATION	ITEM	PROBE	QUANTITY
6. S/W SEPARATOR SIDE BROKEN COLD LEG			
across resistance simulator	diff. press.	DP cell	1
S/W separator to containment tank II	flow rate	venturi	1
multiple points	fluid temp.	T/C	1
	steam temp.	SSP	1
	wall temp.	T/C	1
			sum(5)
7. INTACT COLD LEG			
full length	diff. press.	DP cell	1
across resistance simulator	diff. press.	DP cell	1
across pump simulator	diff. press.	DP cell	1
	flow rate	venturi	1
near resistance simulator	fluid temp.	T/C	1
pump simulator	fluid temp.	T/C	3
	wall temp.	T/C	1
			sum(9)
8. PV SIDE BROKEN COLD-LEG	pressure	DP cell	1
full length	diff. press.	DP cell	1
across resistance simulator	diff. press.	DP cell	1
multiple points	fluid temp.	T/C	4
	wall temp.	T/C	2
	liquid level	DP cell	2
			sum(11)
9. VENT LINE			
across the length	diff. pres.	DP cell	1
			sum(1)

Table A-2 Measurement Items of SCTF (JAERI-provided instruments)
(Continued)

LOCATION	ITEM	PROBE	QUANTITY
10. S/W SEPARATOR			
	pressure	DP cell	1
between inlet and outlet	diff. press.	DP cell	1
SG plenum simulator	diff. press.	DP cell	1
SG plenum simulator	fluid temp.	T/C	2
top and bottom	fluid temp.	T/C	2
wall	wall temp.	T/C	2
full height	liquid level	DP cell	1
liquid extraction	flow rate	DP cell	1
			sum(11)
11. CONTAINMENT TANK-I			
	pressure	DP cell	1
downcomer-CT-I	diff. press.	DP cell	1
CT-I - CT-II	diff. press.	DP cell	1
	flow rate	DP cell	1
full height	liquid level	DP cell	1
		float	1
top, middle & bottom	fluid temp.	T/C	3
wall	wall temp.	T/C	1
			sum(10)
12. CONTAINMENT TANK-II			
	pressure	DP cell	1
upper plenum - CT-II	diff. press.	DP cell	1
separator - CT-II	diff. press.	DP cell	1
steam blow line	flow rate	DP cell	1
full height	liquid level	DP cell	1
top, middle & bottom	fluid temp.	T/C	3
			sum(8)
13. ECC INJECTION SYSTEM			
ACC tank	pressure	DP cell	1
total and LPCI	flow rate	E-M flow meter	2
			1
ACC tank	fluid temp.	T/C	1

Table A-2 Measurement Items of SCTF (JAERI-provided instruments)
(Continued)

LOCATION	ITEM	PROBE	QUANTITY
13. ECC INJECTION SYSTEM			
header	fluid temp.	T/C	2
ACC tank	liquid level	DP cell	1
			sum(8)
14. UCSP WATER EXTRACTION SYSTEM			
extraction line	flow rate	E-M flow meter	4
steam line	flow rate	DP cell	4
extraction line	fluid temp.	T/C	5
steam line	fluid temp.	T/C	1
extraction line	liquid level	DP cell	4
			sum(18)
15. SATURATED WATER TANK			
	fluid temp	T/C	1
	liquid level	DP cell	1
			sum(2)
16. NITROGEN GAS SYSTEM			
	flow rate	DP cell	1
injection port	fluid temp.	T/C	1
			sum(2)

Total 1267

Table A-3 Measurement Items of SCTF (USNRC-provided instruments)

LOCATION	ITEM	PROBE	QUANTITY
1. CORE			
non-heated rods	liquid level	LLD	20×4 = 80
non-heated rods	film thickness and velocity	film probe	6
non-heated rods	void fraction and droplet velocity	flag probe	8
side walls	film thickness and velocity	film probe	8
sub-channel	fluid density	γ-densitometer	10
end box	fluid density	γ-densitometer	5
end box	flow pattern	video optical probe	1
2. UPPER PLENUM			
full height	liquid level	FDG	8×8 = 64
structure surface	film thickness and velocity	film probe	6
side walls	film thickness and velocity	film probe	6
inter structure	void fraction	prong probe	8
above UCSP hole	velocity	turbine	8
inter structure	velocity	turbine	4
inter structure	fluid density	γ-densitometer	4
hot leg inlet	flow pattern	video optical probe	1
3. LOWER PLENUM			
core inlet	velocity	turbine	4
bottom	reference conductivity	reference probe	1
4. DOWNCOMER			
full height	liquid level	FDG	2×3×7 = 42
two levels	velocity	drag disk	3
two levels	void fraction	string probe	3

Table A-3 Measurement Items of SCTF (USNRC-provided instruments)

(Continued)

LOCATION	ITEM	PROBE	QUANTITY
5. HOT LEG	mass flow rate fluid density void fraction	spool piece	1
6. PV SIDE BROKEN COLD-LEG	mass flow rate fluid density void fraction	spool piece	1
7. VENT LINE	mass flow rate void fraction	spool piece	1

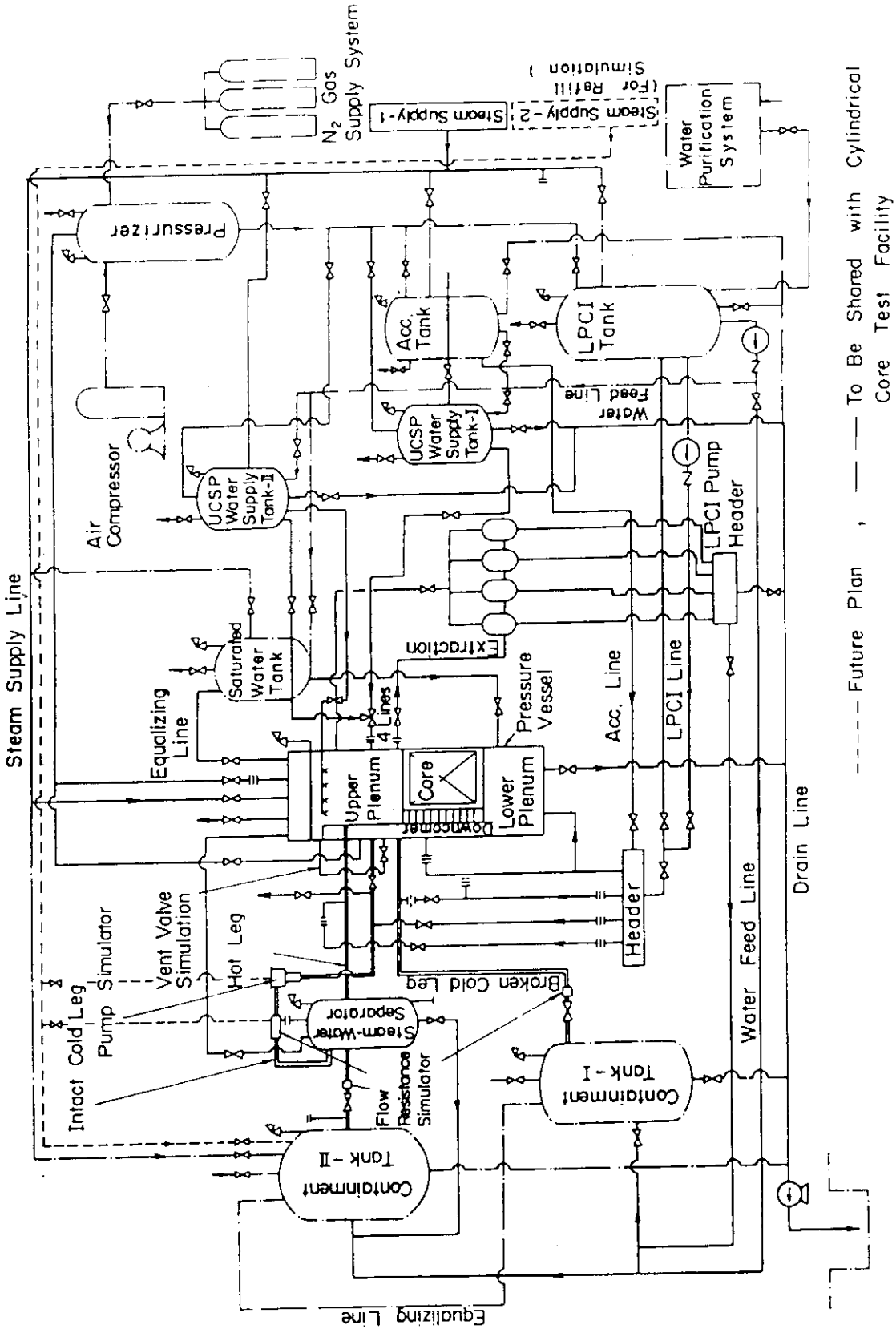

Fig. A-1 Schematic Diagram of Slab Core Test Facility

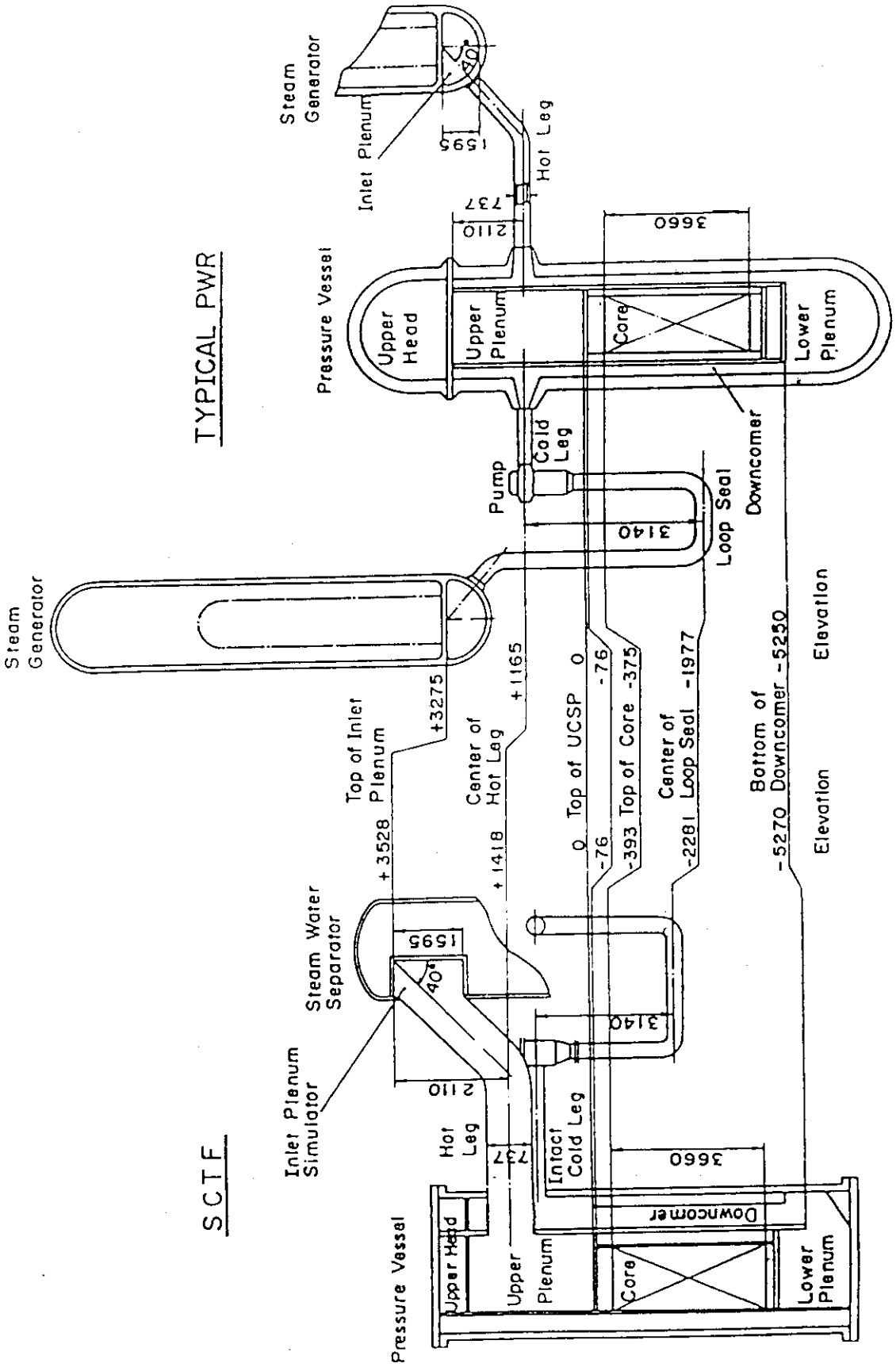

Fig. A-2 Comparison of Dimensions between SCTF and a Reference PWR

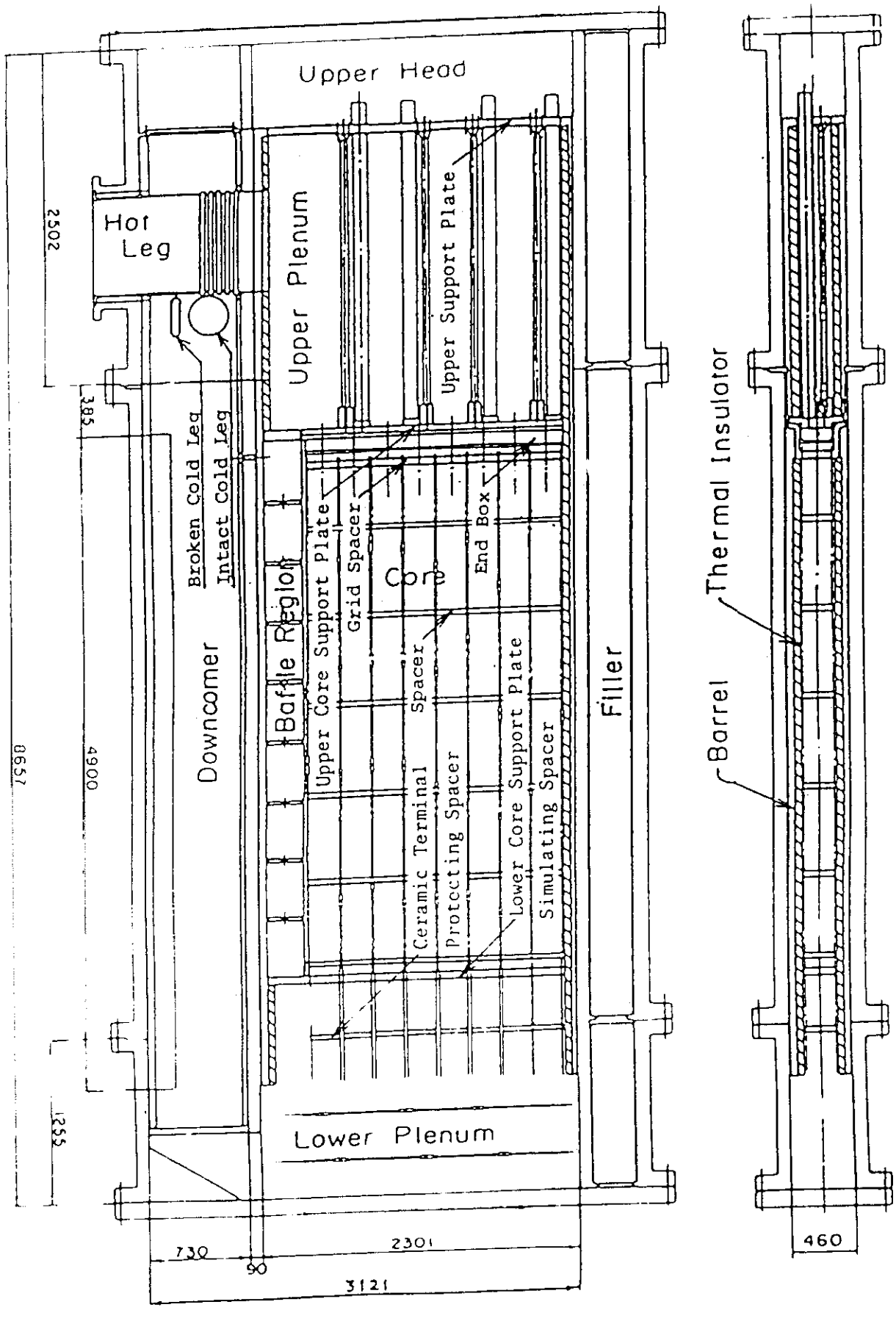

Fig. A-3 Vertical Cross Section of the Pressure Vessel

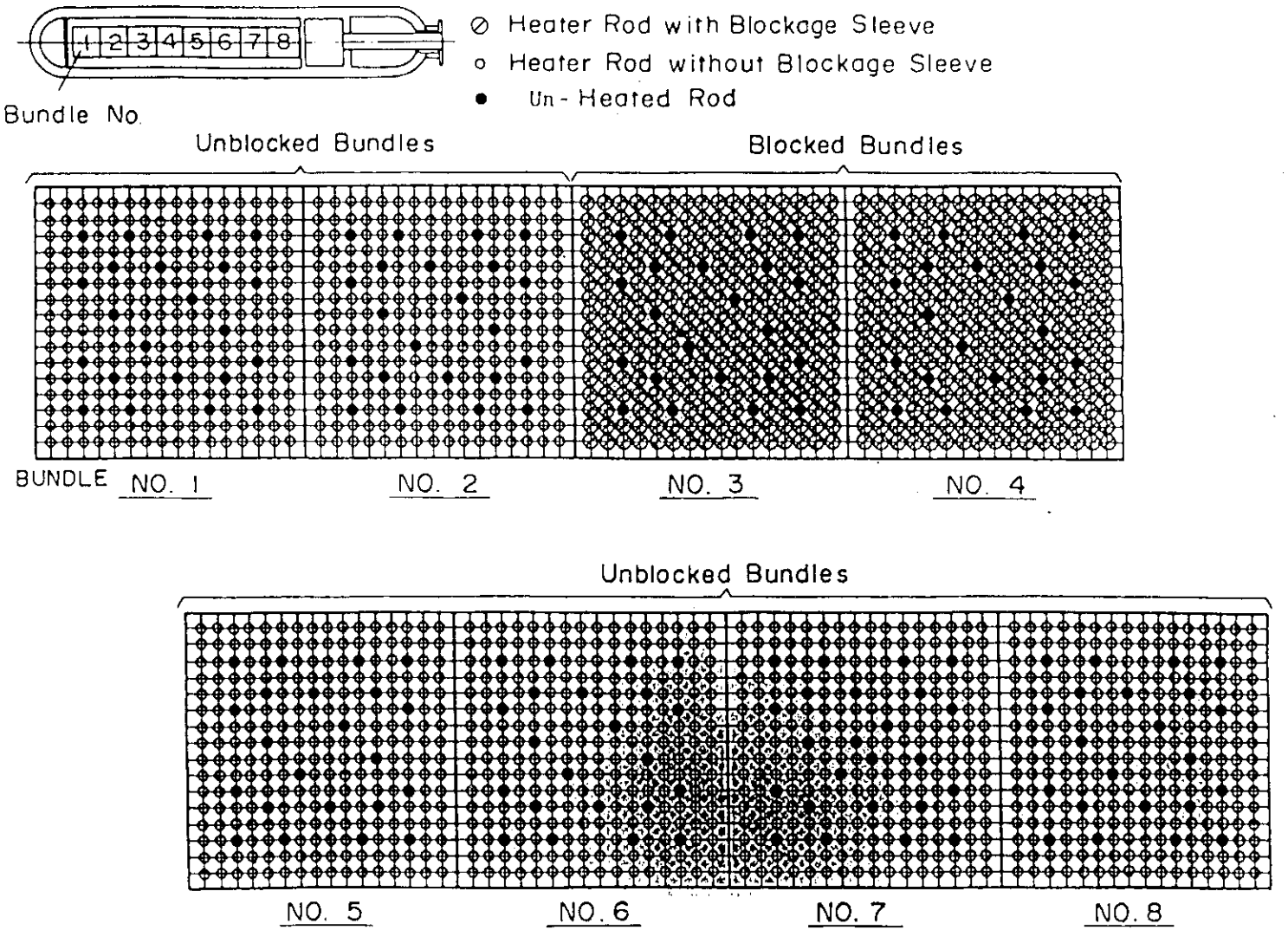

Fig. A-4 Arrangement of Heater Bundles

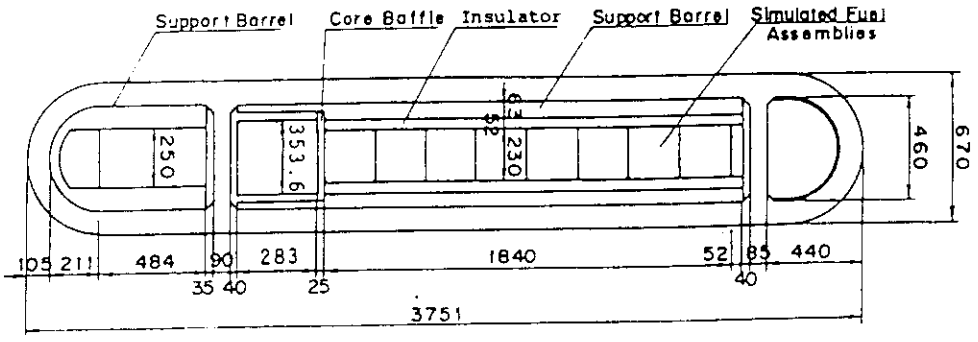

Fig. A-5 Horizontal Cross Section of the Pressure Vessel (1)

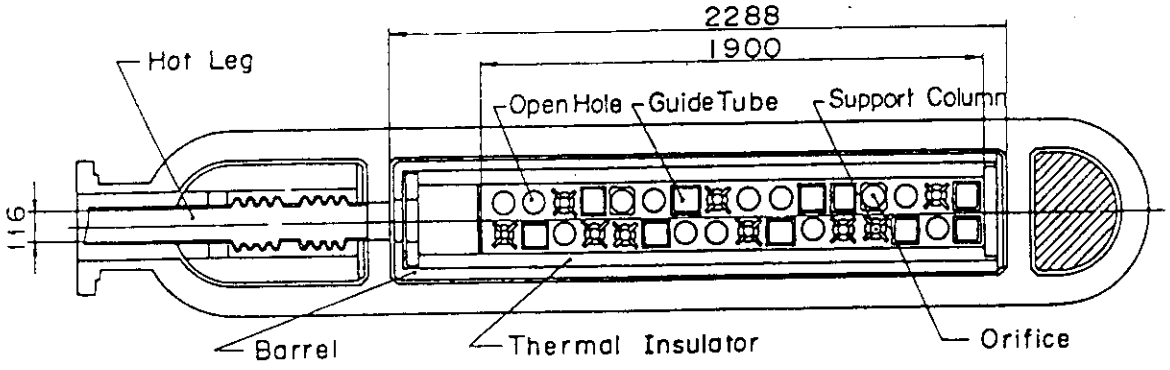

Fig. A-6 Horizontal Cross Section of the Pressure Vessel (2)

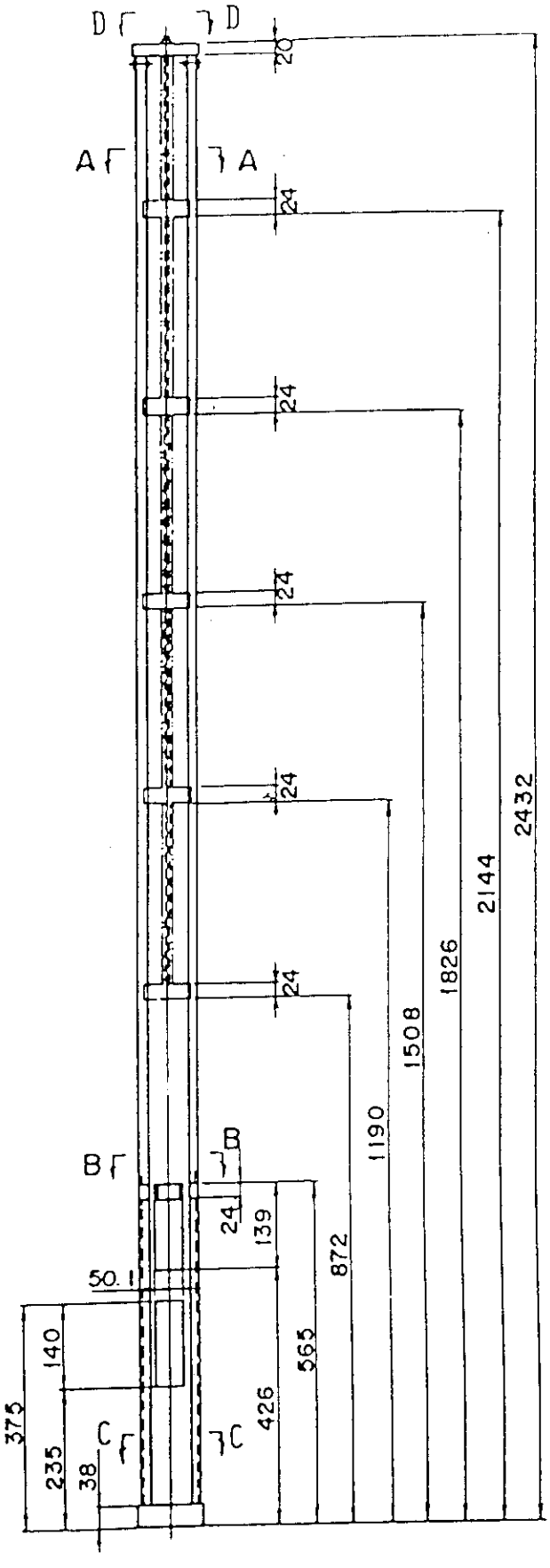

Fig. A-7 Dimension of Guide Tube (1)

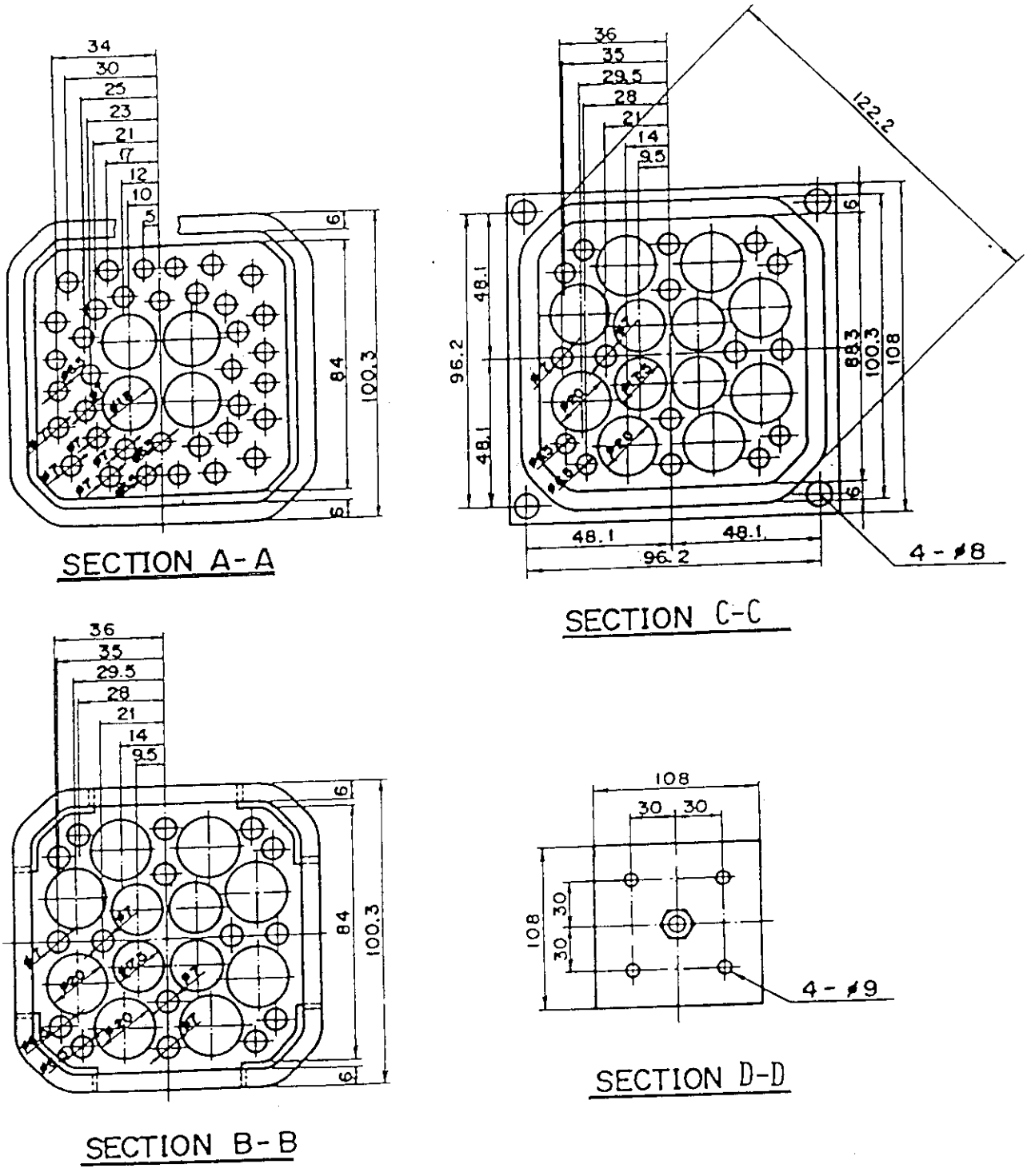

Fig. A-8 Dimension of Guide Tube (2)

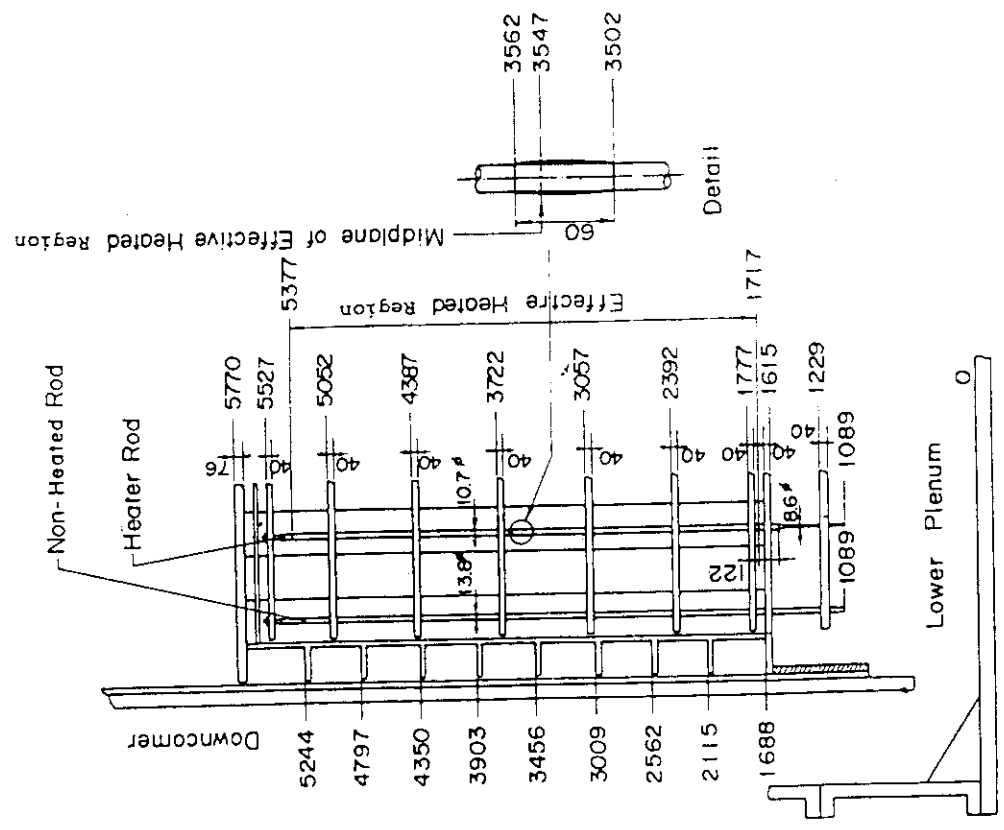

Fig. A-10 Relative Elevation and Dimension of the Core in SCTF

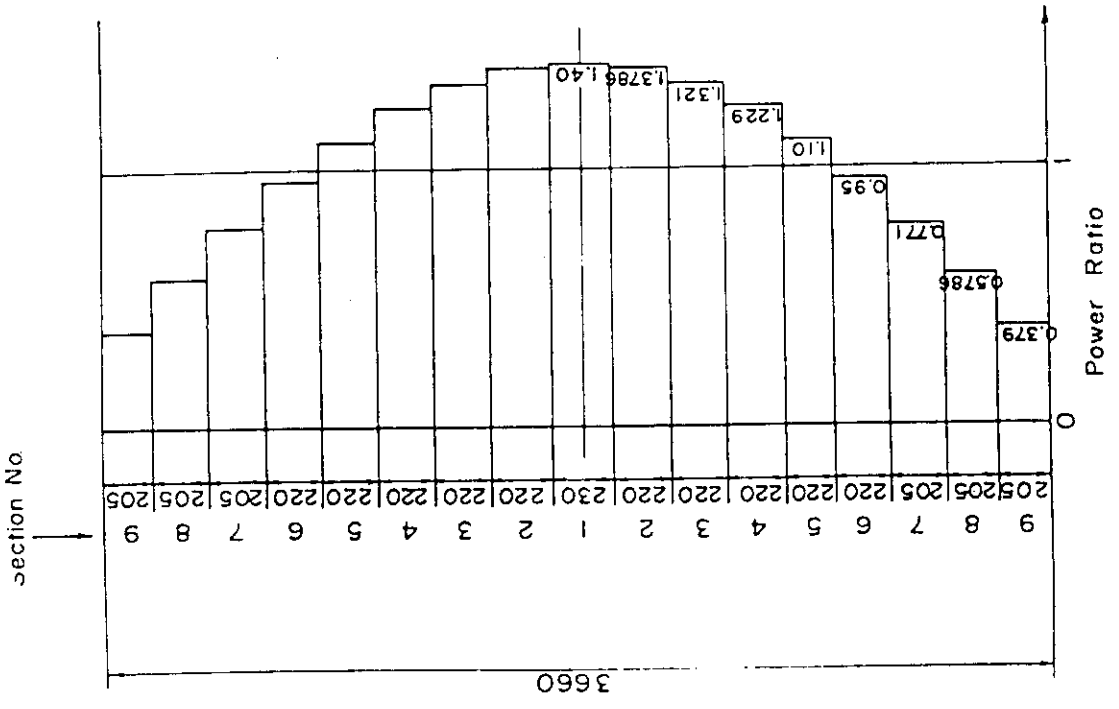

Fig. A-9 Axial Power Distribution of Heater Rod

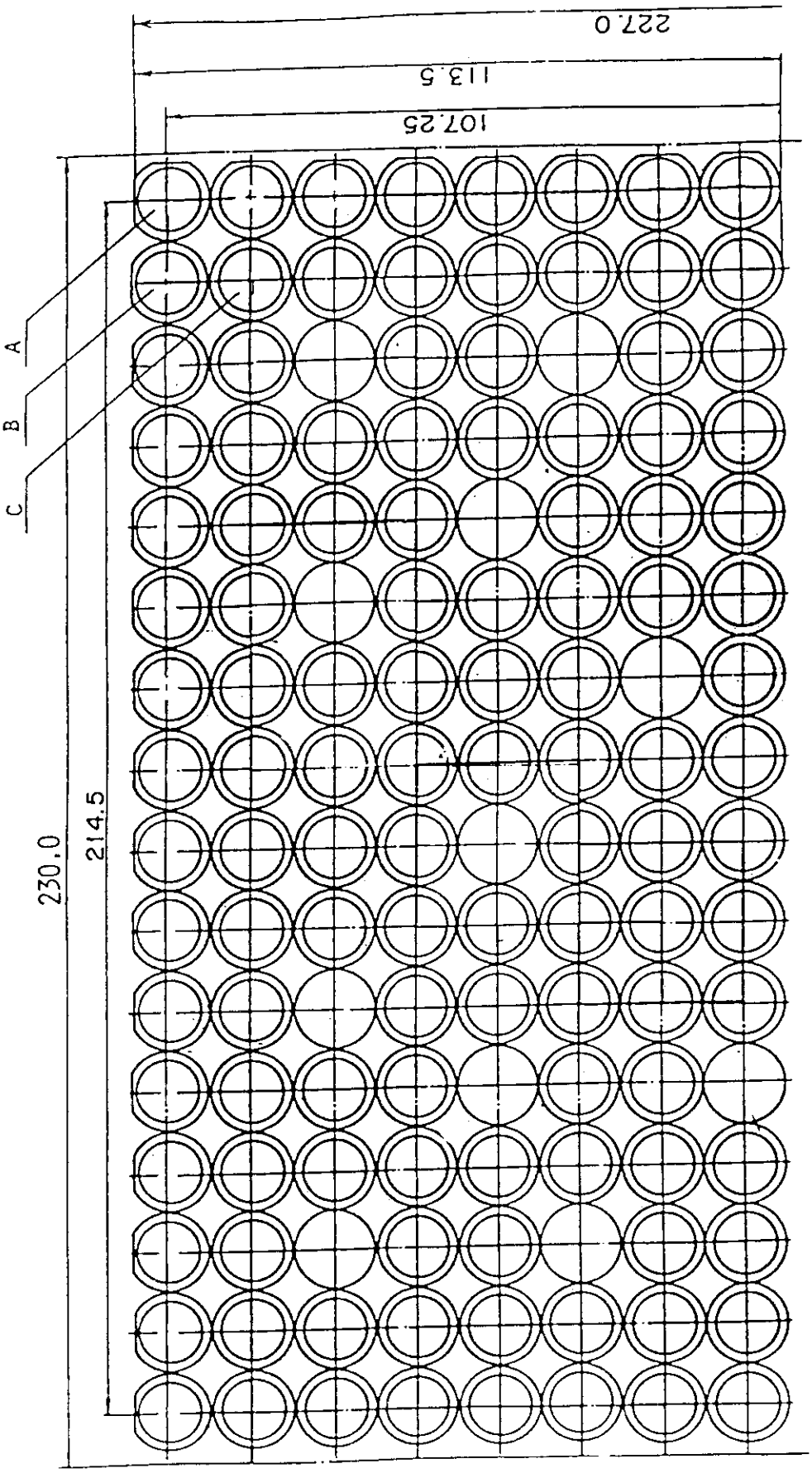

Fig. A-11 Arrangement of the Heater Rods with Three Kinds of Blockage Sleeve

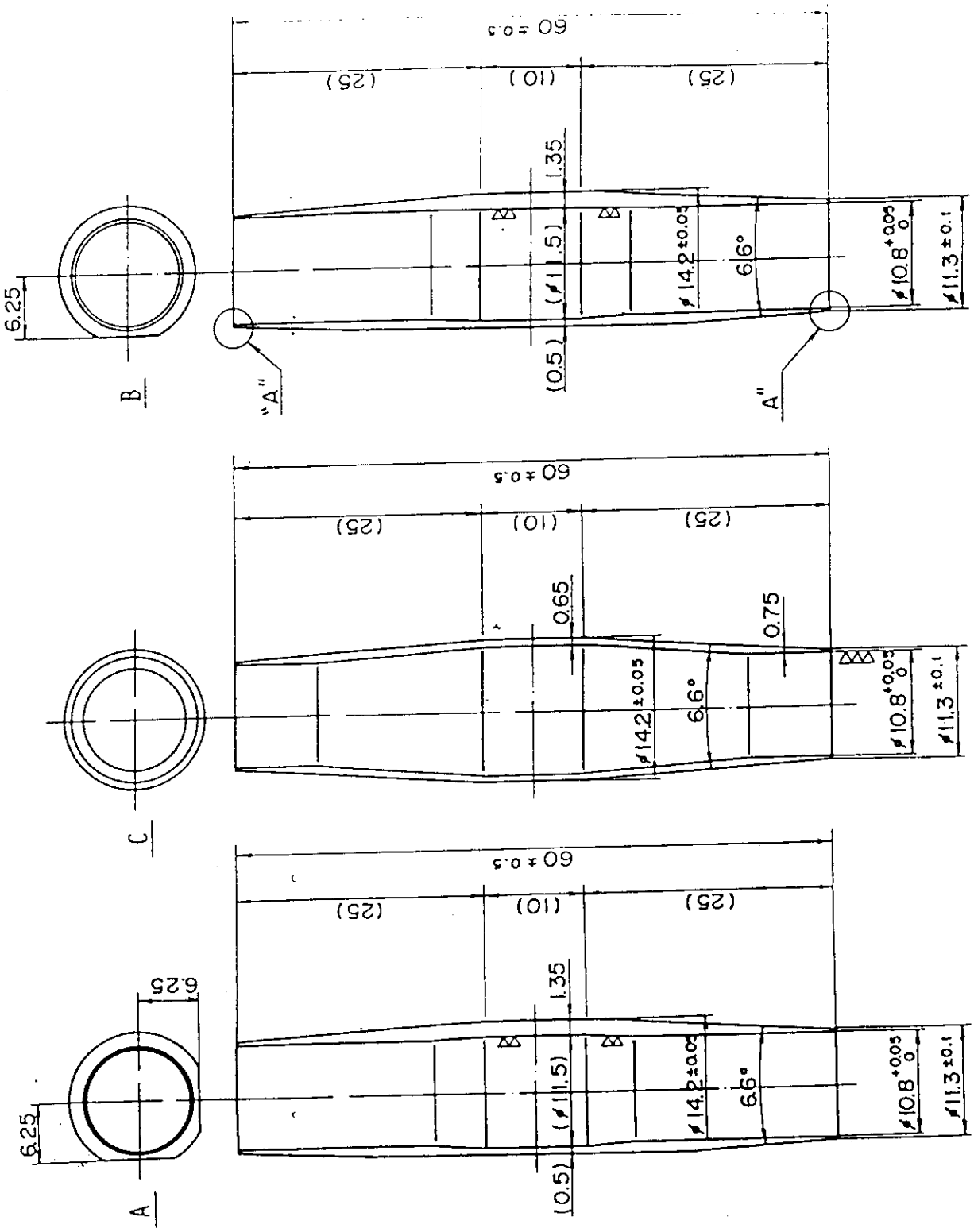

Fig. A-12 Configuration and Dimension of the Thre Blockage Sleeves

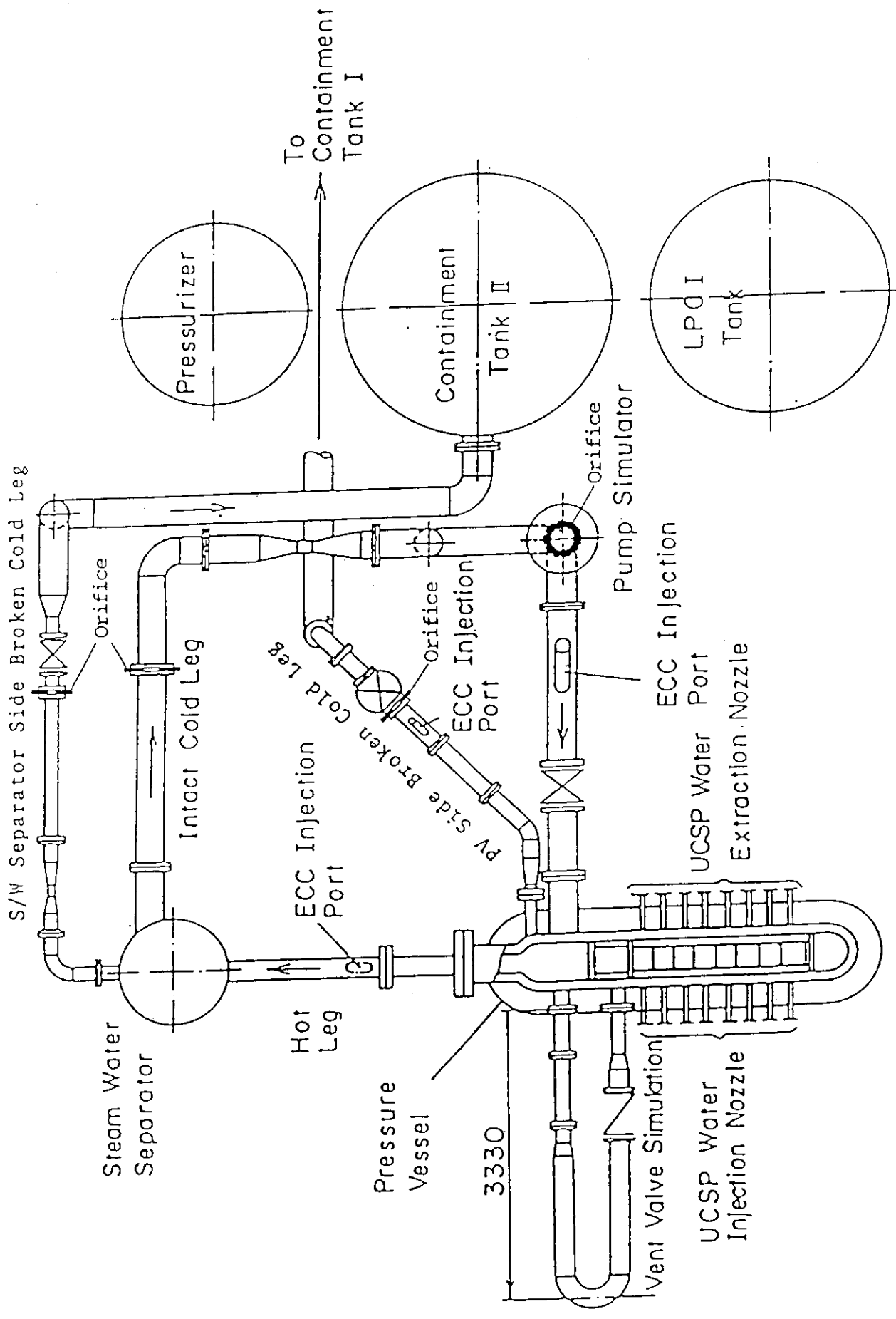

Fig. A-13 Overview of the Arrangements of the SCTF

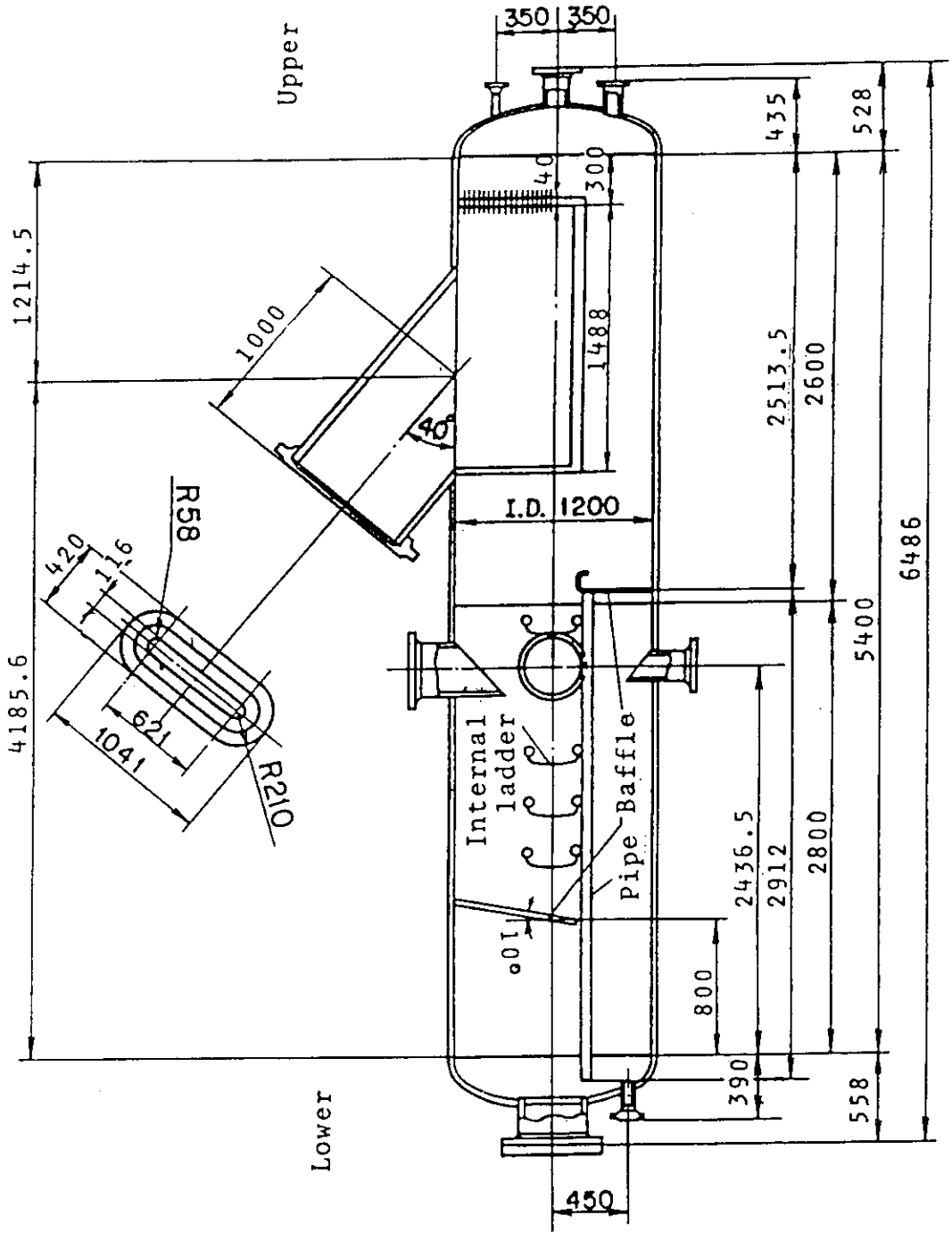

Fig. A-14 Steam Water Separator

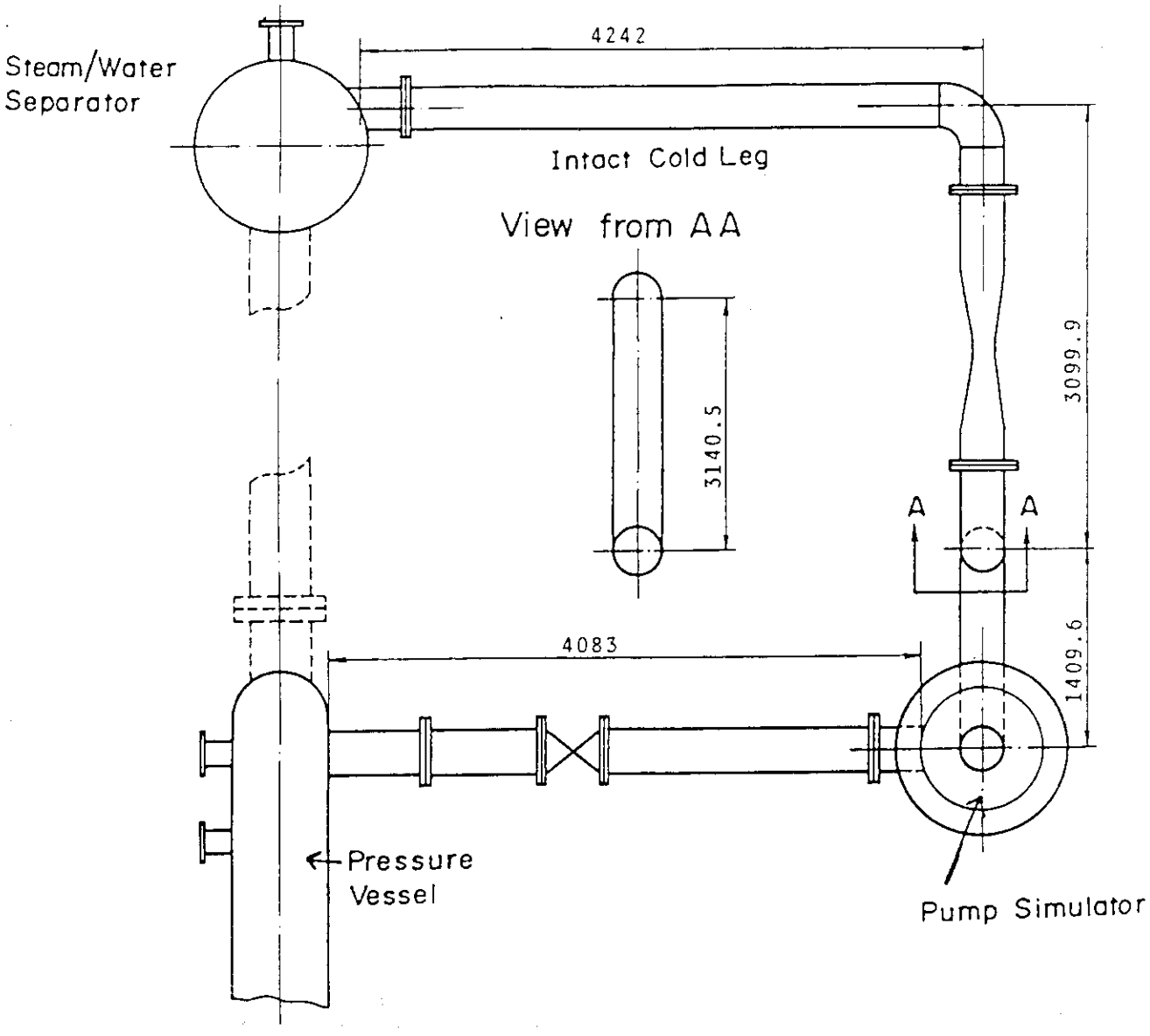

Fig. A-15 Arrangement of Intact Cold Leg

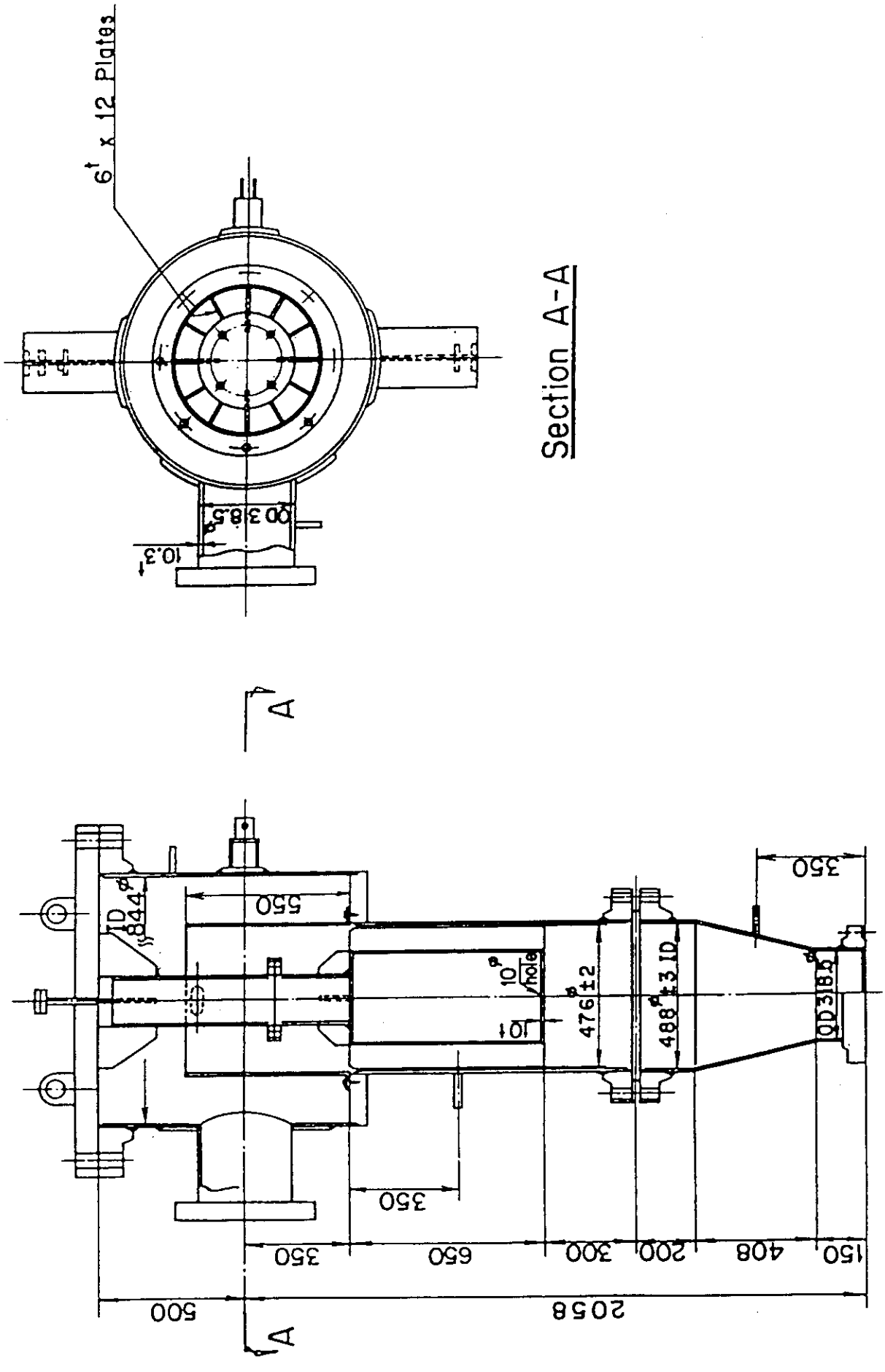

Fig. A-16 Configuration and Dimension of Pump Simulator

Appendix B
Selected Data from Test S1-SH2 (Run 506)

Note:

In Appendix B selected data from Test S1-SH2 are introduced. Each figure shows the following data.

* Figs. B-1(1) through B-8(2) :

Heater rod cladding temperatures are shown in these figures. B denotes "Test S1-SH2". Numbers 1 through 8 denote "Bundle Nos. 1 through 8", respectively. (1) denotes "bottom half core", on the other hand, (2) denotes "top half core".

Identification mark, thermocouple elevation number and measuring elevation based on the bottom of heated length for each curve are as follows:

○	T/C 1	110 mm	Bottom half core
△	T/C 2	520 mm	
+	T/C 3	950 mm	
×	T/C 4	1380 mm	
◇	T/C 5	1735 mm	
○	T/C 6	1905 mm	Top half core
△	T/C 7	2330 mm	
+	T/C 8	2760 mm	
×	T/C 9	3190 mm	
◇	T/C 10	3620 mm	

* Figs. B-9(1) and B-9(2) :

Differential pressures across the core full height are shown in these figures.

Identification mark and measuring bundle for each curve are as follows :

- ○ Bundles 1 and 5
- △ Bundles 2 and 6
- + Bundles 3 and 7
- × Bundles 4 and 8

* Figs. B-10 and 11 :

Horizontal differential pressures in the core are shown in these figures. Fig. B-10 gives the differential pressures between Bundles 5 and 8 and Fig. 8-11 gives those between Bundles 1 and 8

Identification mark and measuring elevation based on the bottom

of heated length for each curve are as follows :

○ Below spacer 4 (1905 mm)

△ Below spacer 6 (3235 mm)

+ Below end box tie plate (3821 mm)

* Figs. B-12(1) and B-12(2) :

Differential pressures across end box tie plates are shown in these figures.

Identification mark and corresponding bundle for each curve are the same as Figs. B-9(1) and B-9(2).

* Figs. B-13(1) and B-13(2) :

Collapsed water levels in the end boxes are shown in these figures.

Identification mark and corresponding bundle for each curve are the same as Figs. B-9(1) and B-9(2).

* Figs. B-14(1) and B-14(2) :

Collapsed water levels above the UCSP are shown in these figures.

Identification mark and corresponding bundle for each curve are the same as Figs. B-9(1) and B-9(2). In addition, collapsed water level above the core baffle region is also shown in Fig. B-14(2), by using the following identification mark :

◇ Above core baffle region

* Fig. B-15 :

System pressures at the various locations are shown in this figure as follows :

○ Top of pressure vessel

△ Core center

+ Core inlet

× Upper part of downcomer

* Figs. B-16(1) and B-16(2)

Heating powers for each the bundle are shown in these figures.

Identification mark and measuring bundle for each curve are the same as Figs. B-9(1) and B-9(2).

* Fig. B-17 :

ECC water injection rate into the lower plenum is shown in this figure.

Identification mark is as follows:

○ Injection into lower plenum

* Figs. B-18 through B-21 :

Steam flow rates at the intact cold leg, steam-water separator side broken cold leg, between containment tanks-I and -II, and discharge line from containment-II are shown in these figures, respectively.

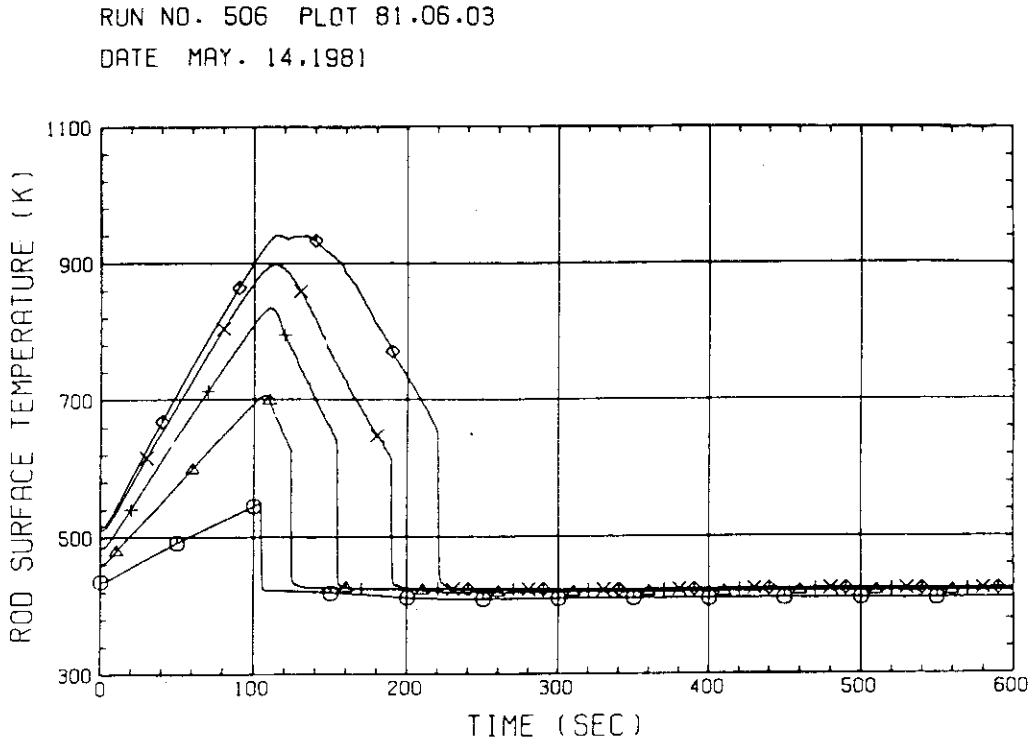

FIG. B-1(1) Heater Rod Temperatures (Lower Half of Bundle 1)

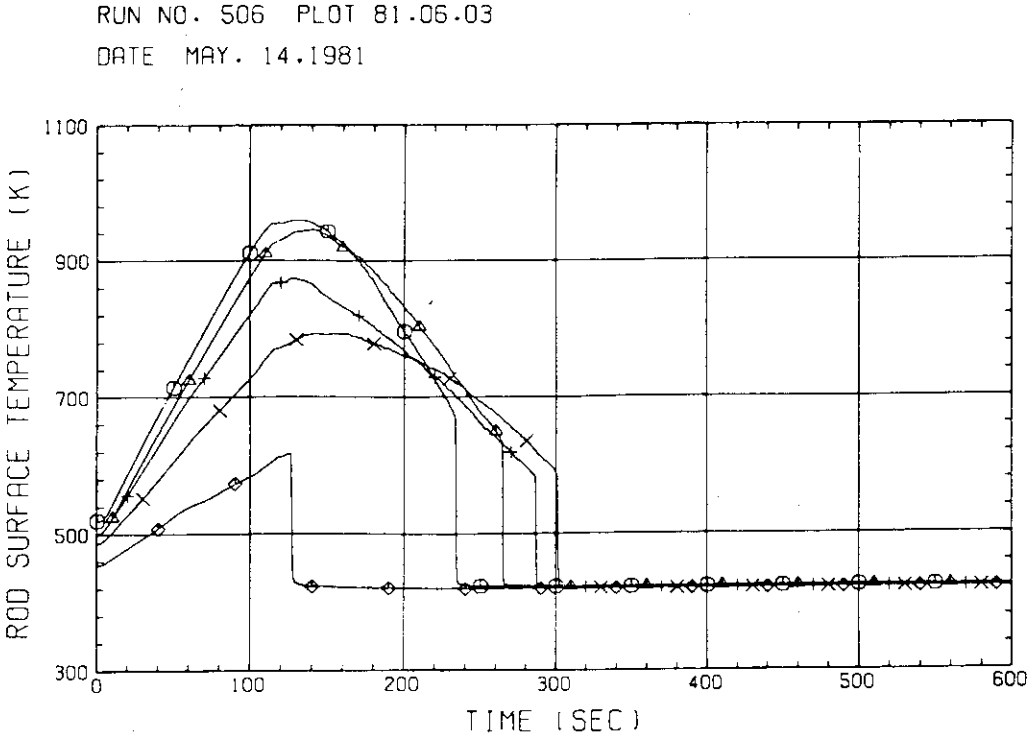

FIG. B-1(2) Heater Rod Temperatures (Upper Half of Bundle 1)

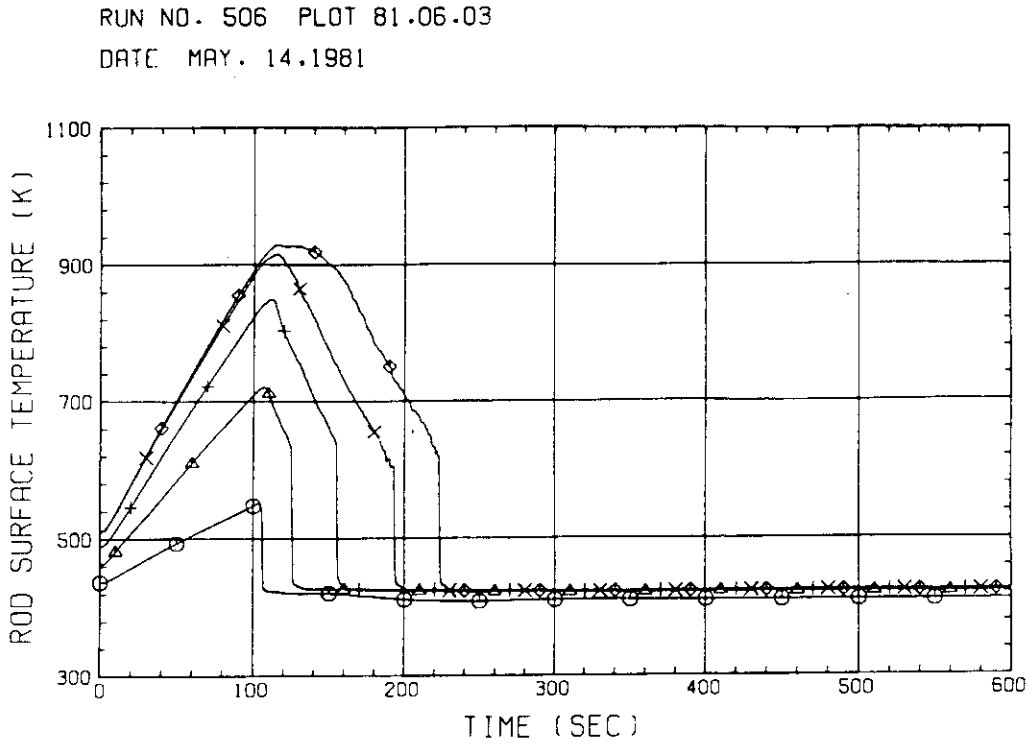

FIG. B-2(1) Heater Rod Temperatures (Lower Half of Bundle 2)

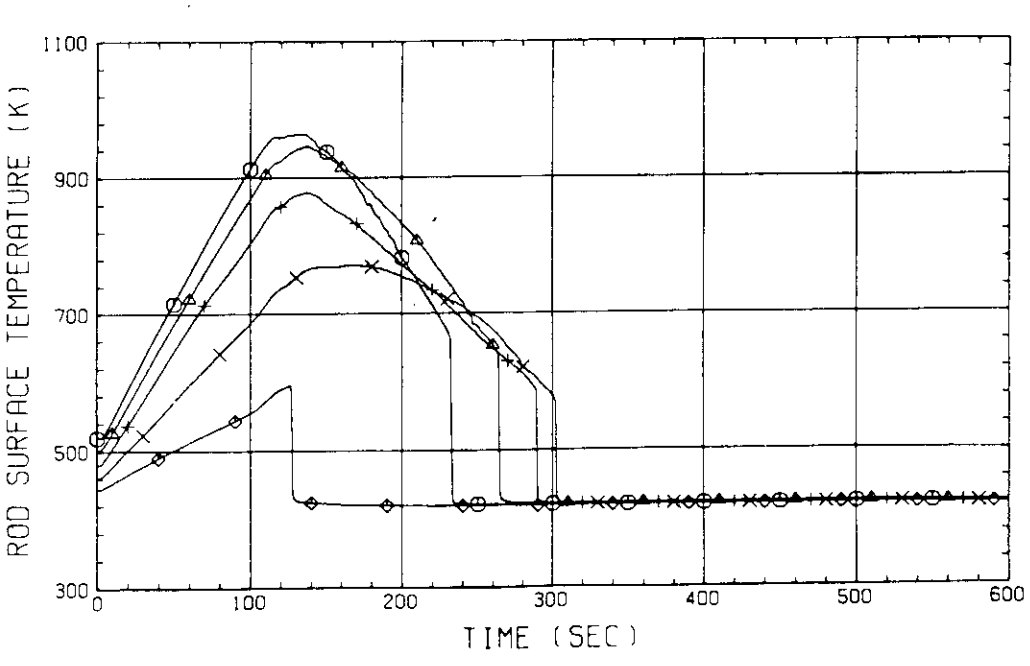

FIG. B-2(2) Heater Rod Temperatures (Upper Half of Bundle 2)

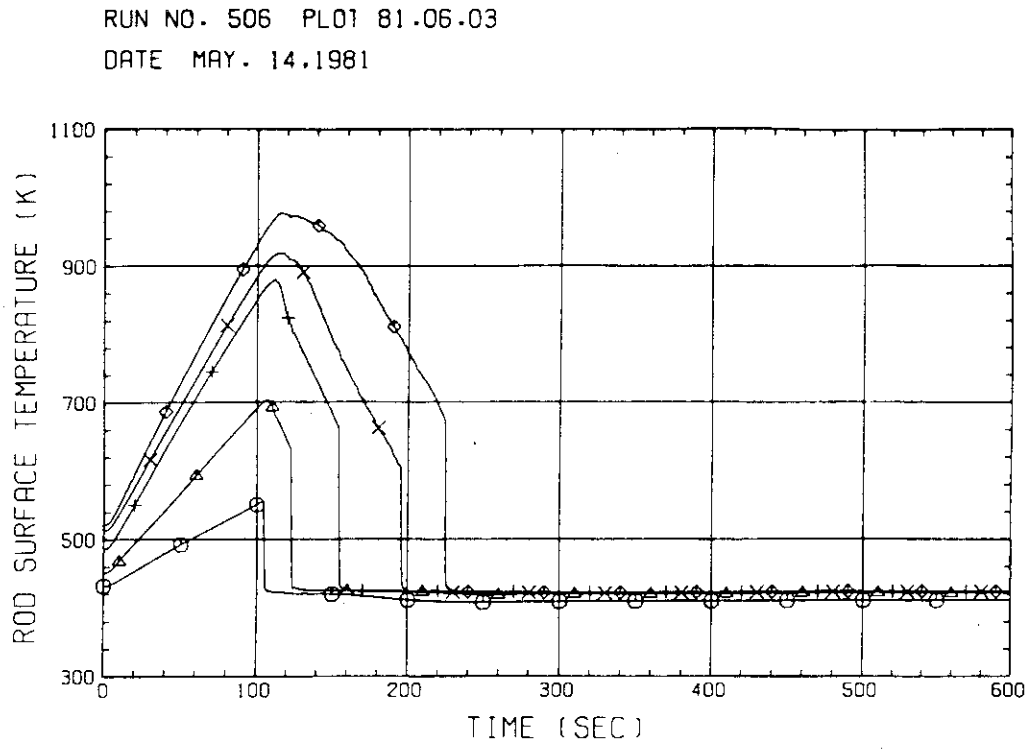

FIG. B-3(1) Heater Rod Temperatures (Lower Half of Bundle 3)

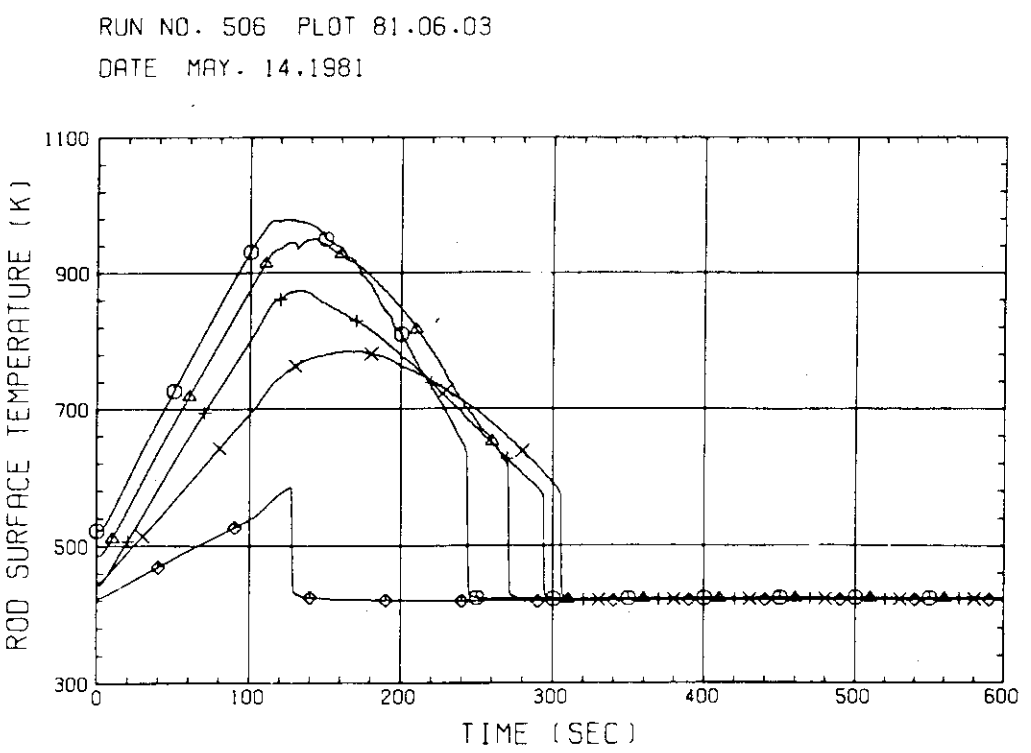

FIG. B-3(2) Heater Rod Temperatures (Upper Half of Bundle 3)

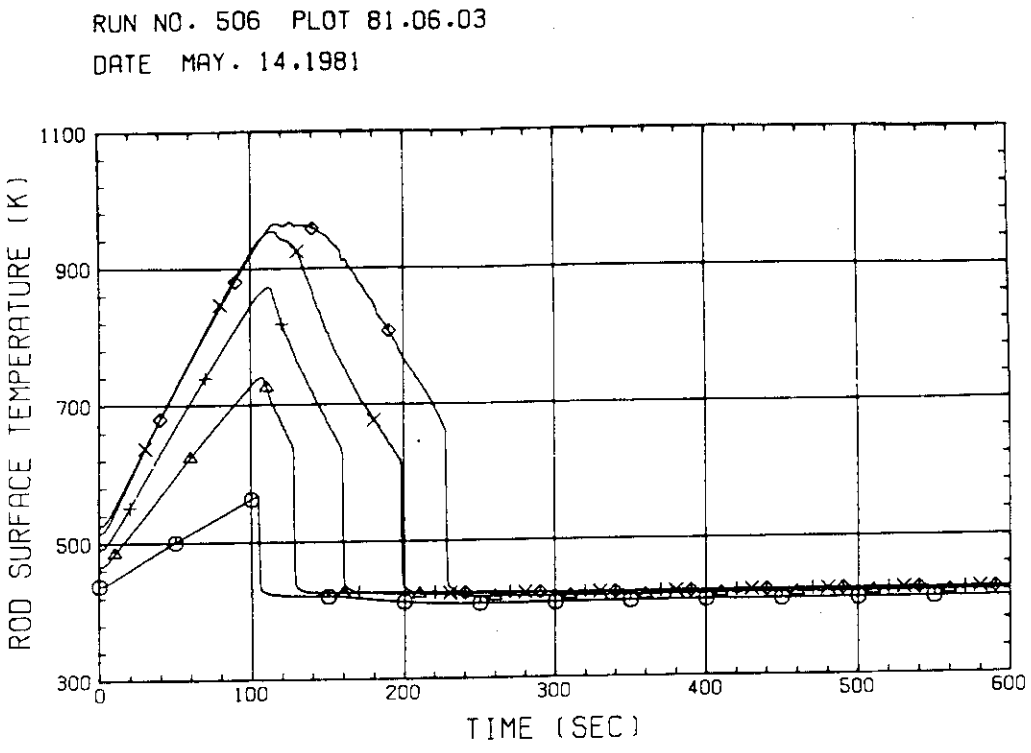

FIG. B-4(1) Heater Rod Temperatures (Lower Half of Bundle 4)

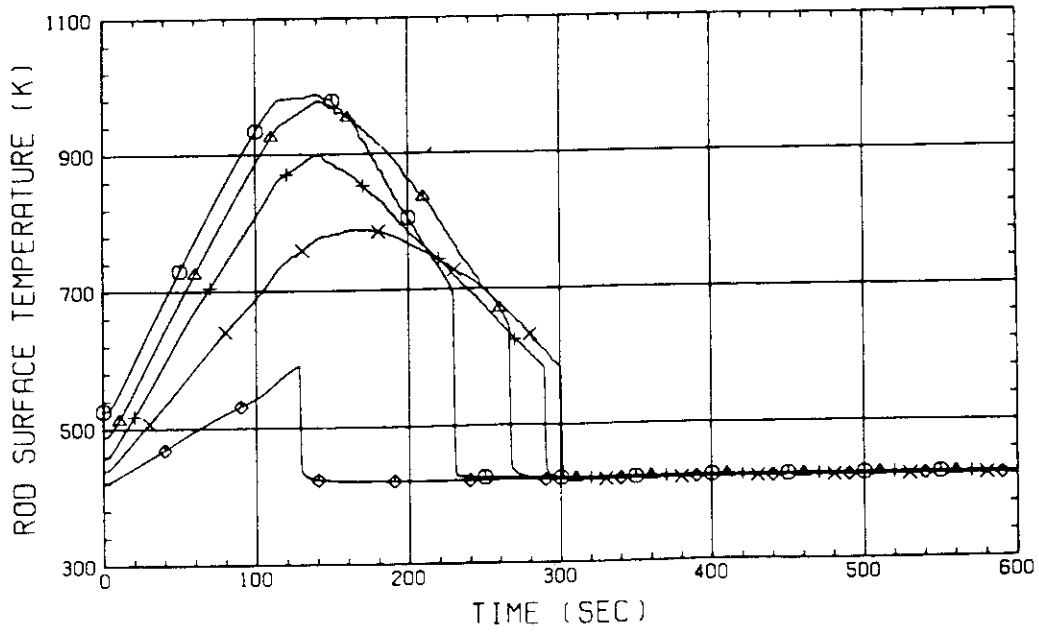

FIG. B-4(2) Heater Rod Temperatures (Upper Half of Bundle 4)

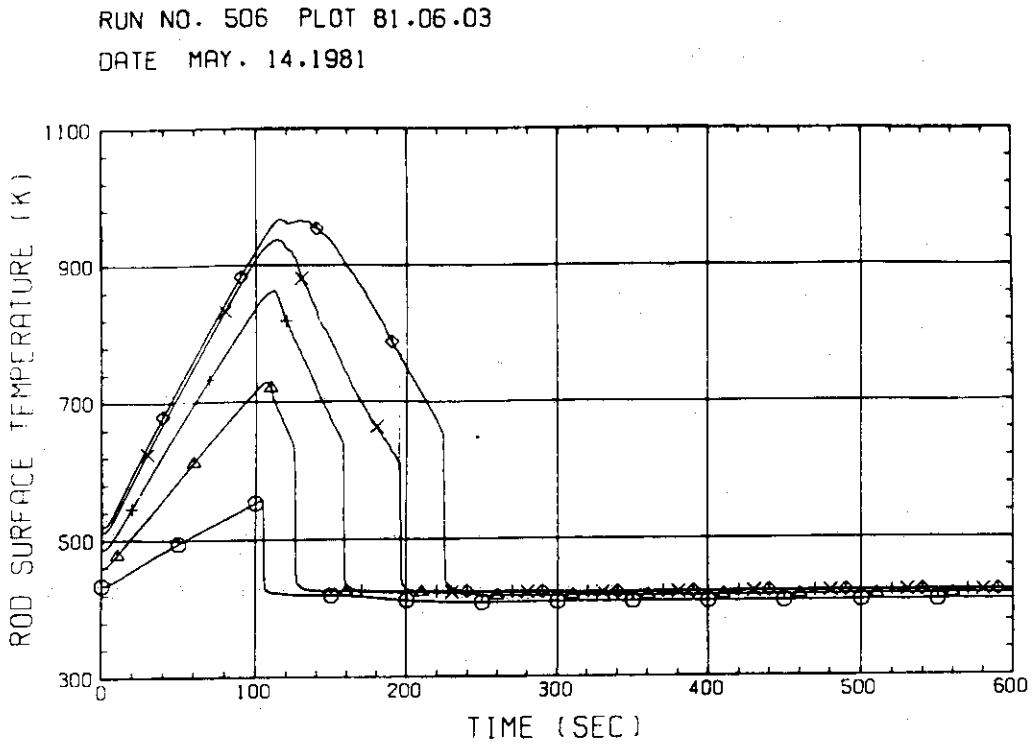

FIG. B-5(1) Heater Rod Temperatures (Lower Half of Bundle 5)

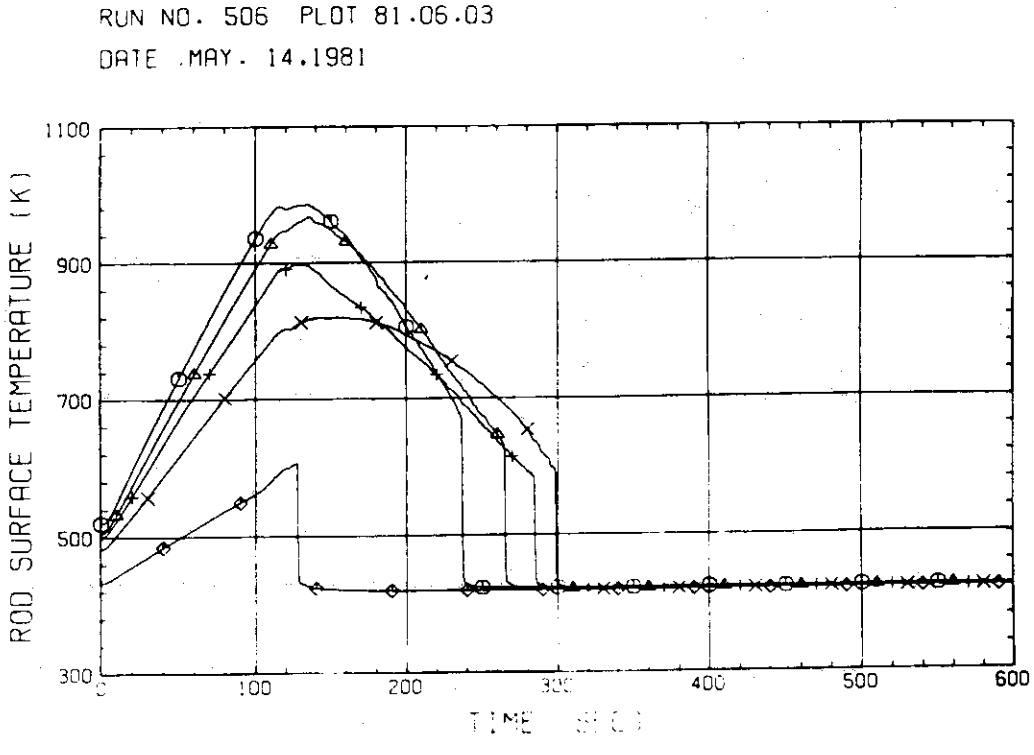

FIG. B-5(2) Heater Rod Temperatures (Upper Half of Bundle 5)

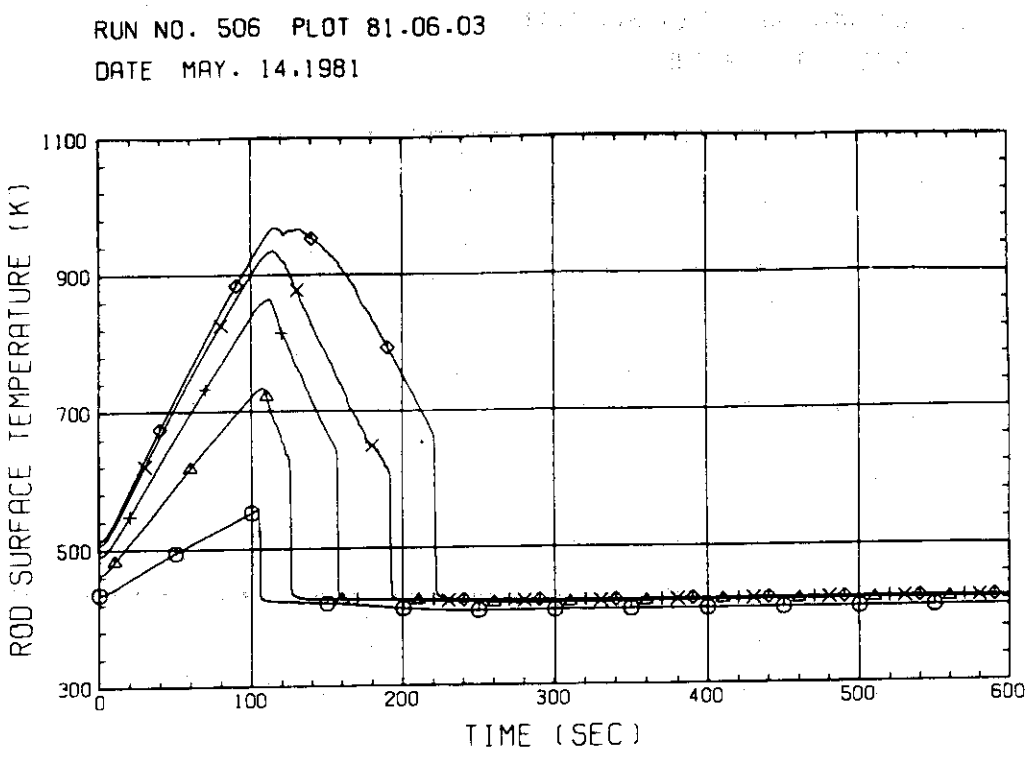

FIG. B-6(1) Heater Rod Temperatures (Lower Half of Bundle 6)

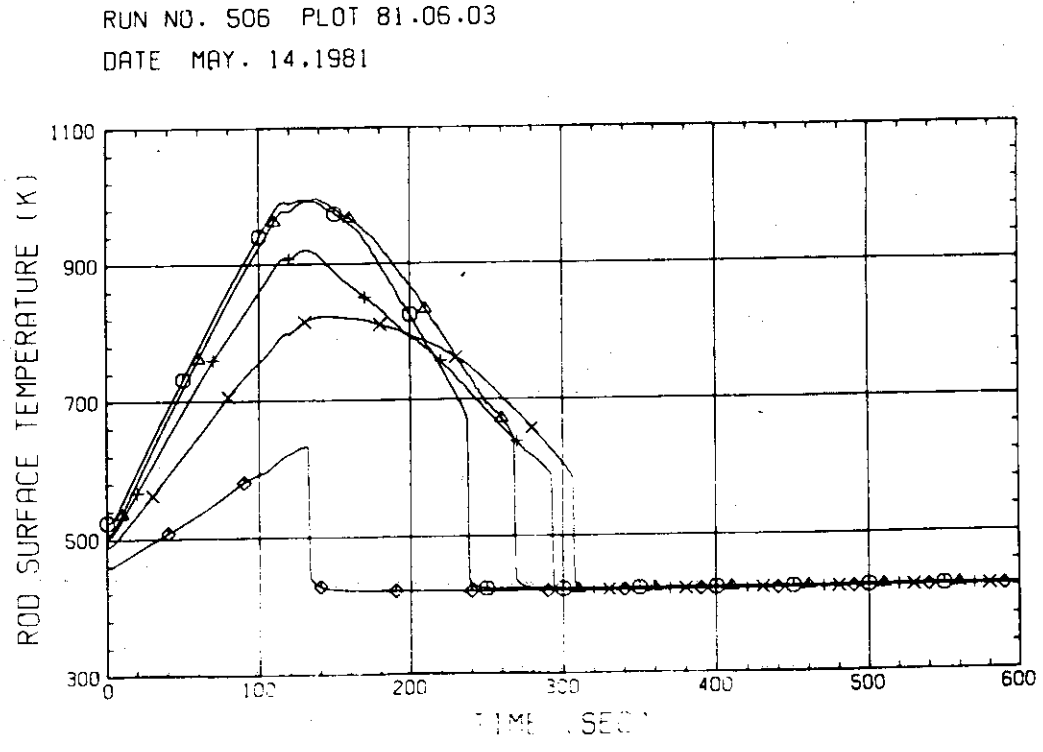

FIG. B-6(2) Heater Rod Temperatures (Upper Half of Bundle 6)

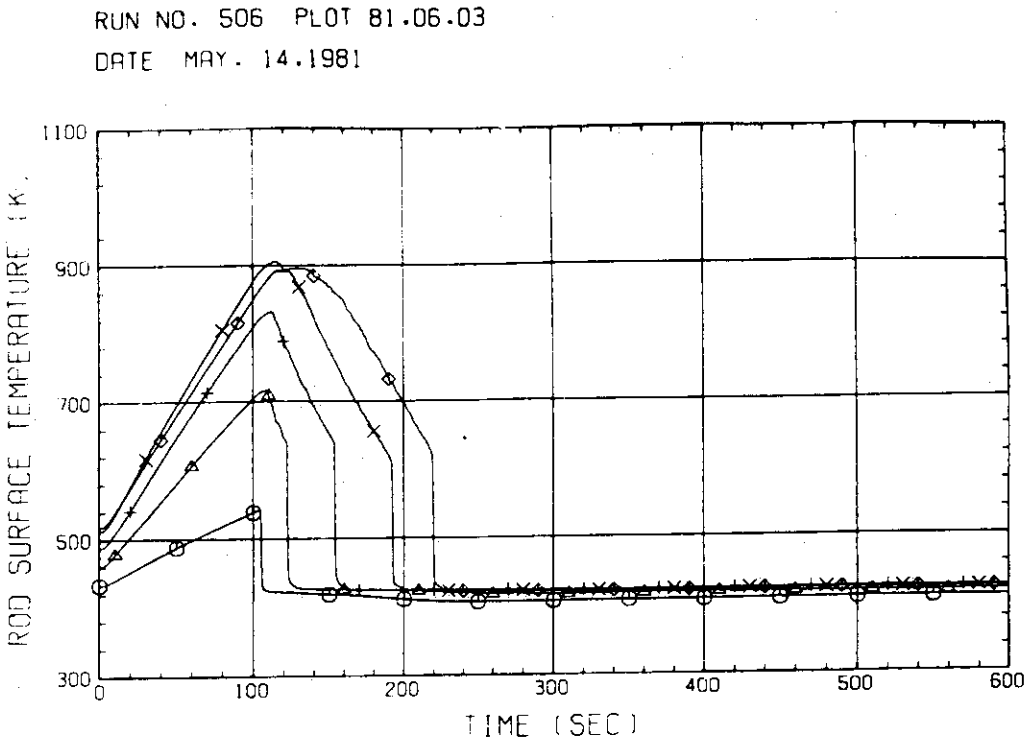

FIG. B-7(1) Heater Rod Temperatures (Lower Half of Bundle 7)

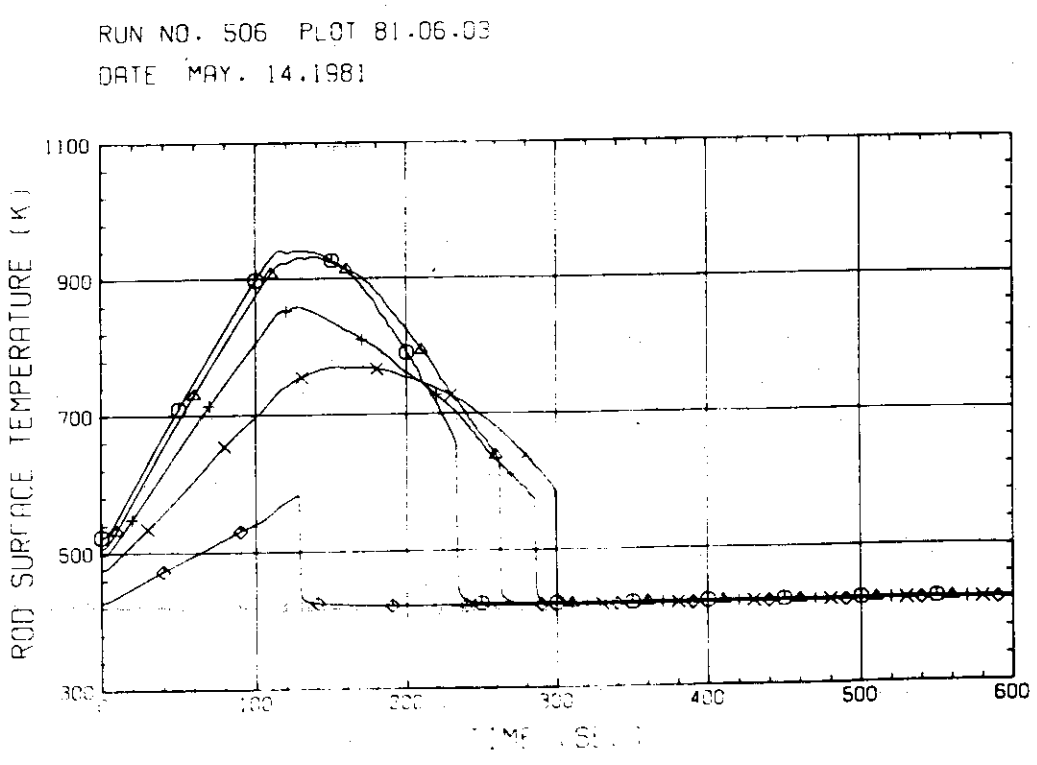

FIG. B-7(2) Heater Rod Temperatures (Upper Half of Bundle 7)

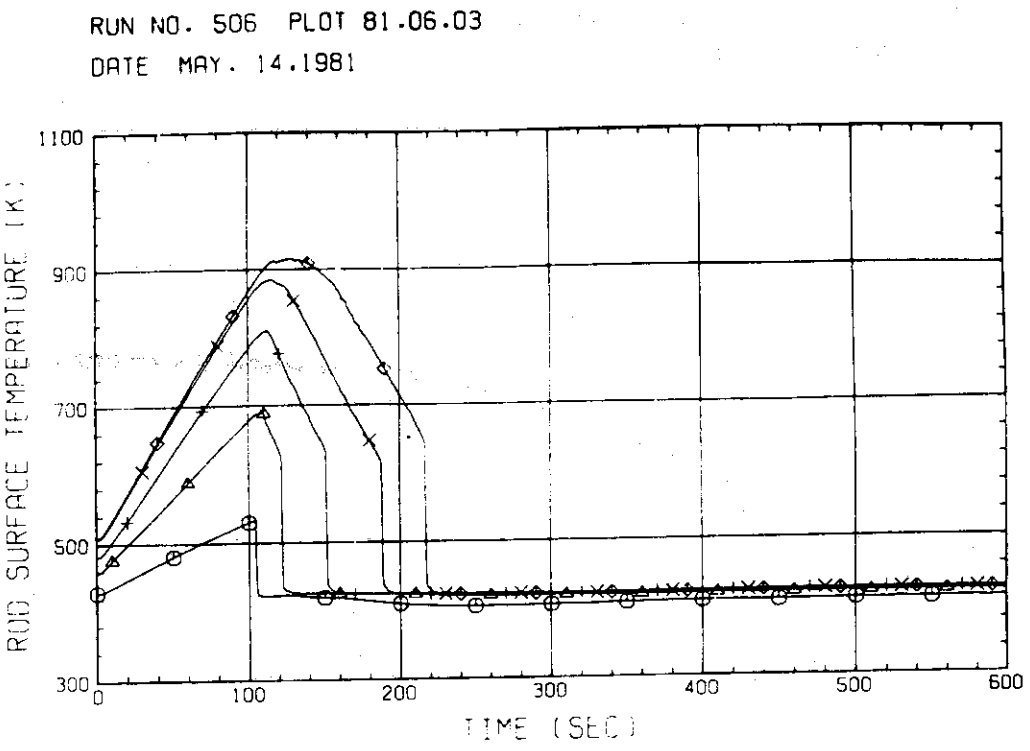

FIG. B-8(1) Heater Rod Temperatures (Lower Half of Bundle 8)

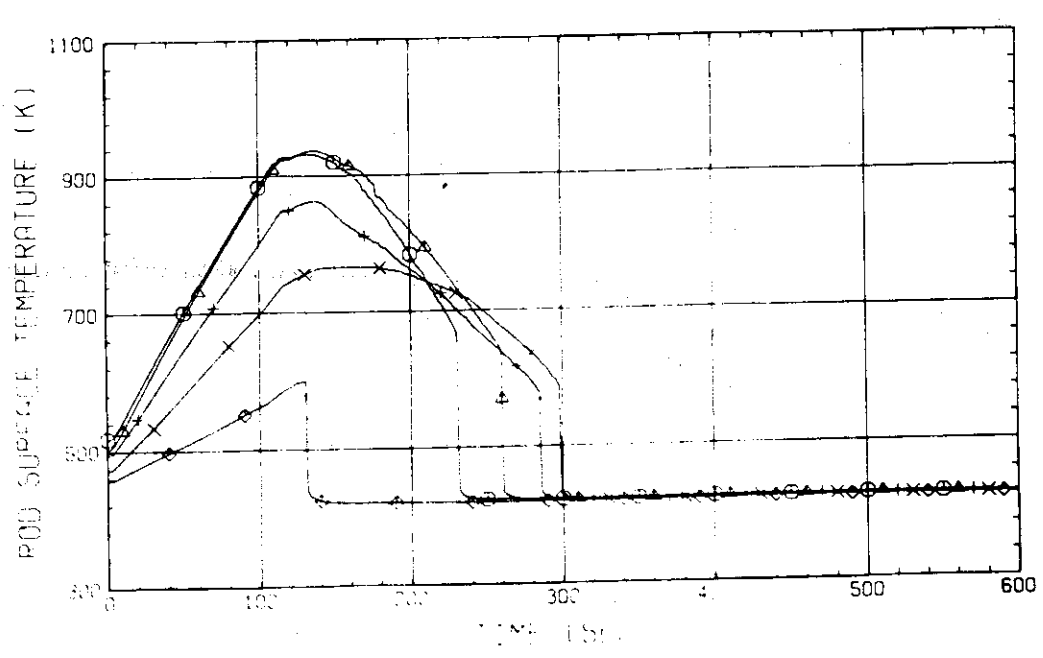

FIG. B-8(2) Heater Rod Temperatures (Upper Half of Bundle 8)

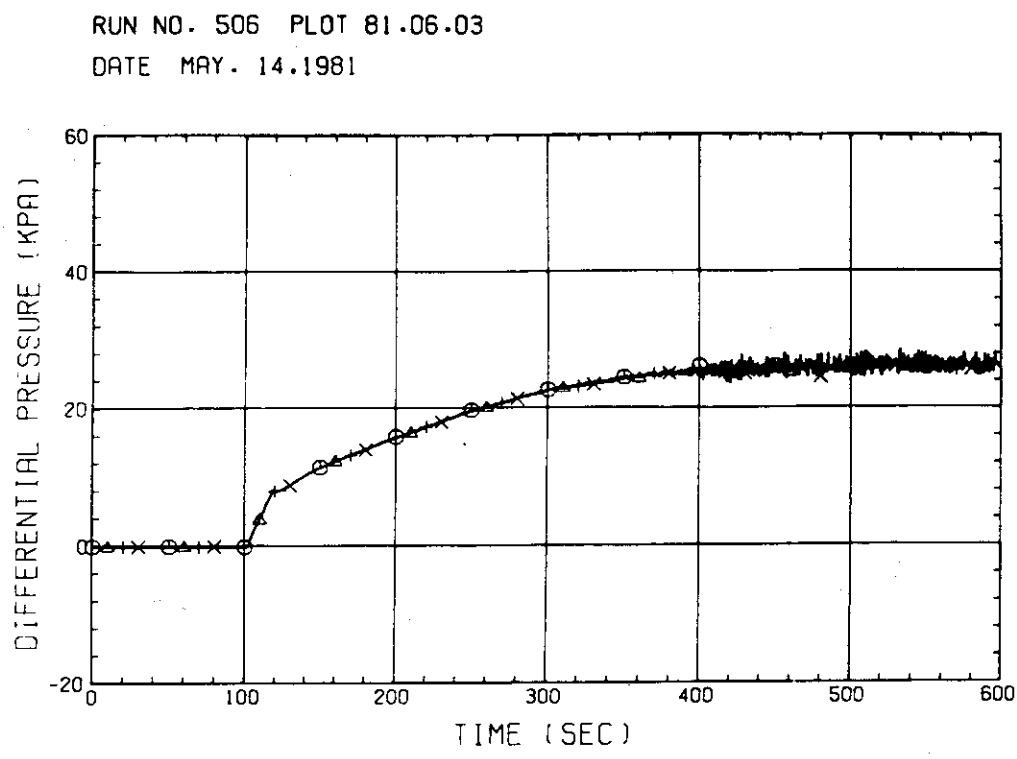

FIG. B-9(1) Differential Pressures across Core Full Height (Bundles 1 through 4)

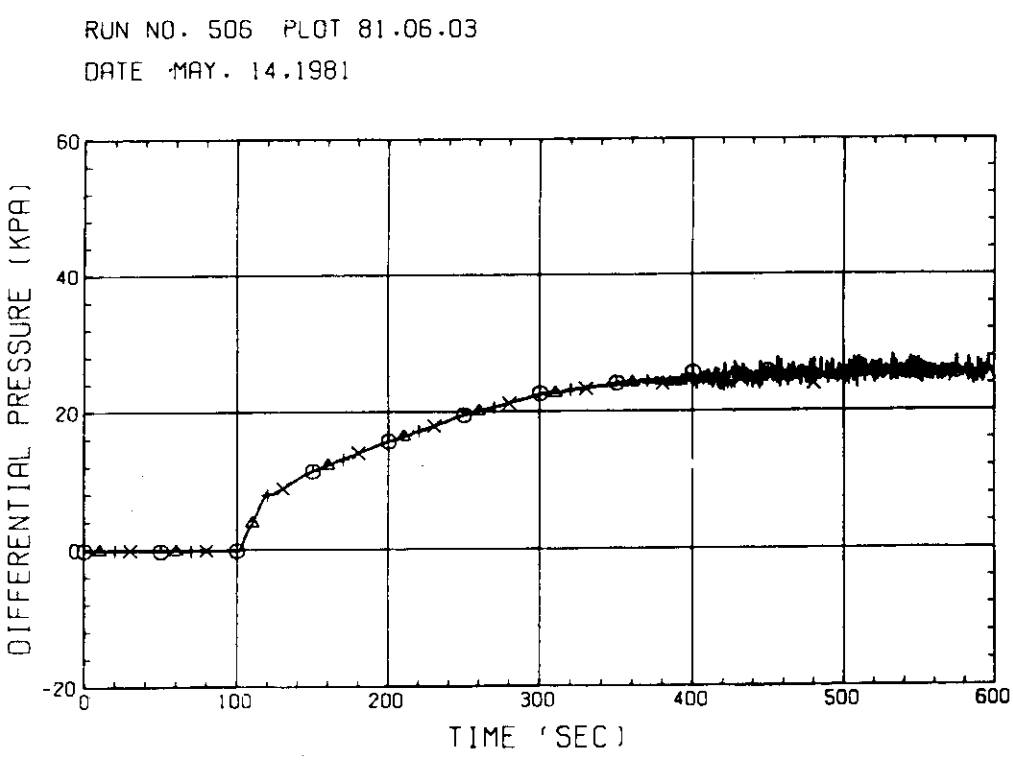

FIG. B-9(2) Differential Pressures across Core Full Height (Bundles 5 through 8)

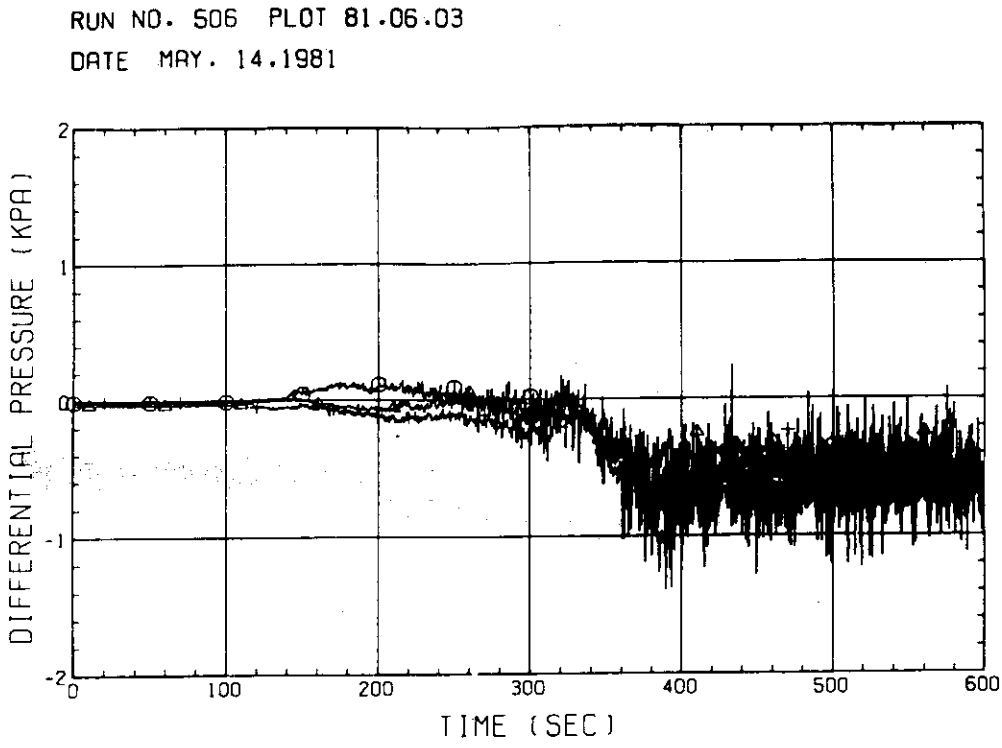

FIG. B-10 Horizontal Differential Pressures in Core (Pressure in Bundle 5 - Pressure in Bundle 8)

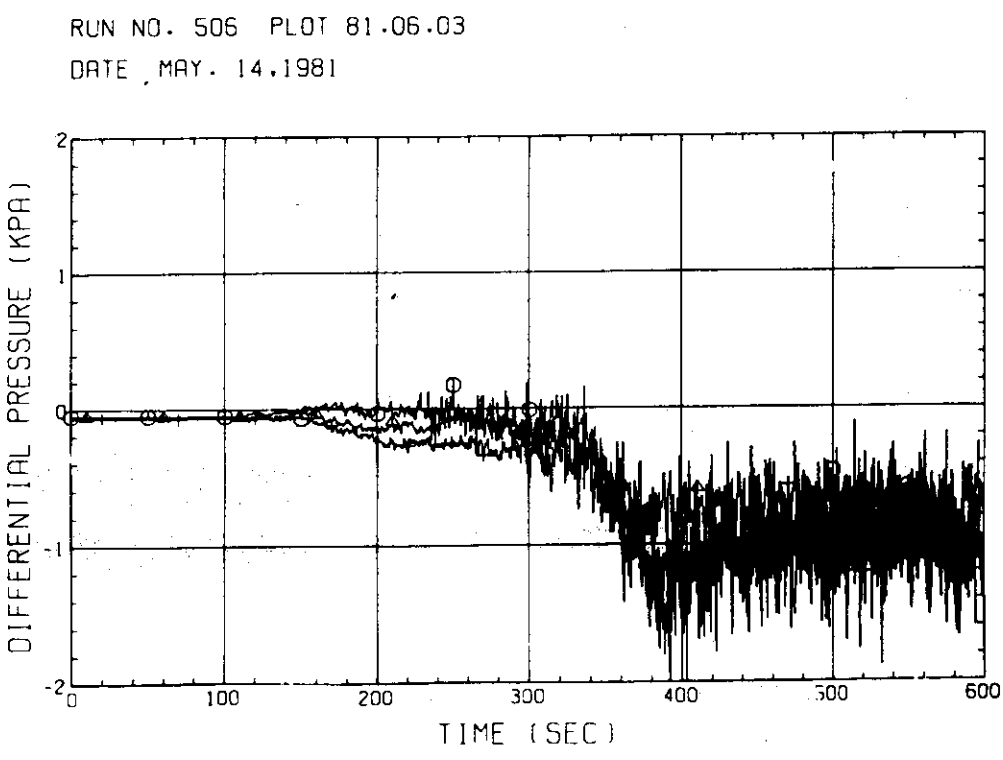

FIG. B-11 Horizontal Differential Pressures in Core (Pressure in Bundle 1 - Pressure in Bundle 8)

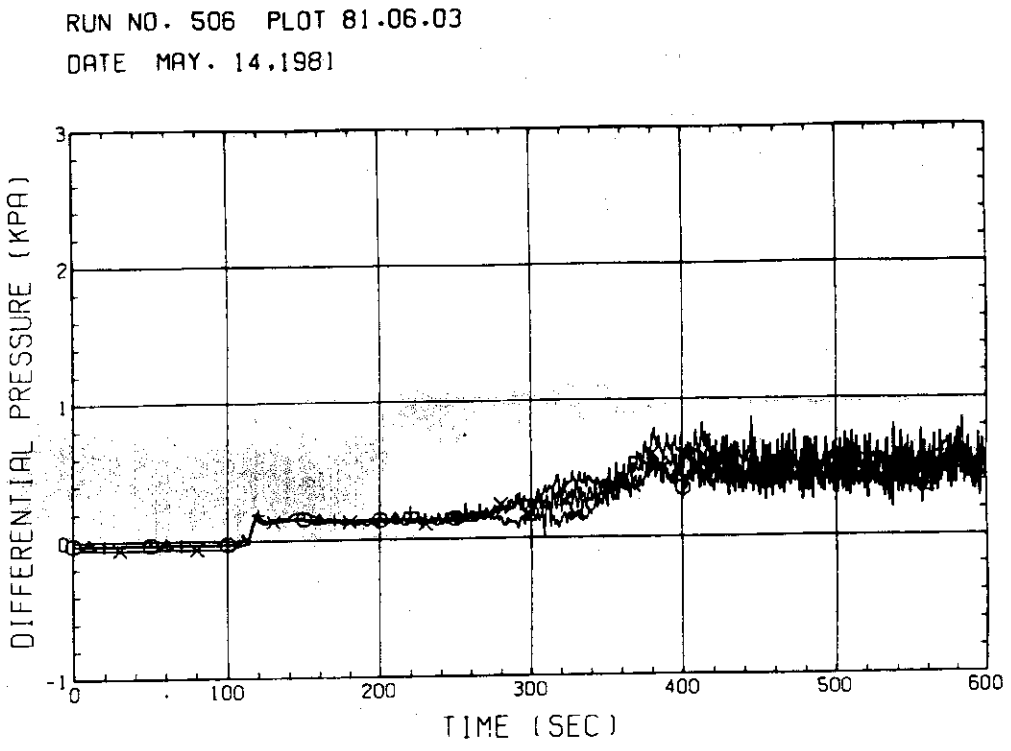

FIG. B-12(1) Differential Pressures across End Box Tie Plates (Bundles 1 through 4)

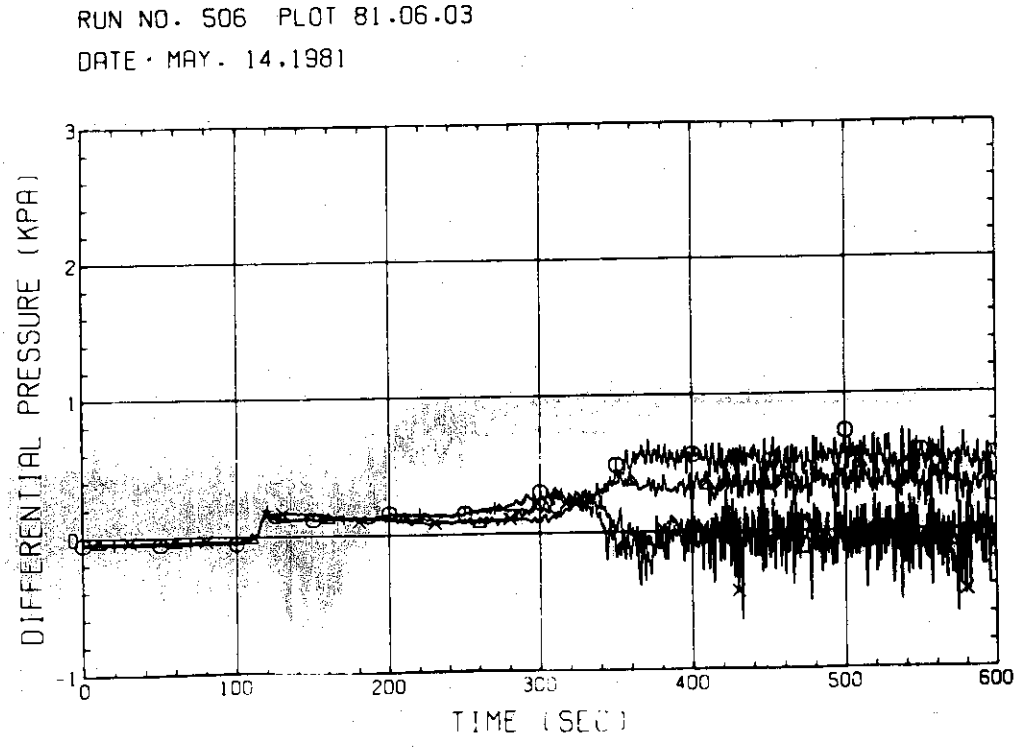

FIG. B-12(2) Differential Pressures across End Box Tie Plates (Bundles 5 through 8)

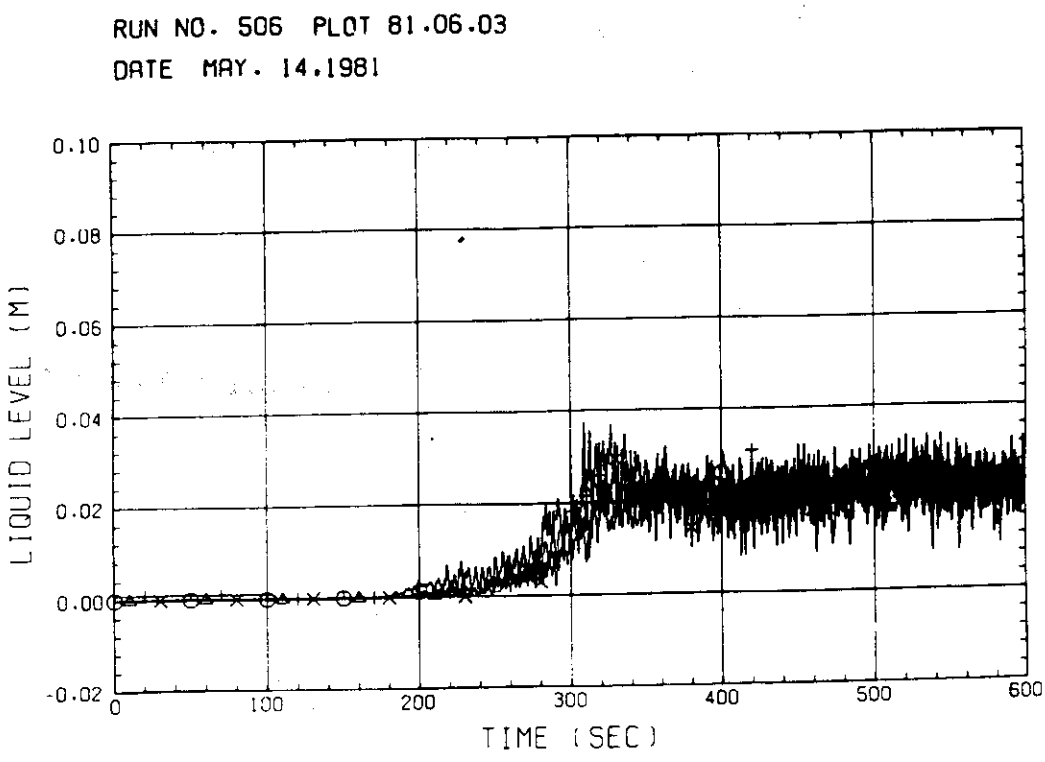

FIG. B-13(1) Collapsed Water Levels in End Boxes (Bundles 1 through 4)

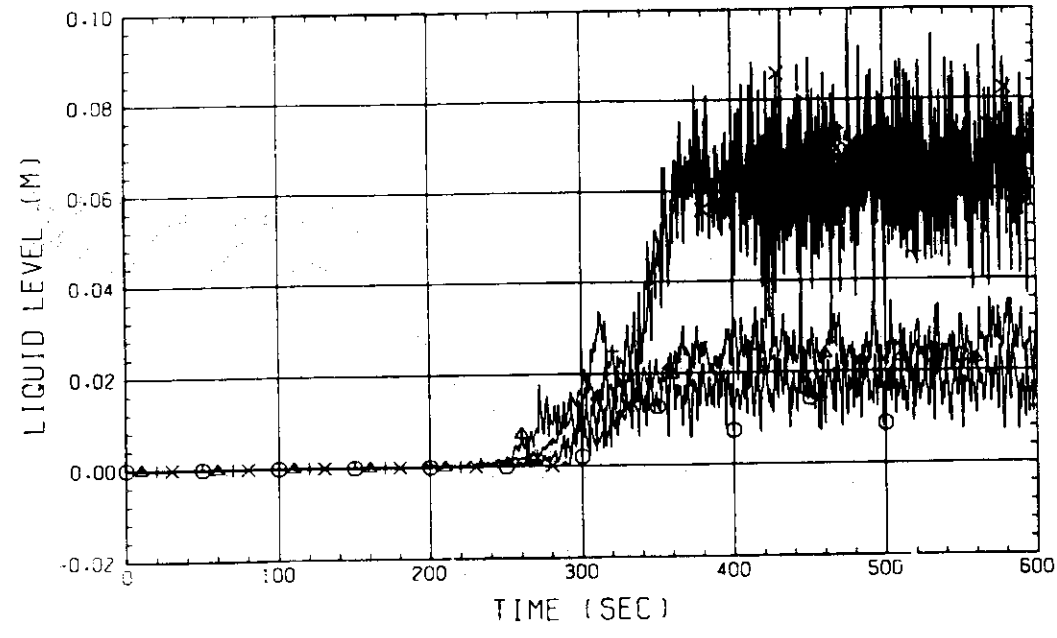

FIG. B-13(2) Collapsed Water Levels in End Boxes (Bundles 5 through 8)

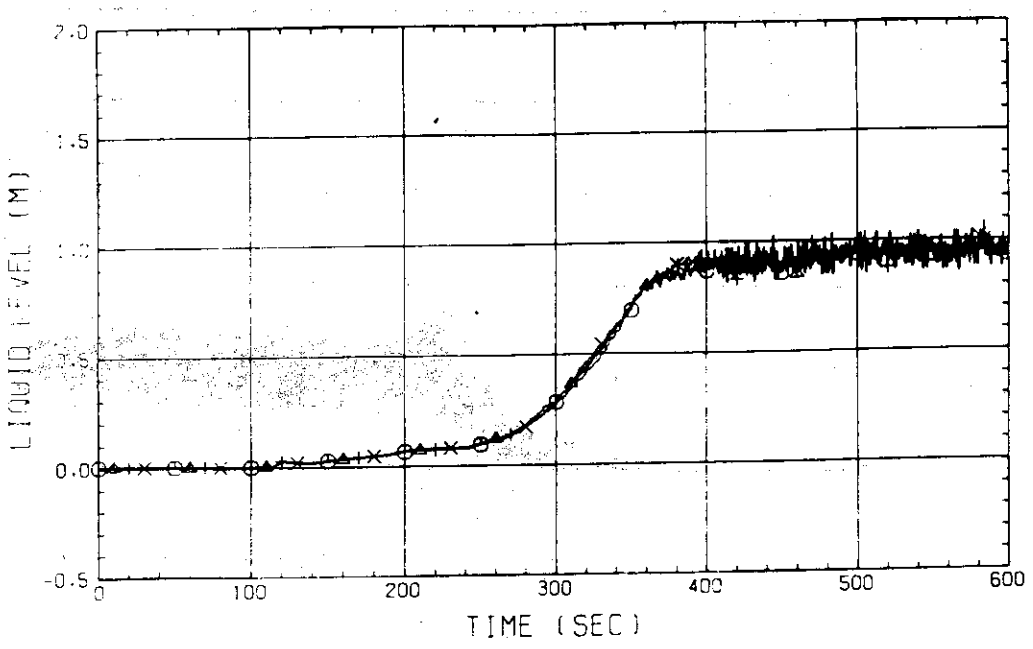

FIG. B-14(1) Collapsed Water Levels above UCSP (Bundles 1 through 4)

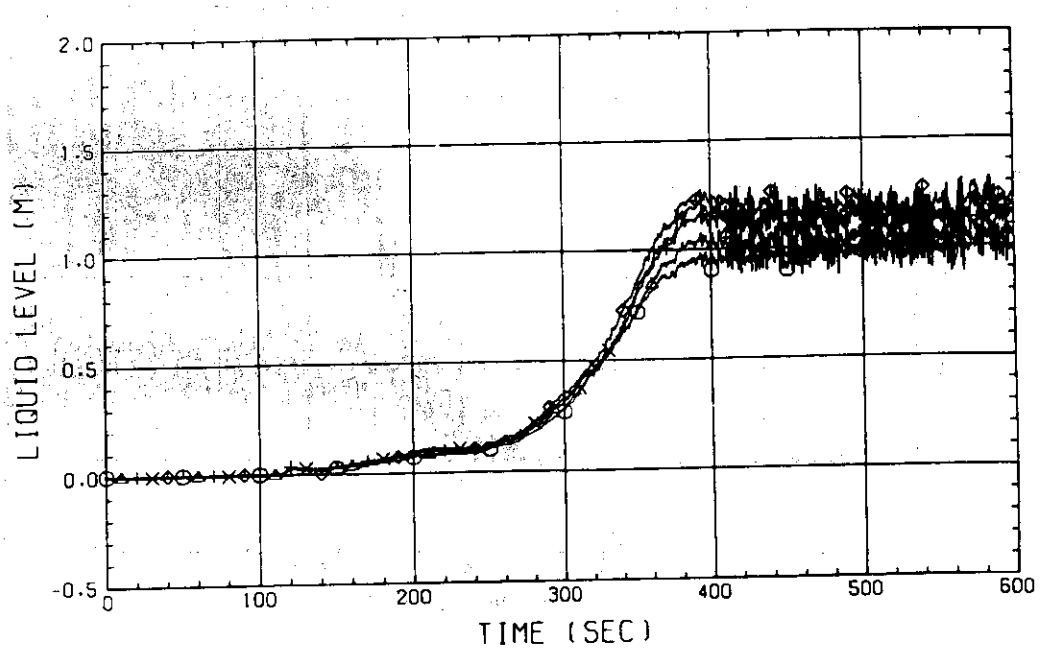

FIG. B-14(2) Collapsed Water Levels above UCSP (Bundles 5 through 8 and Core Baffle)

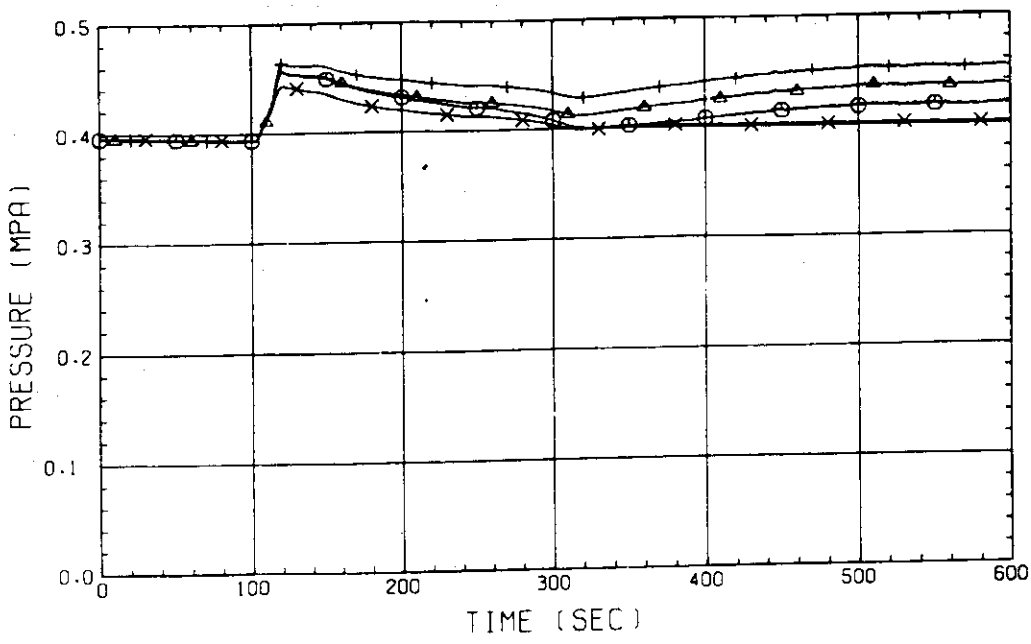

FIG. B-15 System Pressures at Top of Pressure Vessel, Core Center, Core Inlet and Upper Part of Downcomer

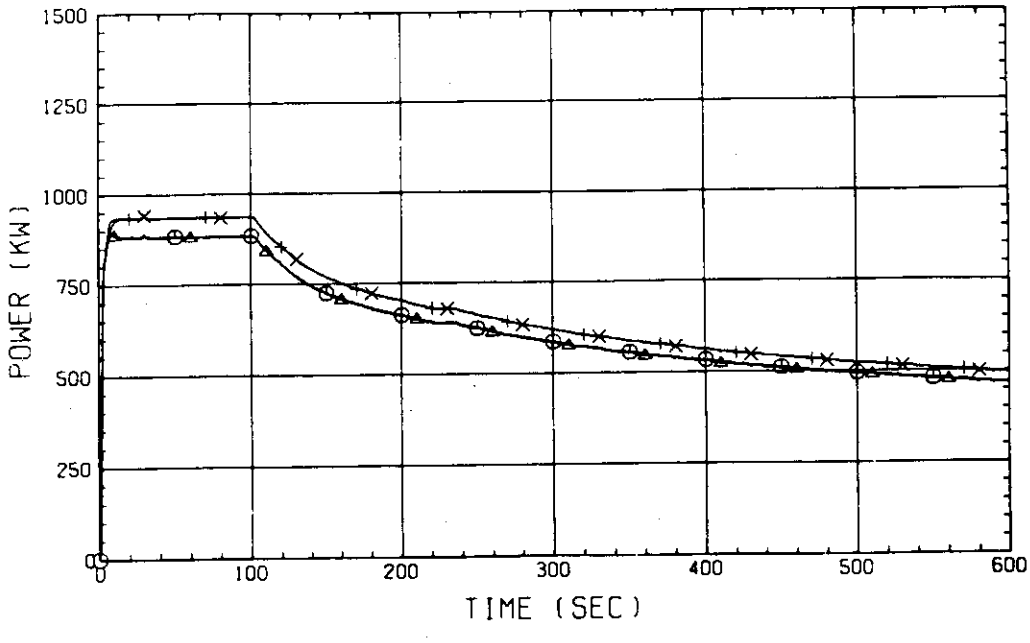

FIG. B-16(1) Heating Powers (Bundles 1 through 4)

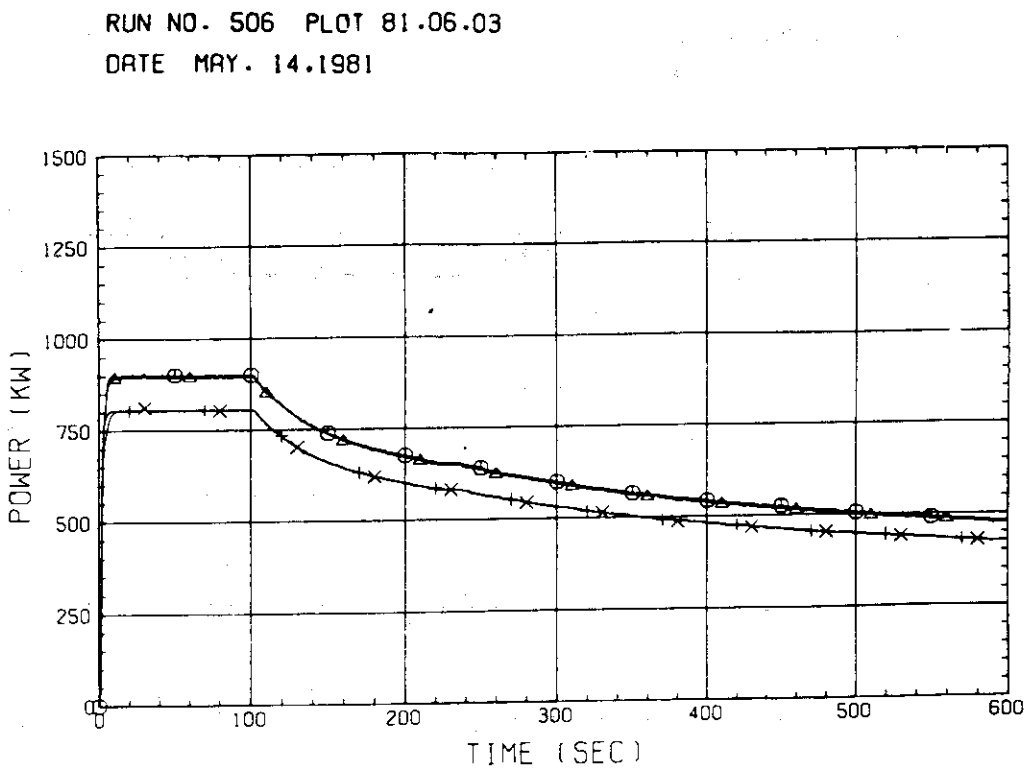

FIG. B-16(2) Heating Powers (Bundles 5 through 8)

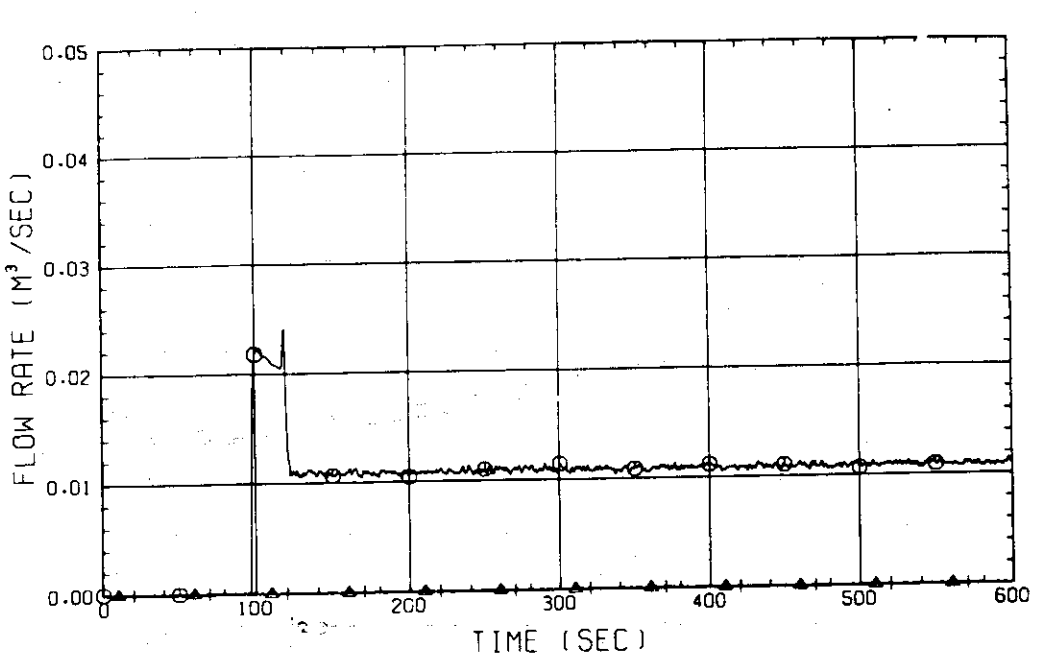

FIG. B-17 ECC Water Injection Rate into Lower Plenum

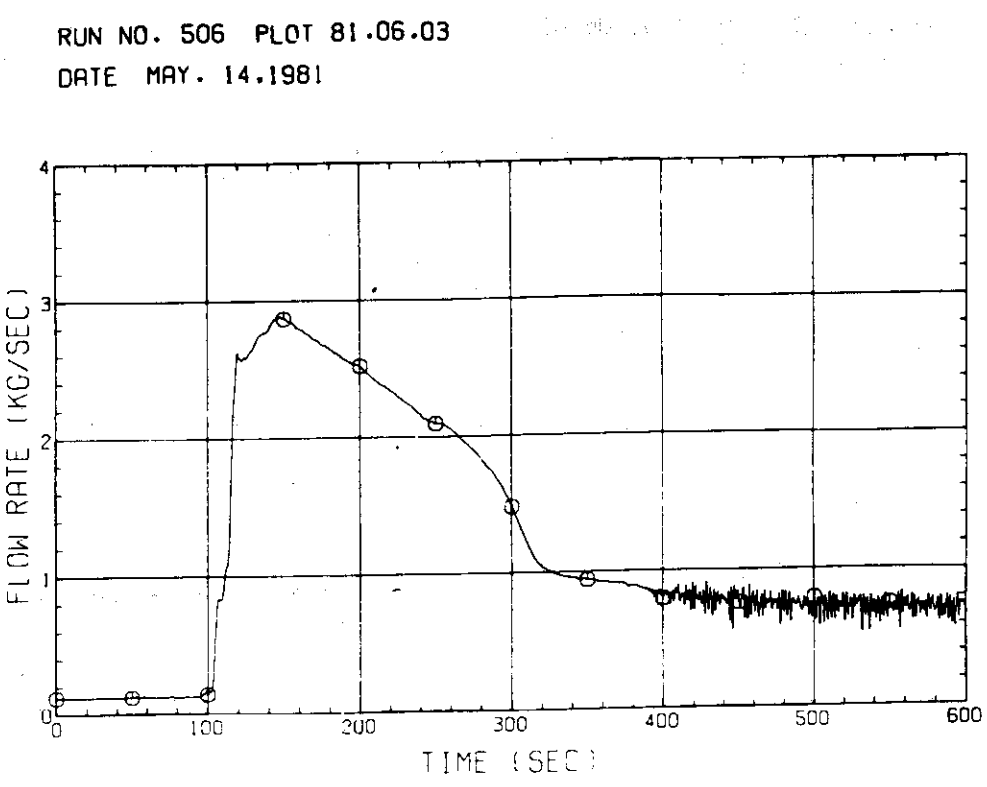

FIG. B-18 Steam Flow Rate at Intact Cold Leg

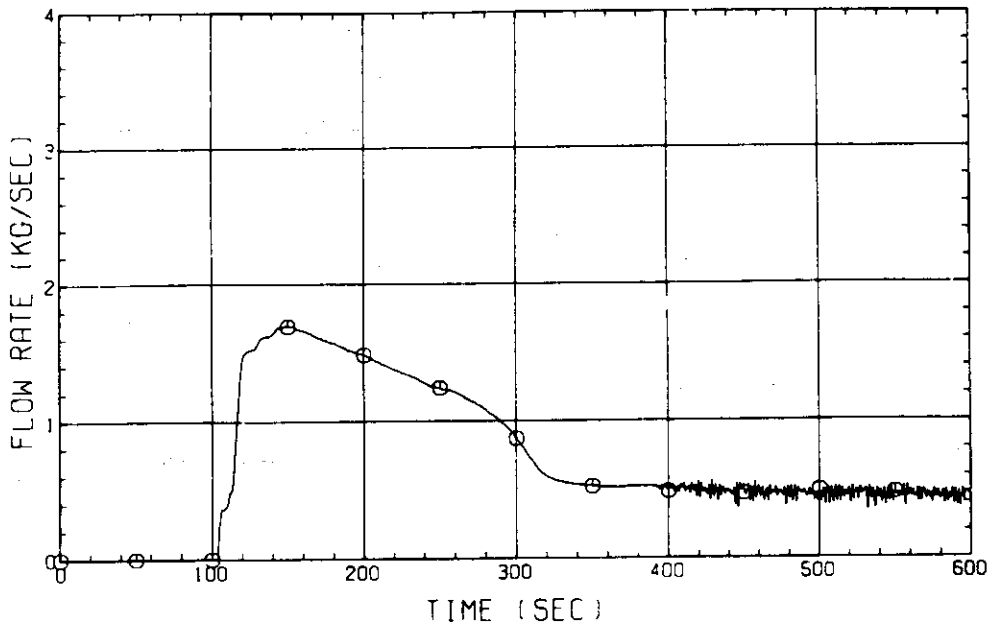

FIG. B-19 Steam Flow Rate at Steam-Water Separator Side Borken Cold Leg

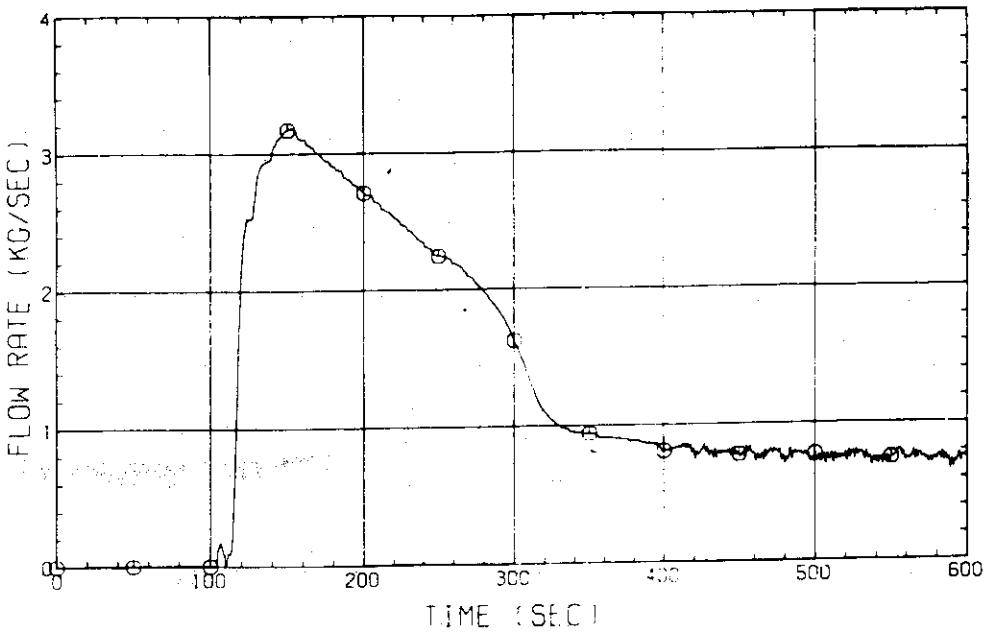

FIG. B-20 Steam Flow Rate between Containment Tanks-I and -II

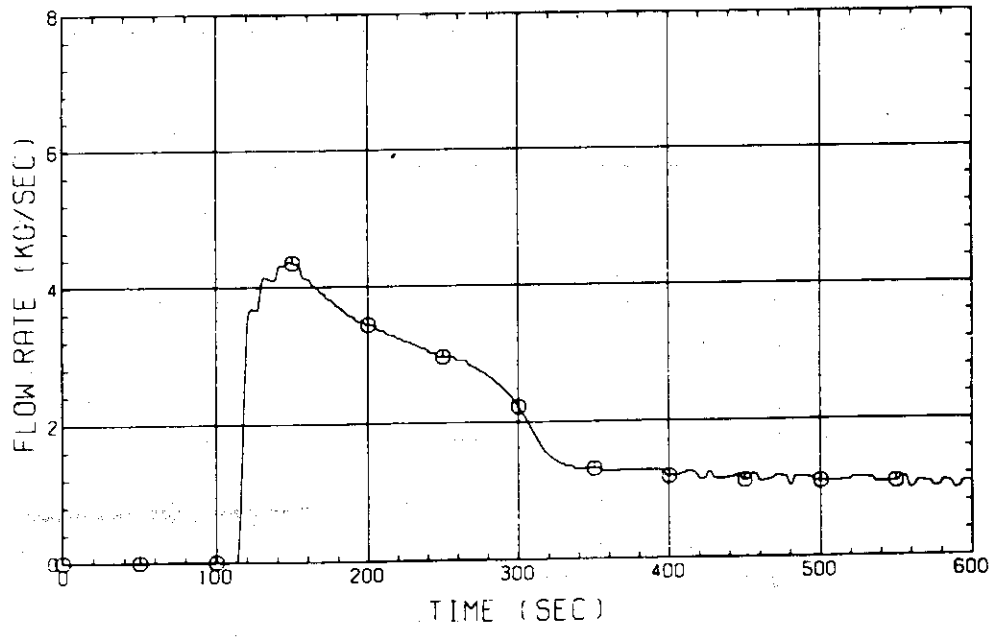

FIG. B-21 Steam Flow Rate at Discharge Line from Containment Tank-II

Appendix C
Selected Data from Test S1-01 (Run 507)

Note:

In Appendix C, selected data from Test S1-01 are introduced. Figure number for each measurement is the same as in Appendix B, except but the test identification character is C instead of B.

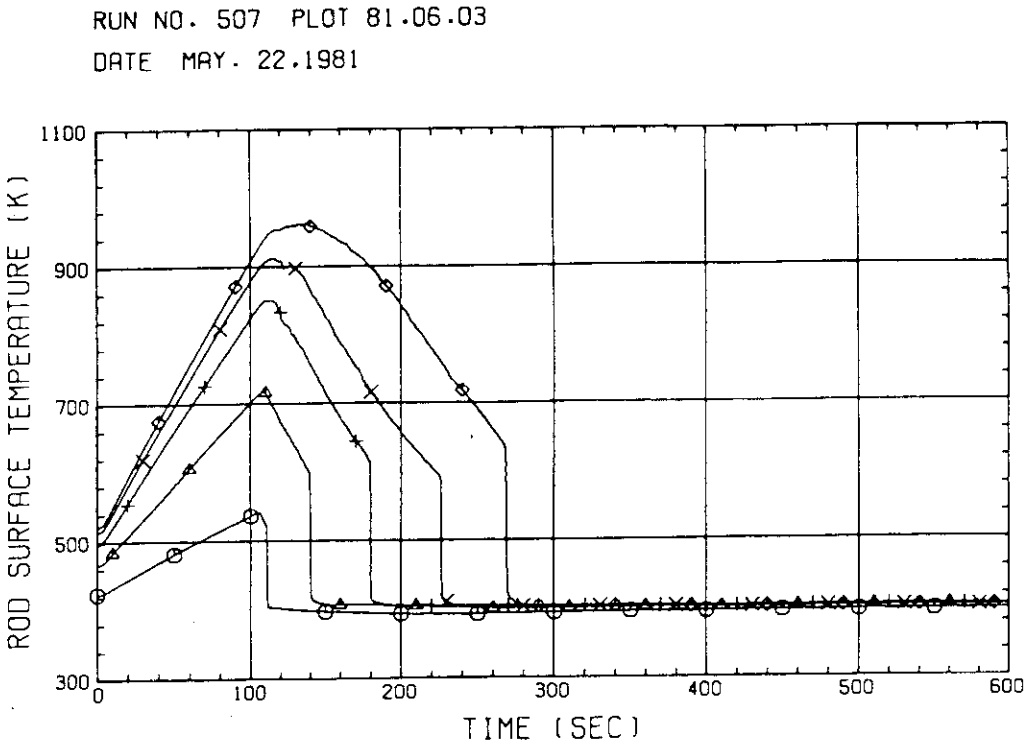

FIG. C-1(1) Heater Rod Temperatures (Lower Half of Bundle 1)

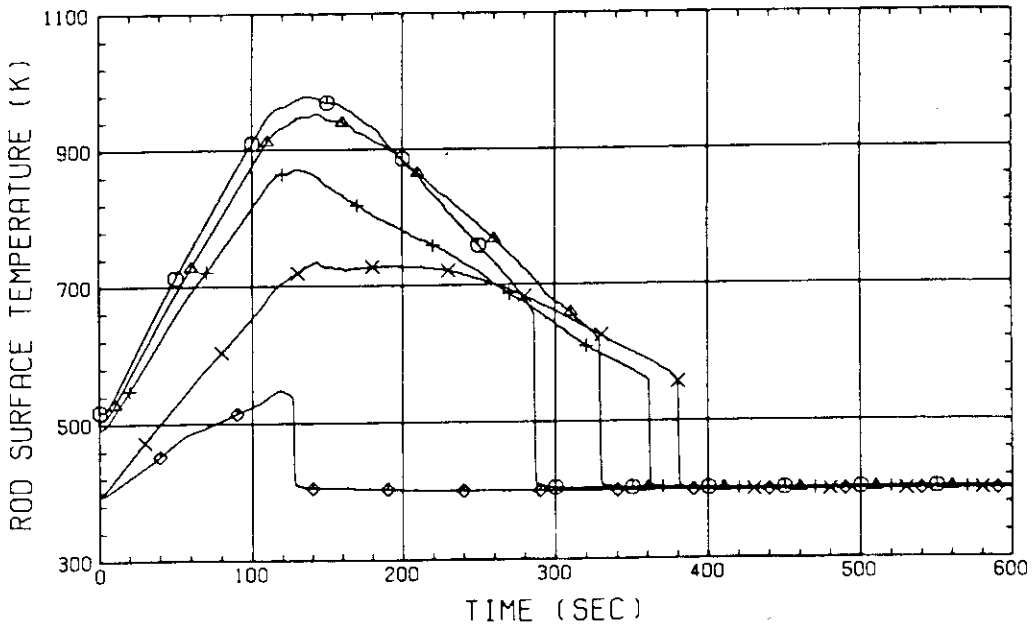

FIG. C-1(2) Heater Rod Temperatures (Upper Half of Bundle 1)

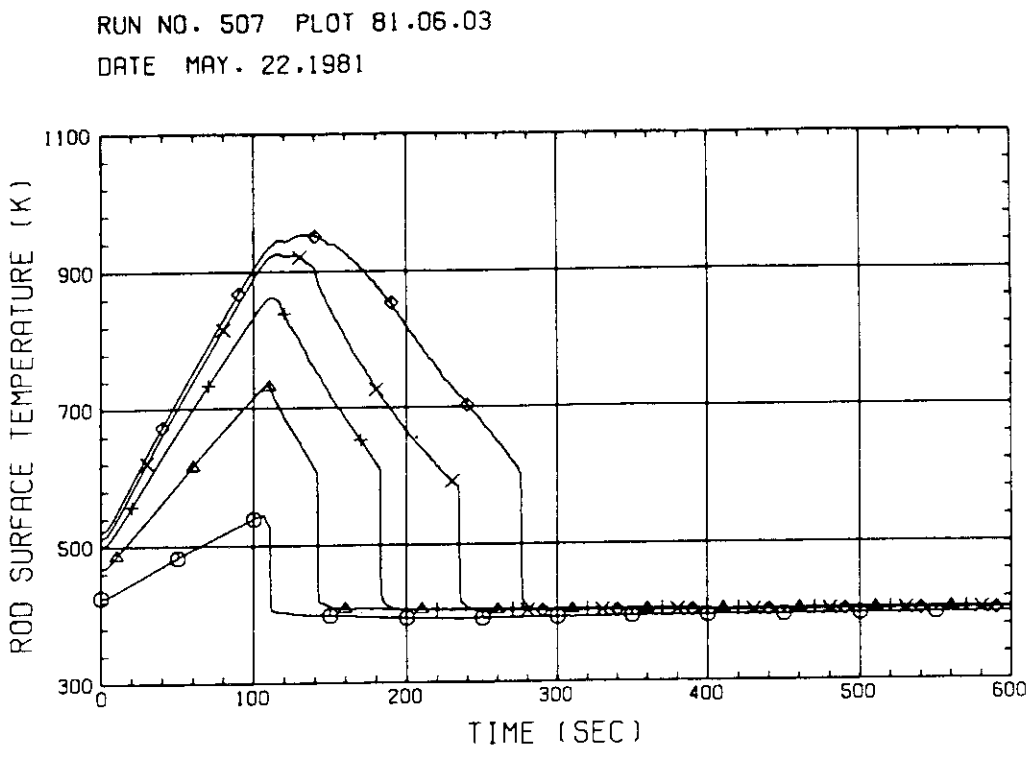

FIG. C-2(1) Heater Rod Temperatures (Lower Half of Bundle 2)

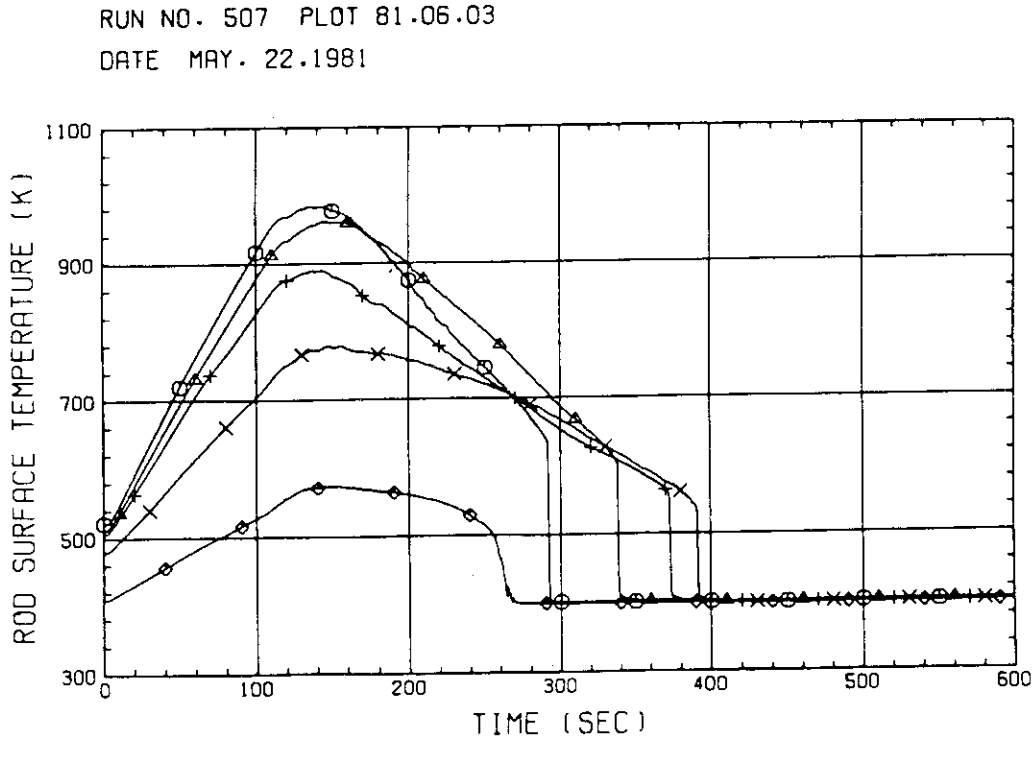

FIG. C-2(2) Heater Rod Temperatures (Upper Half of Bundle 2)

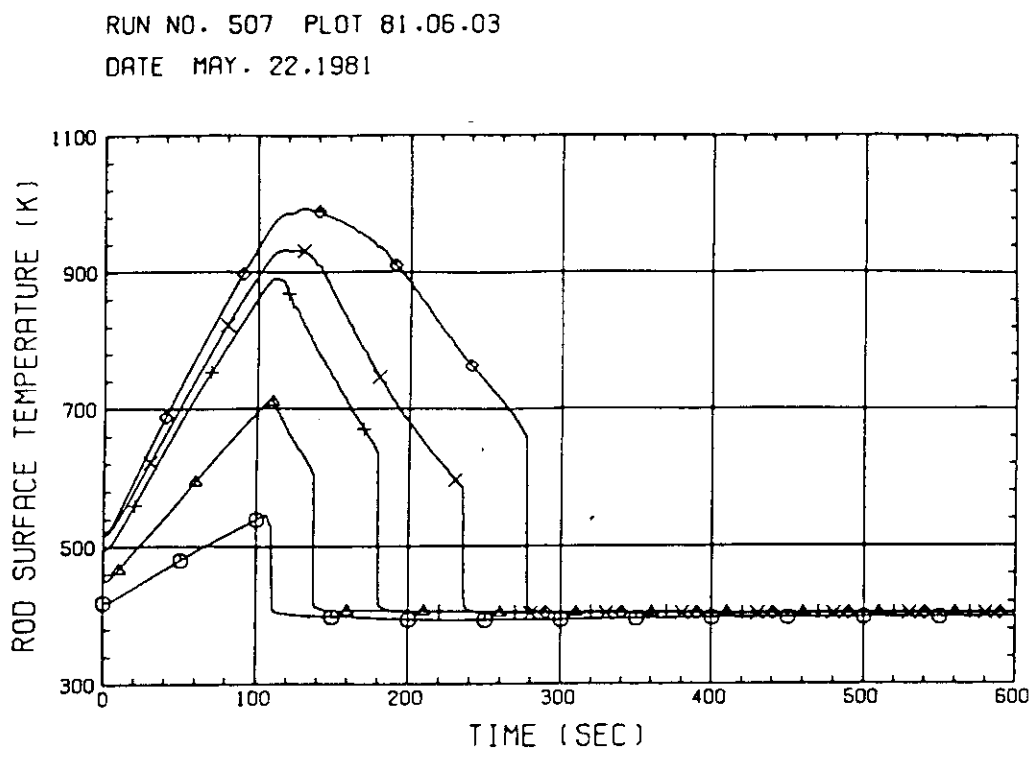

FIG. C-3(1) Heater Rod Temperatures (Lower Half of Bundle 3)

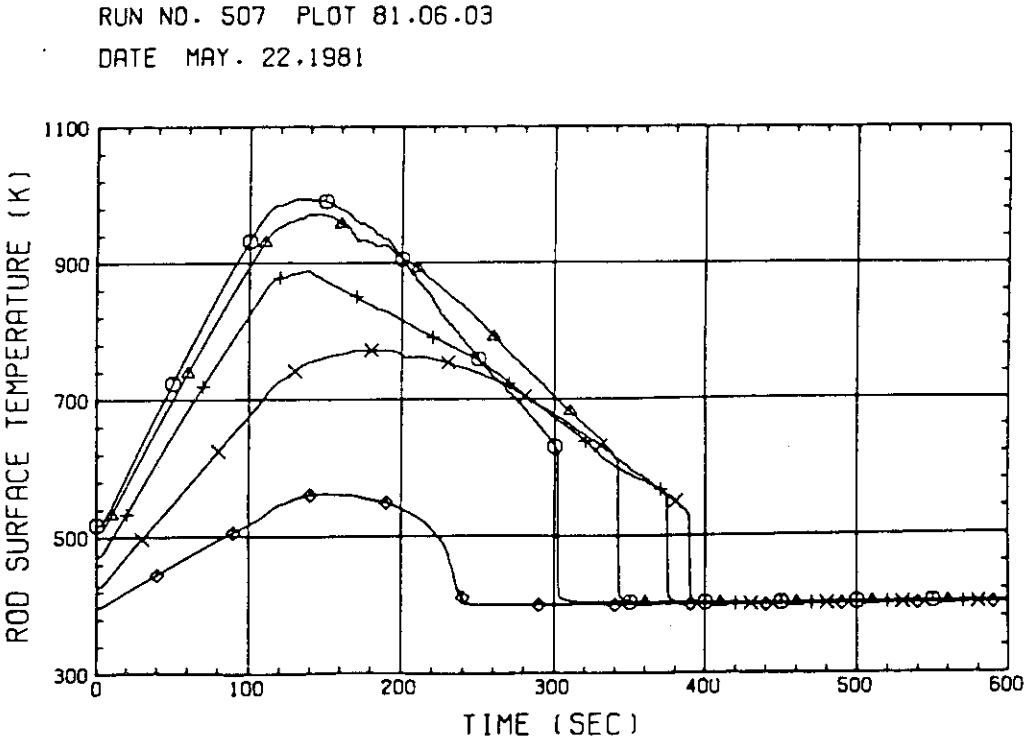

FIG. C-3(2) Heater Rod Temperatures (Upper Half of Bundle 3)

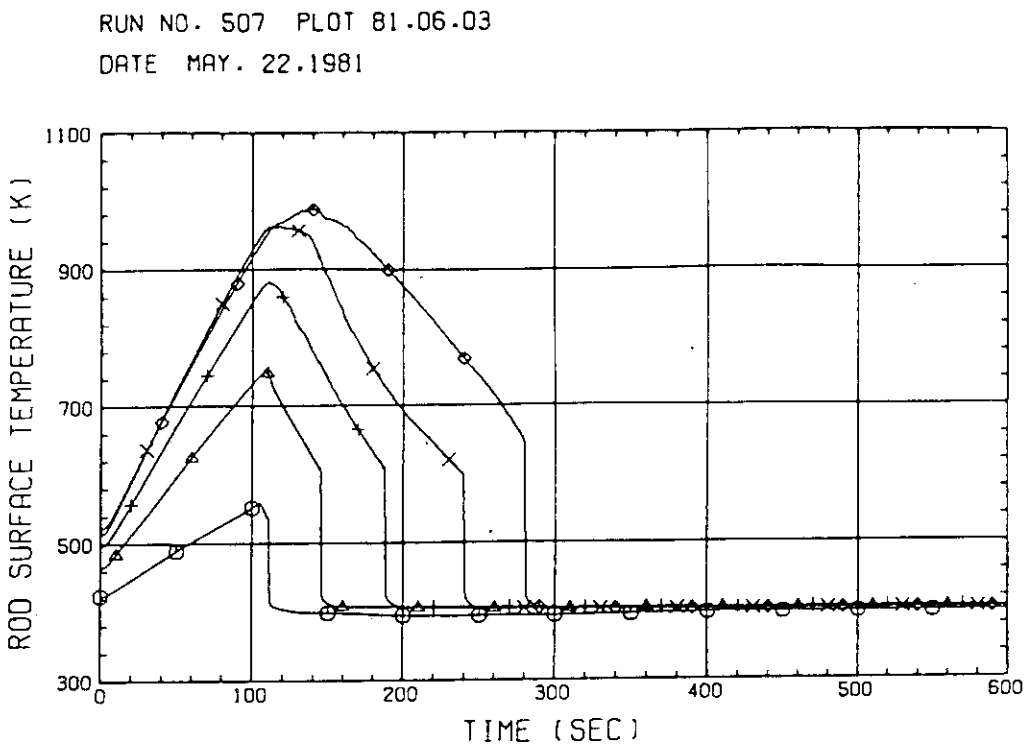

FIG. C-4(1) Heater Rod Temperatures (Lower Half of Bundle 4)

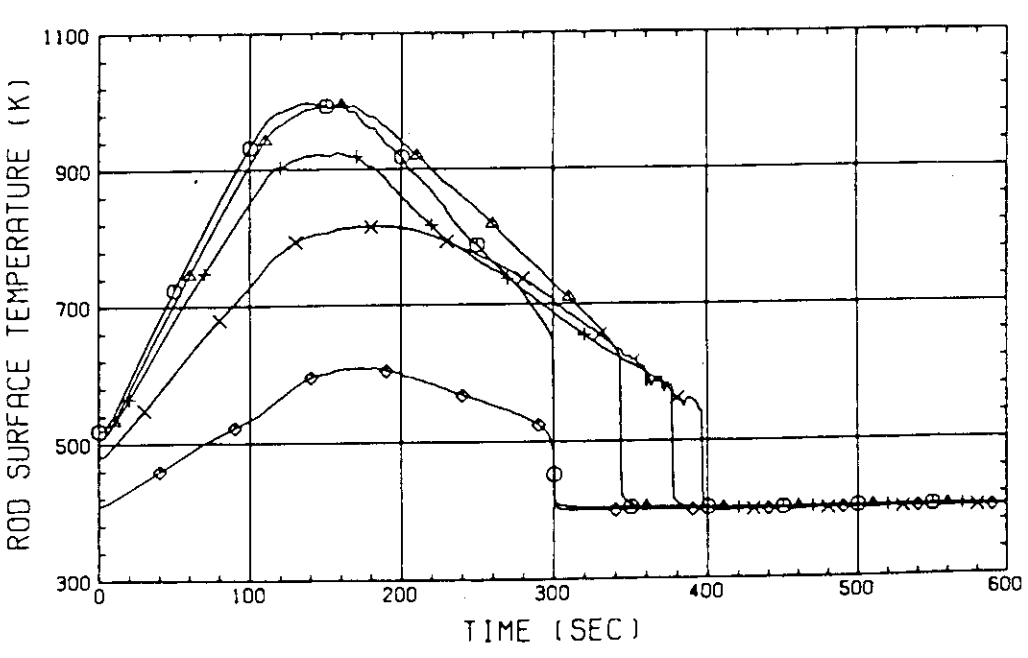

FIG. C-4(2) Heater Rod Temperatures (Upper Half of Bundle 4)

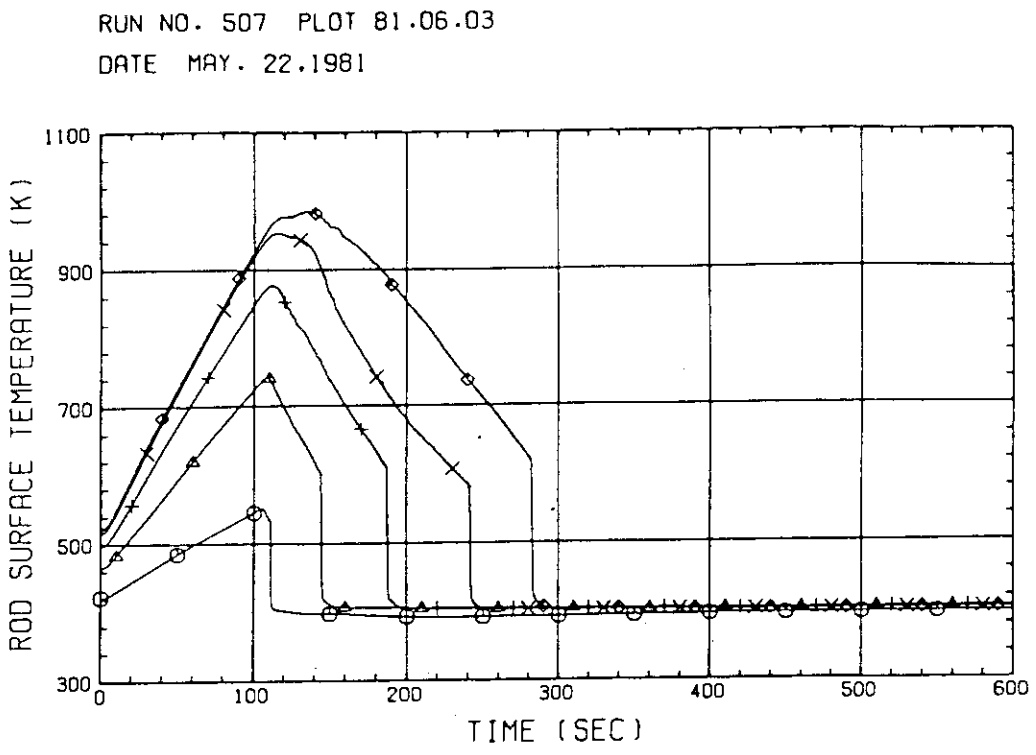

FIG. C-5(1) Heater Rod Temperatures (Lower Half of Bundle 5)

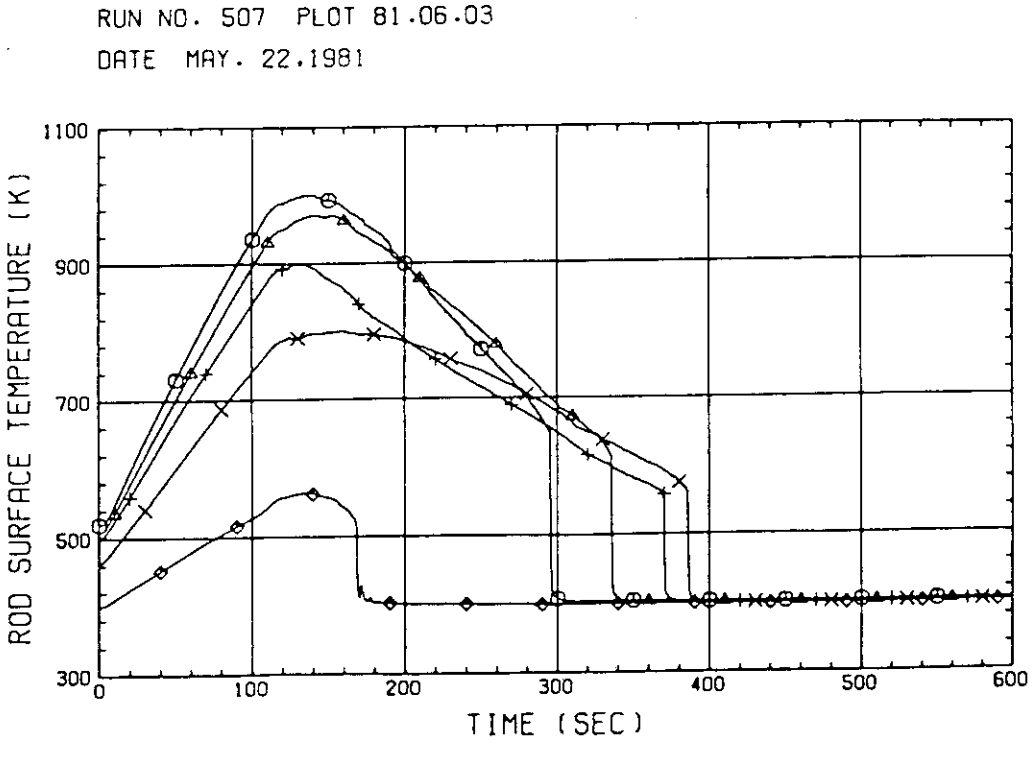

FIG. C-5(2) Heater Rod Temperatures (Upper Half of Bundle 5)

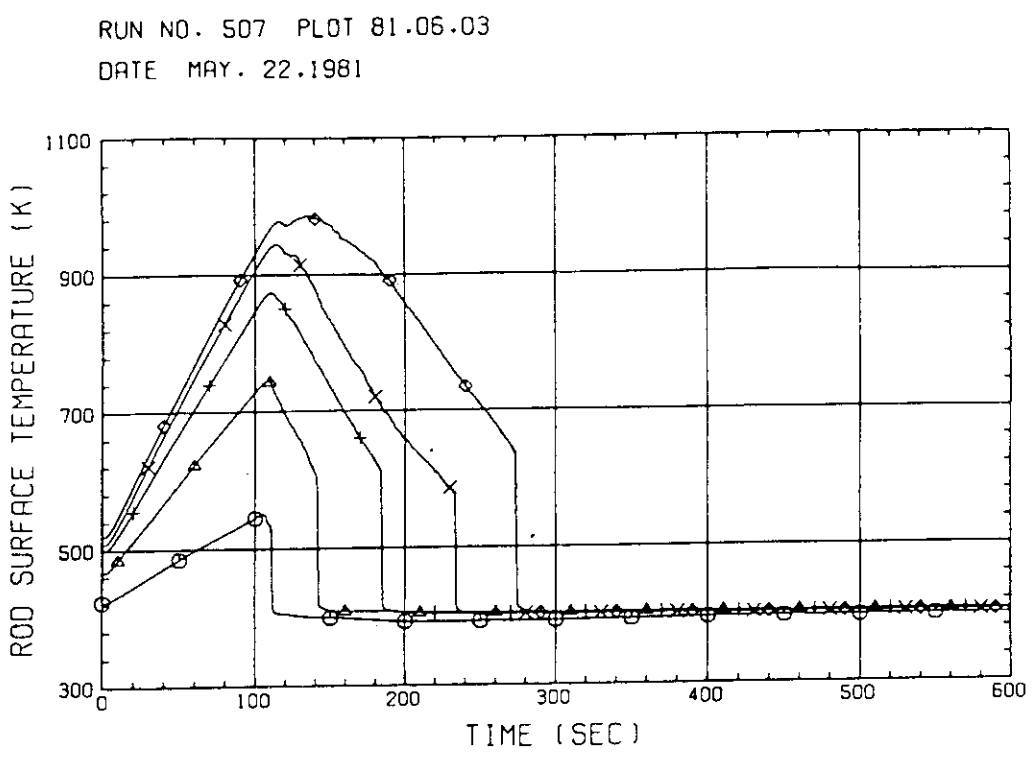

FIG. C-6(1) Heater Rod Temperatures (Lower Half of Bundle 6)

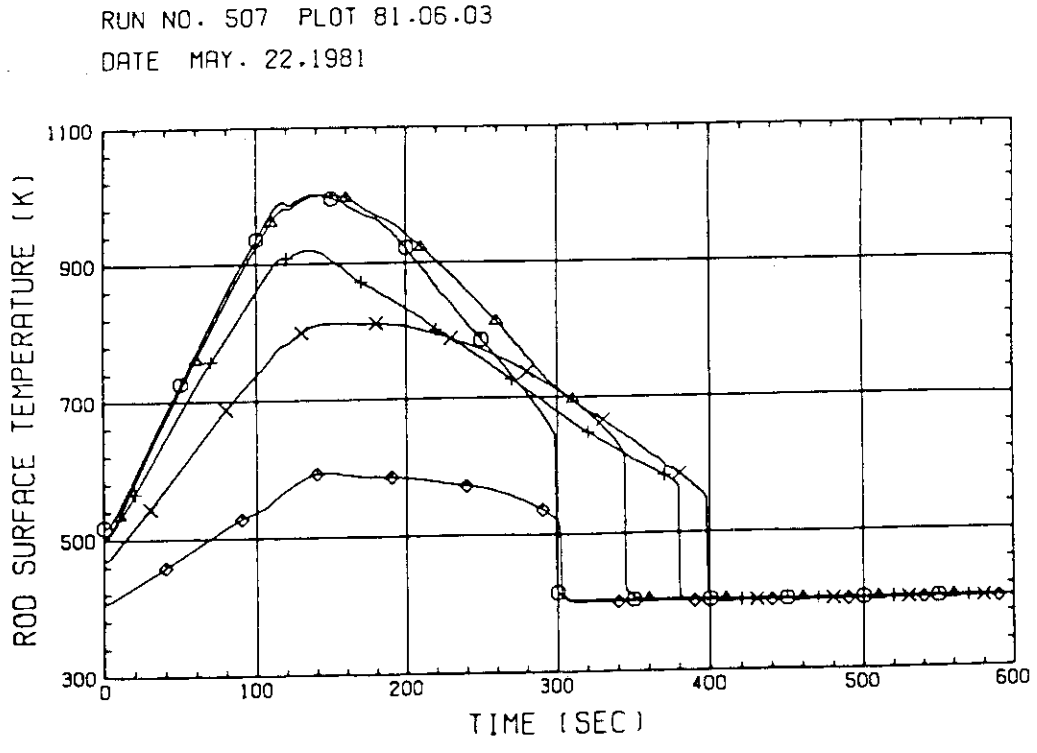

FIG. C-6(2) Heater Rod Temperatures (Upper Half of Bundle 6)

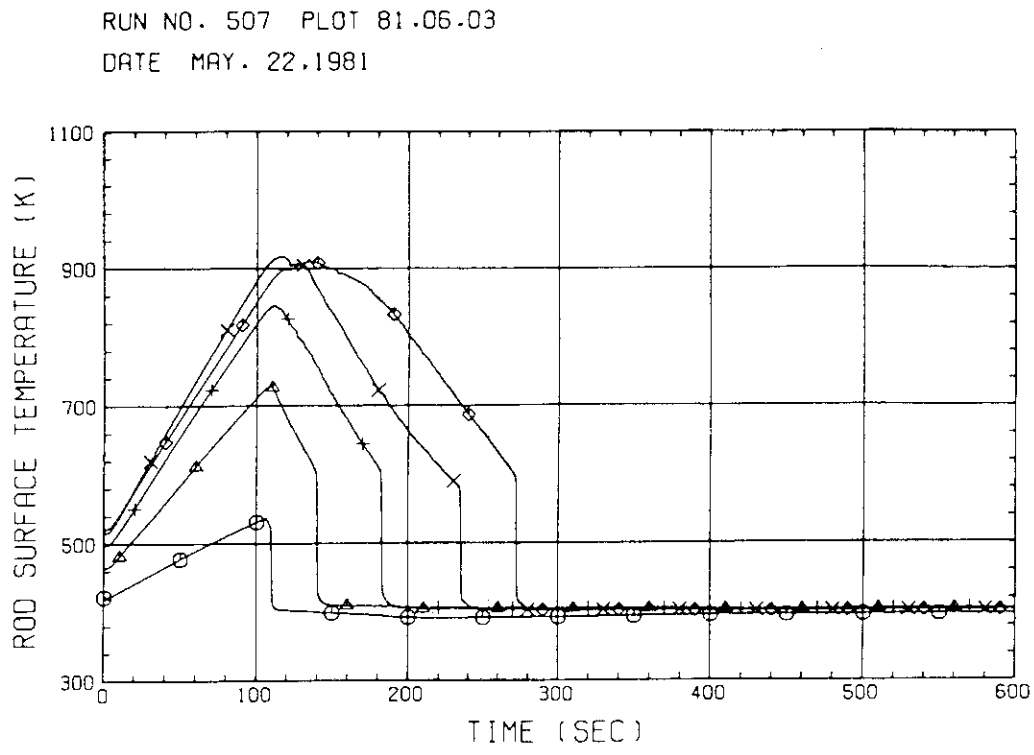

FIG. C-7(1) Heater Rod Temperatures (Lower Half of Bundle 7)

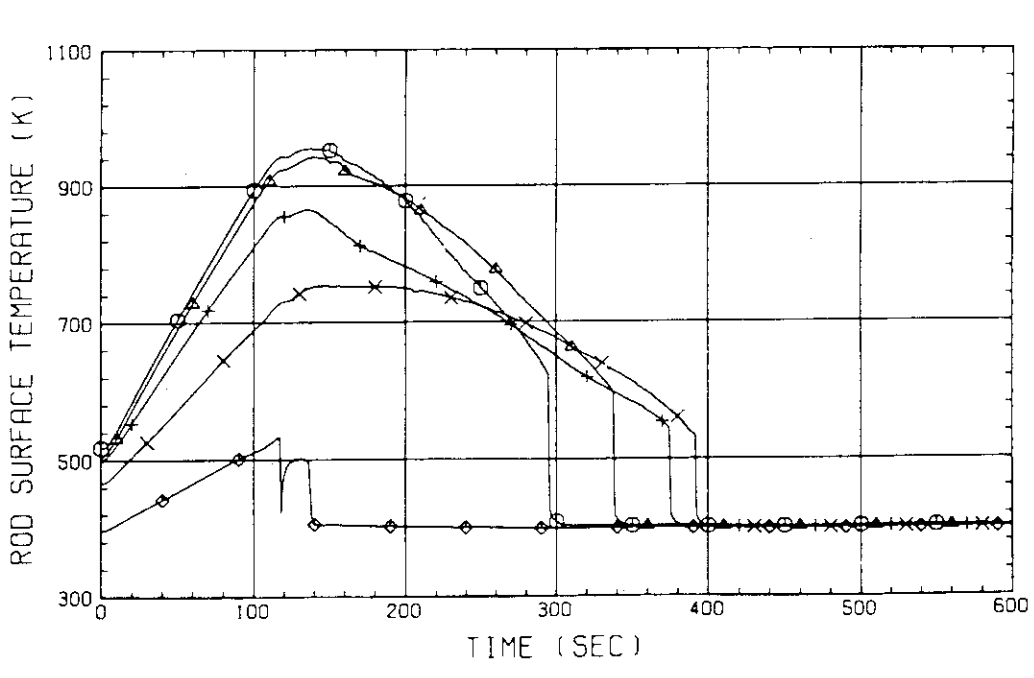

FIG. C-7(2) Heater Rod Temperatures (Upper Half of Bundle 7)

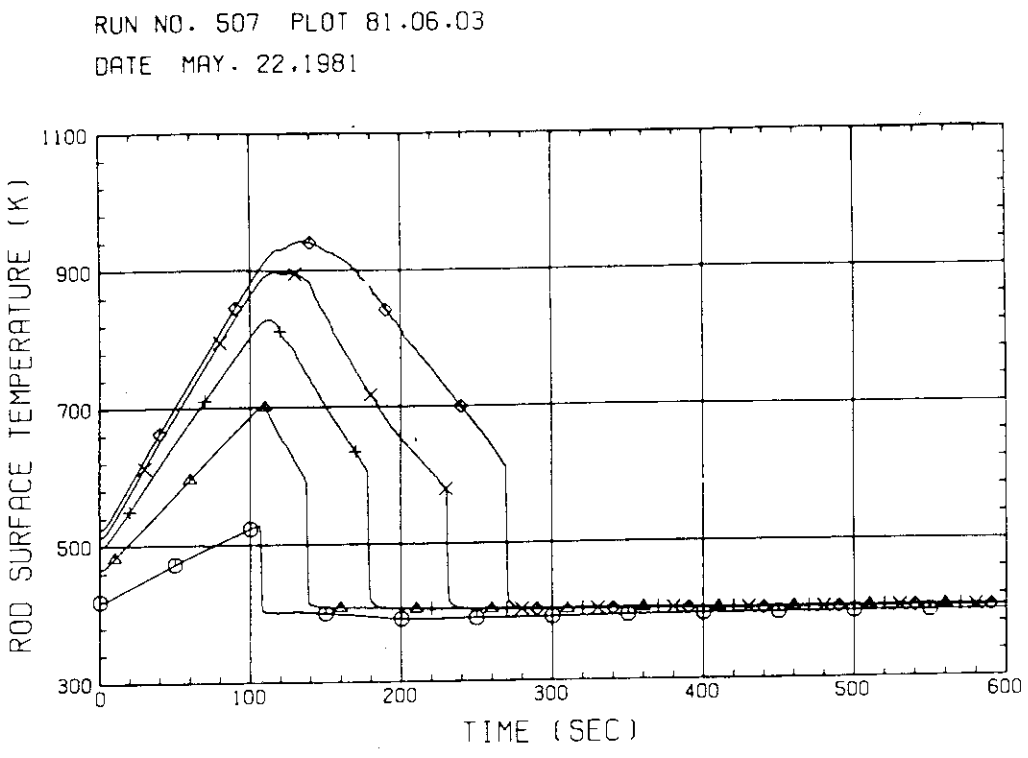

FIG. C-8(1) Heater Rod Temperatures (Lower Half of Bundle 8)

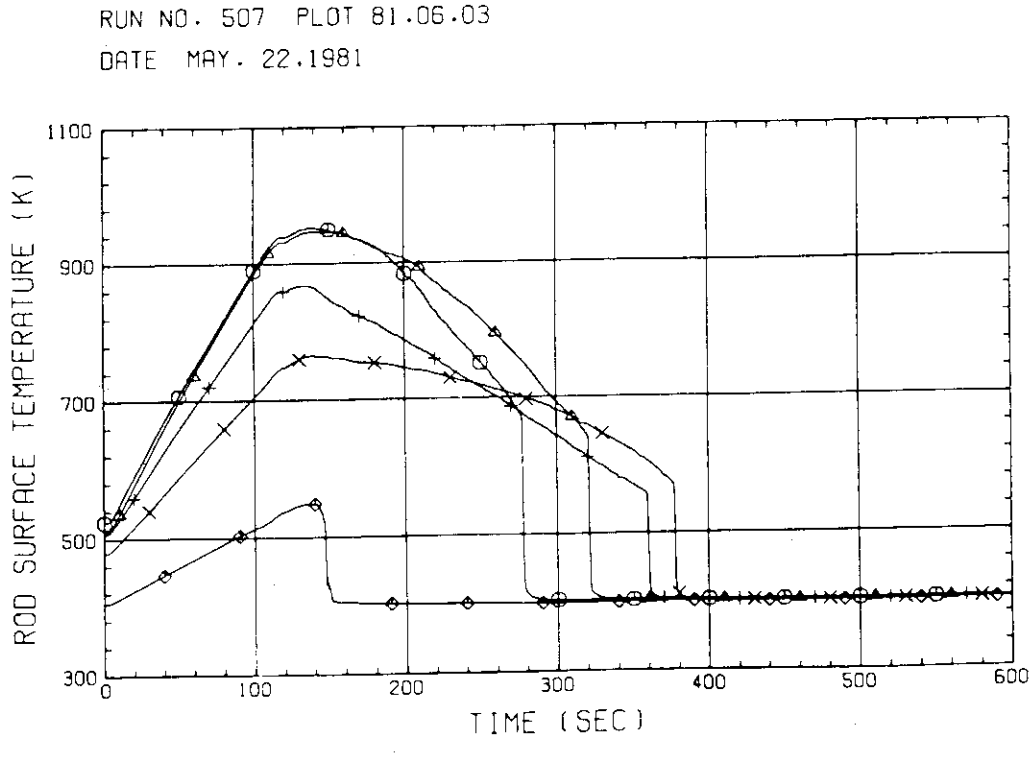

FIG. C-8(2) Heater Rod Temperatures (Upper Half of Bundle 8)

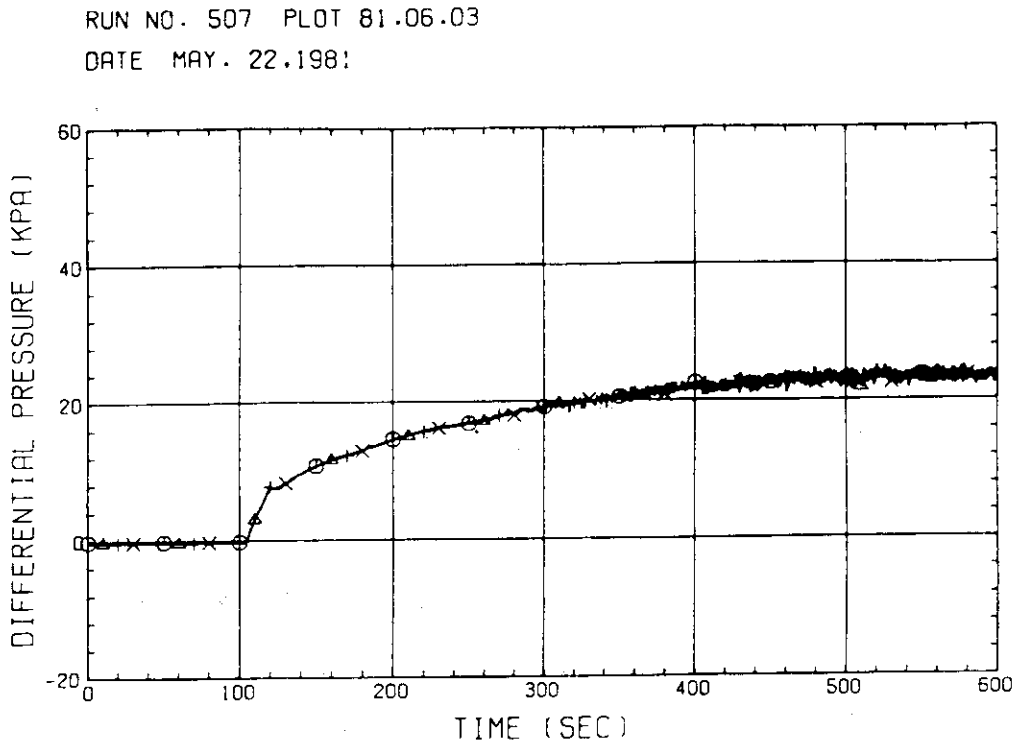

FIG. C-9(1) Differential Pressure across Core Full Height (Bundles 1 through 4)

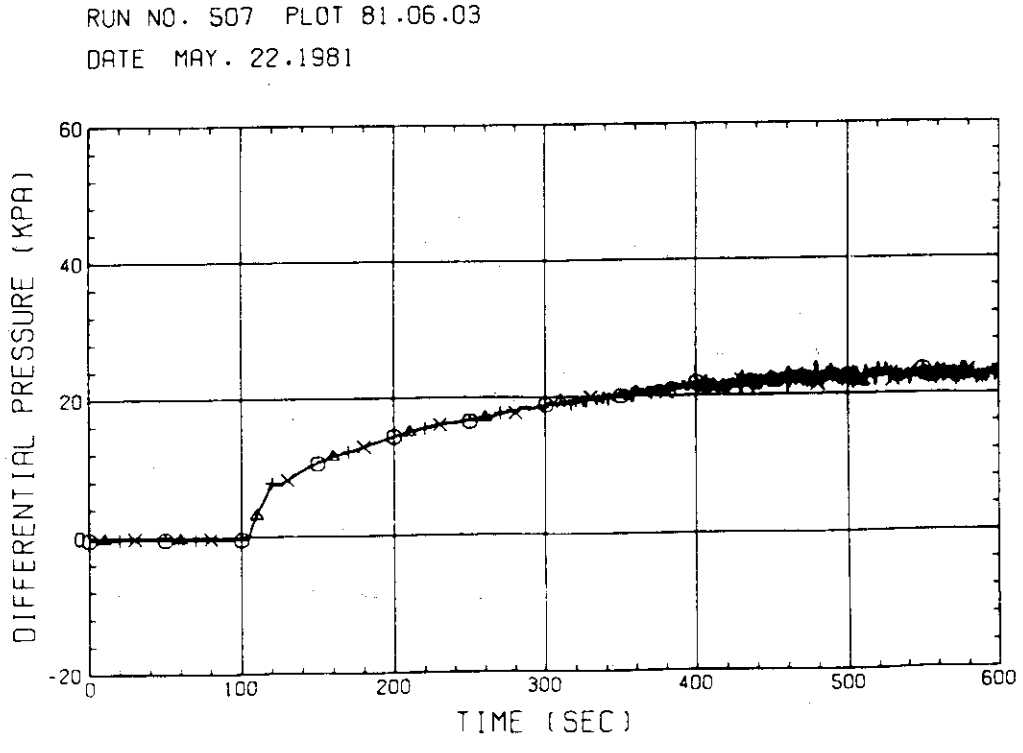

FIG. C-9(2) Differential Pressure across Core Full Height (Bundles 5 through 8)

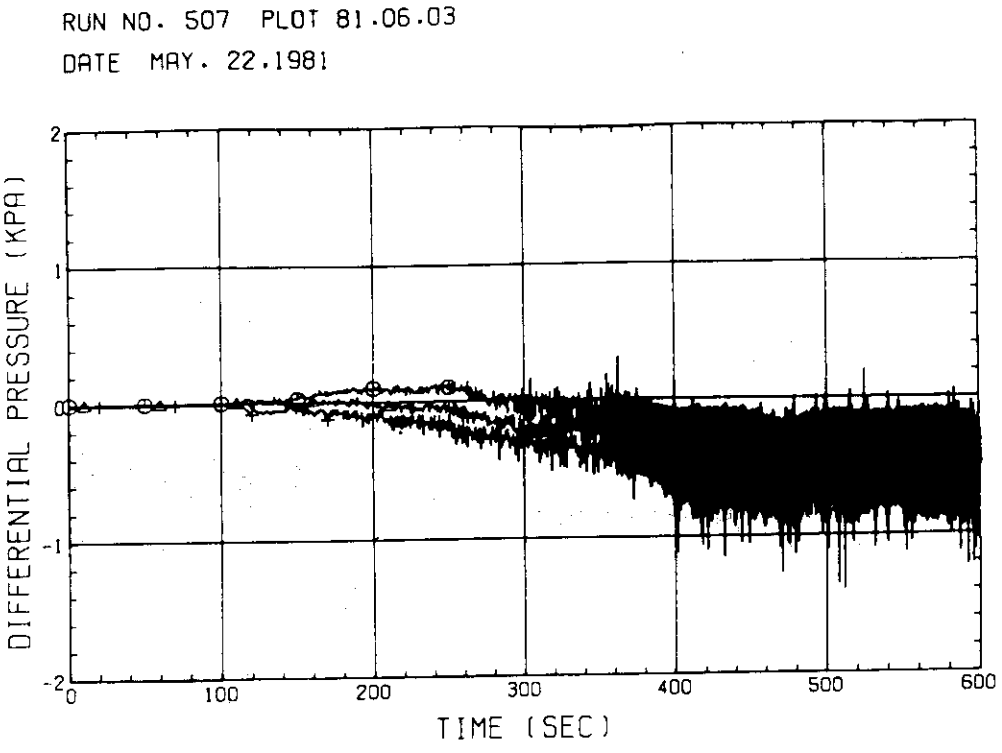

FIG. C-10 Horizontal Differential Pressures in Core (Pressure in Bundle 5 - Pressure in Bundle 8)

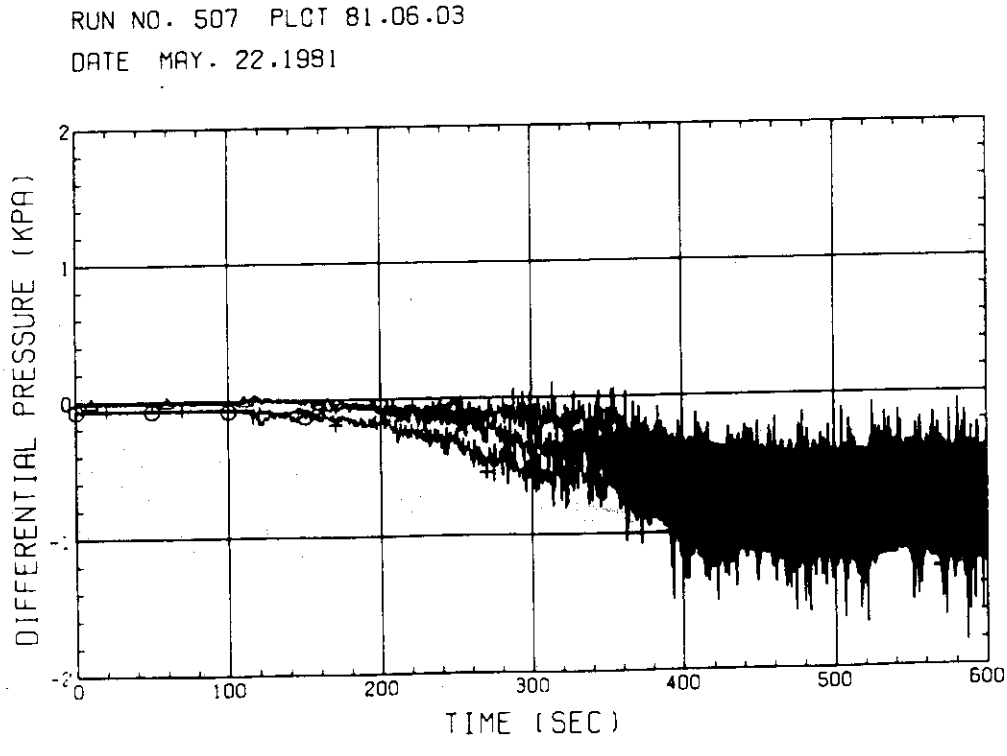

FIG. C-11 Horizontal Differential Pressures in Core (Pressure in Bundle 1 - Pressure in Bundle 8)

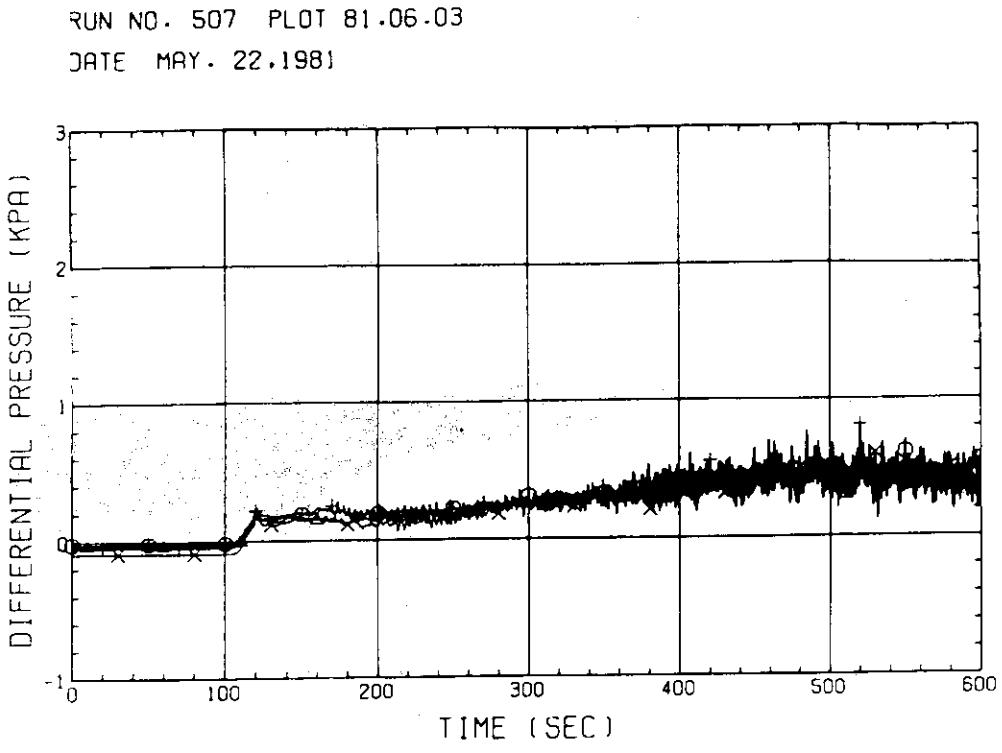

FIG. C-12(1) Differential Pressures across End Box Tie Plates (Bundles 1 through 4)

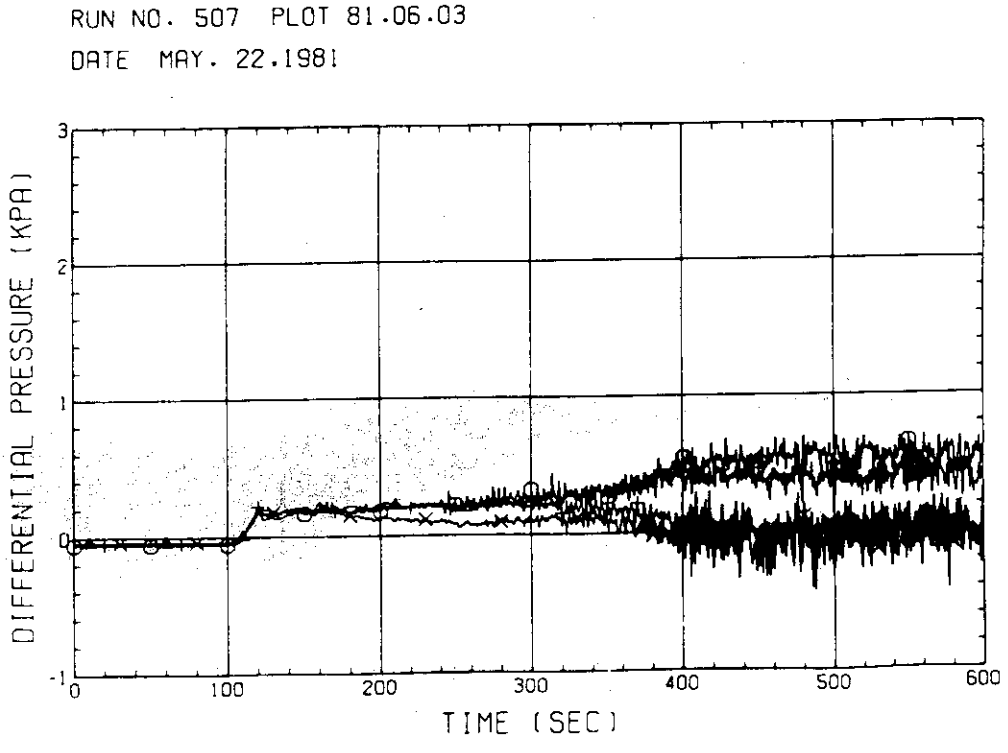

FIG. C-12(2) Differential Pressures across End Box Tie Plates (Bundles 5 through 8)

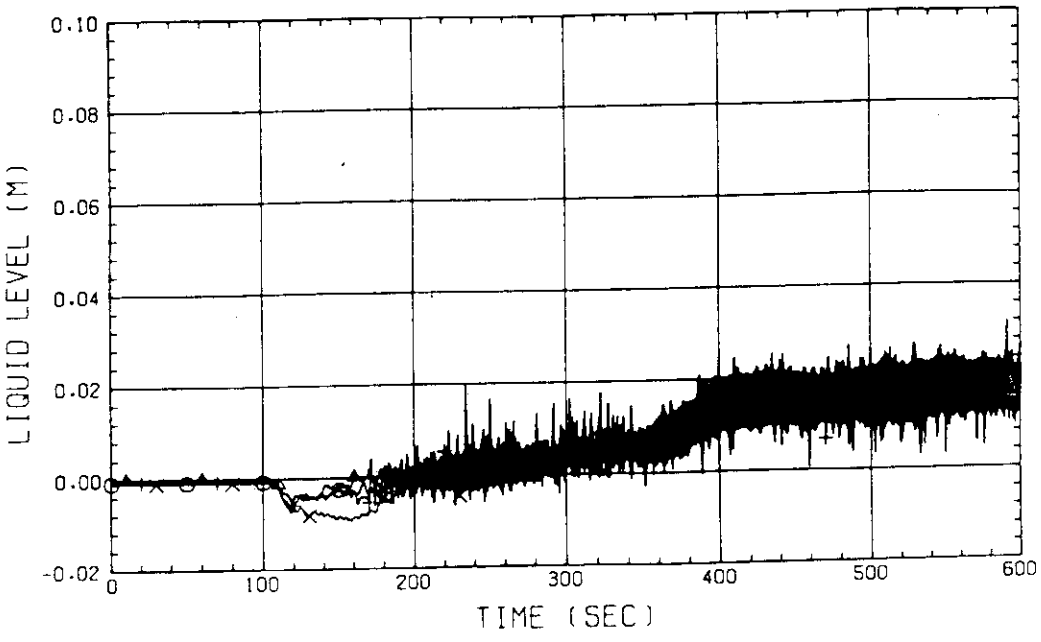

FIG. C-13(1) Collapsed Water Levels in End Boxes (Bundles 1 through 4)

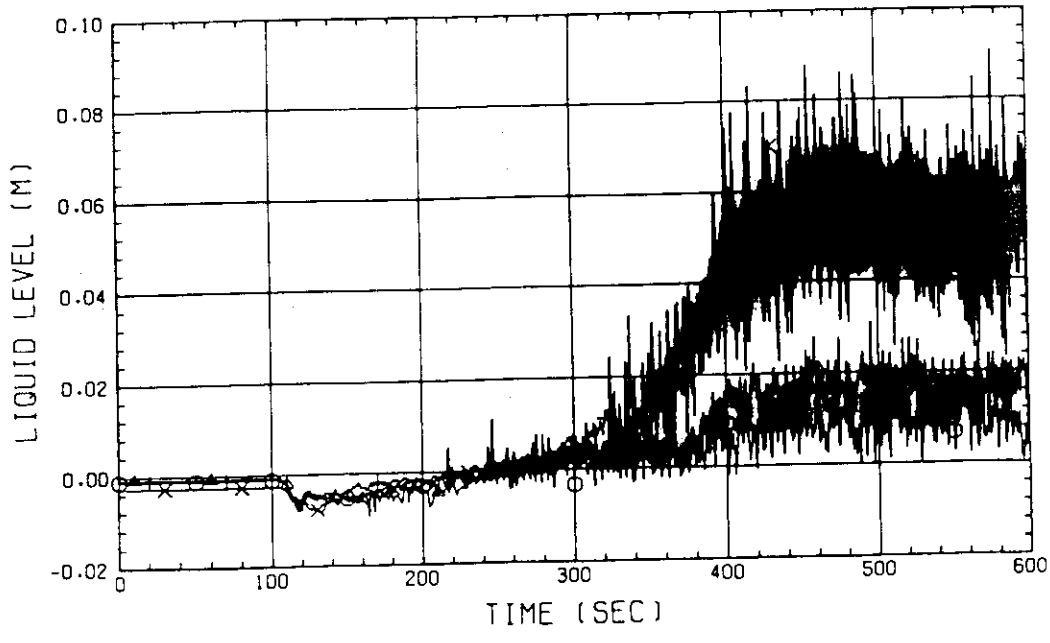

FIG. C-13(2) Collapsed Water Levels in End Boxes (Bundles 5 through 8)

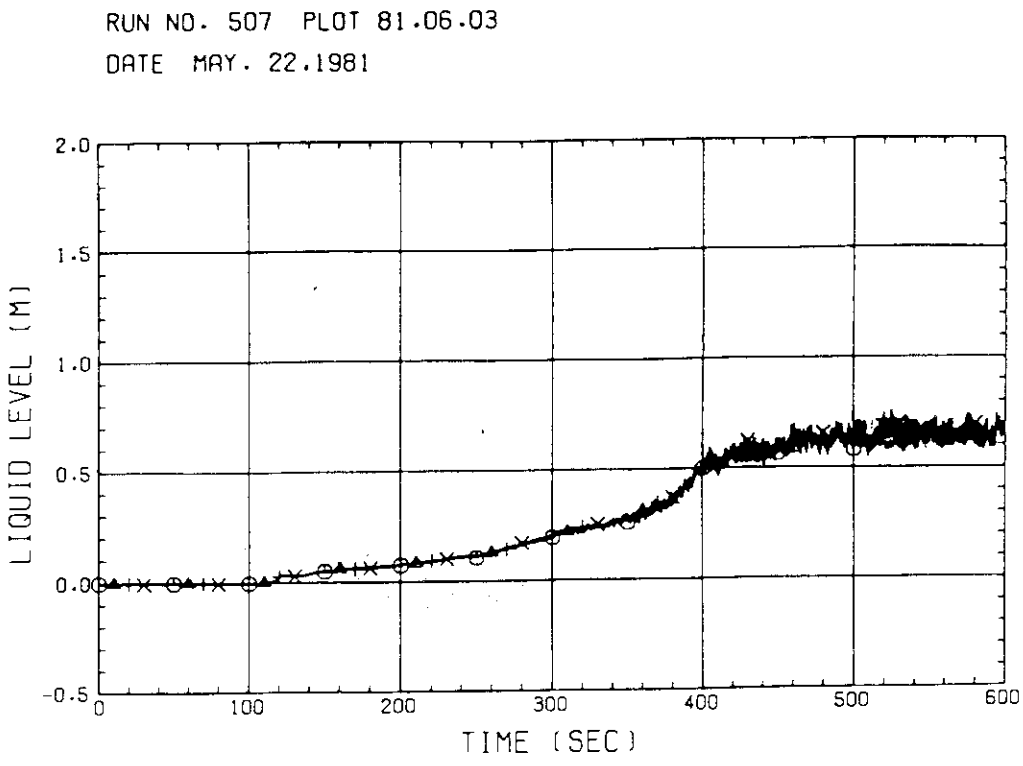

FIG. C-14(1) Collapsed Water Levels above UCSP (Bundles 1 through 4)

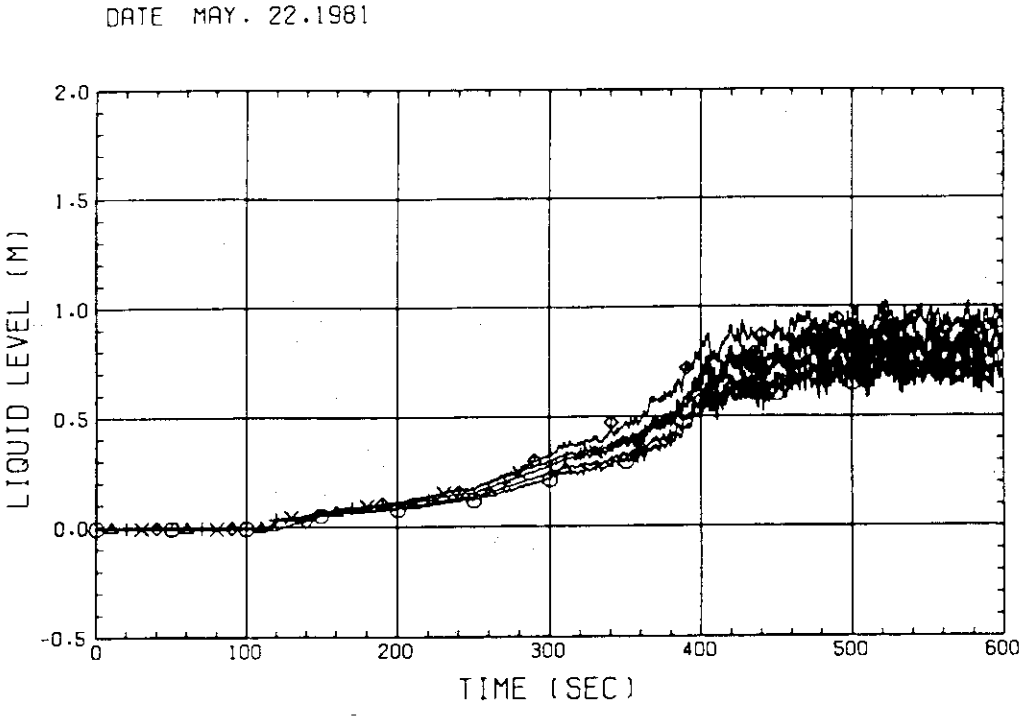

FIG. C-14(2) Collapsed Water Levels above UCSP (Bundles 5 through 8 and Core Baffle)

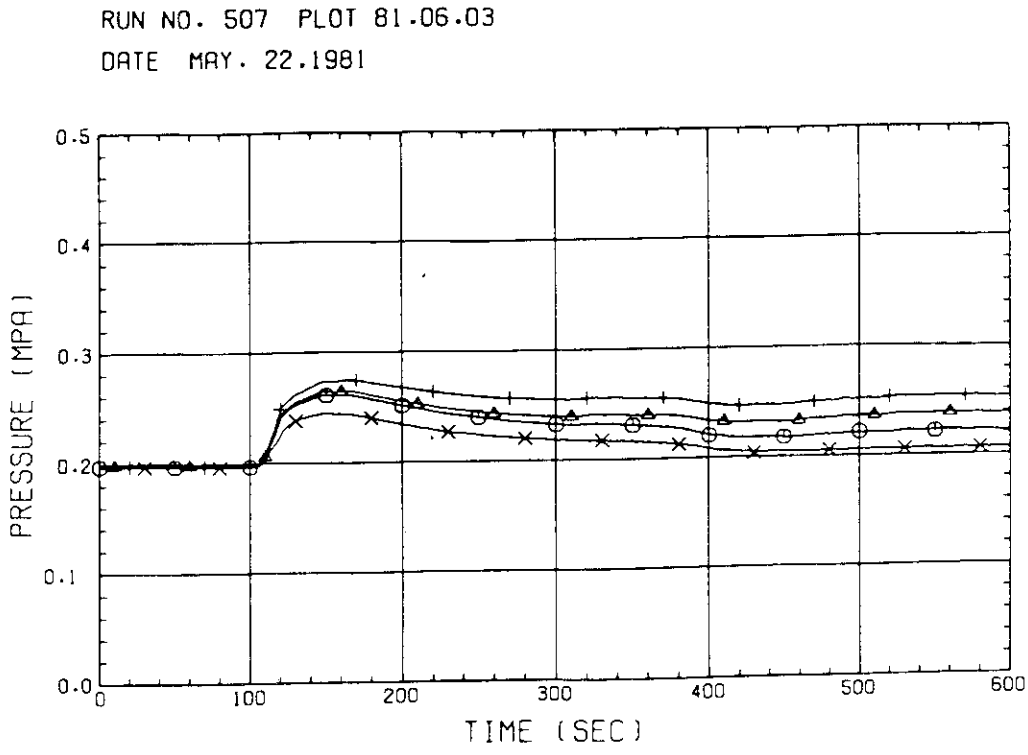

FIG. C-15 System Pressures at Top of Pressure Vessel, Core Center, Core Inlet and Upper Part of Downcomer

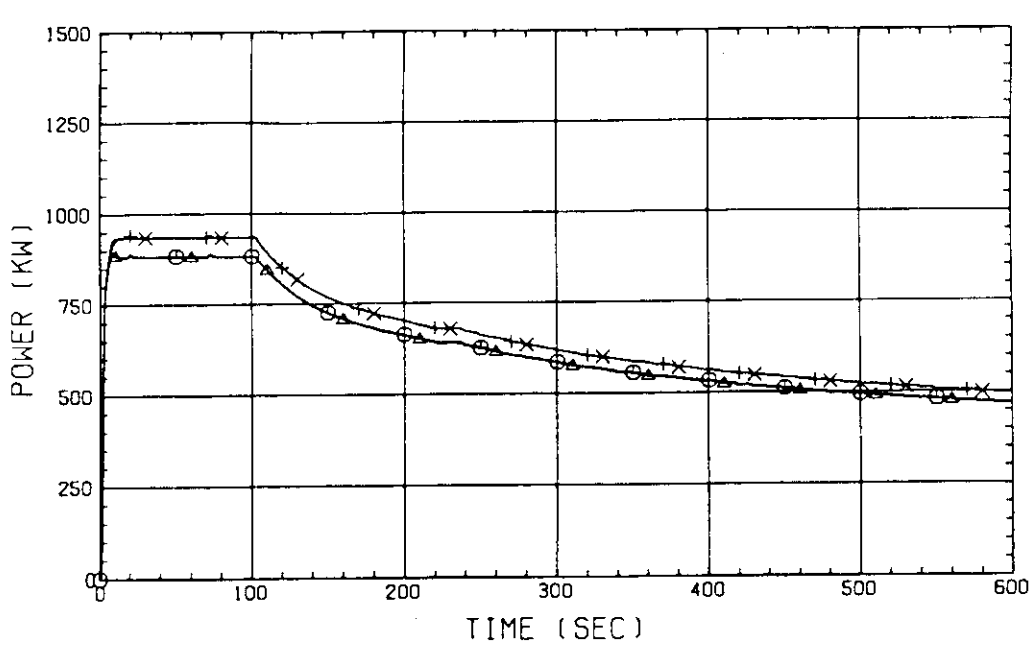

FIG. C-16(1) Heating Powers (Bundles 1 through 4)

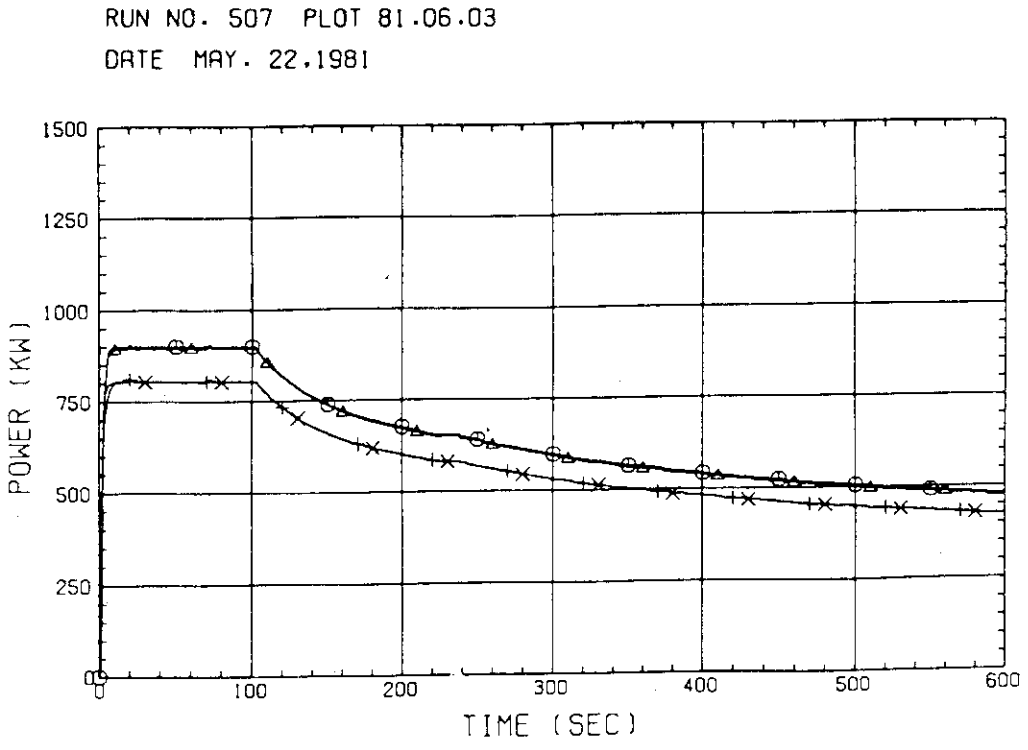

FIG. C-16(2) Heating Powers (Bundles 5 through 8)

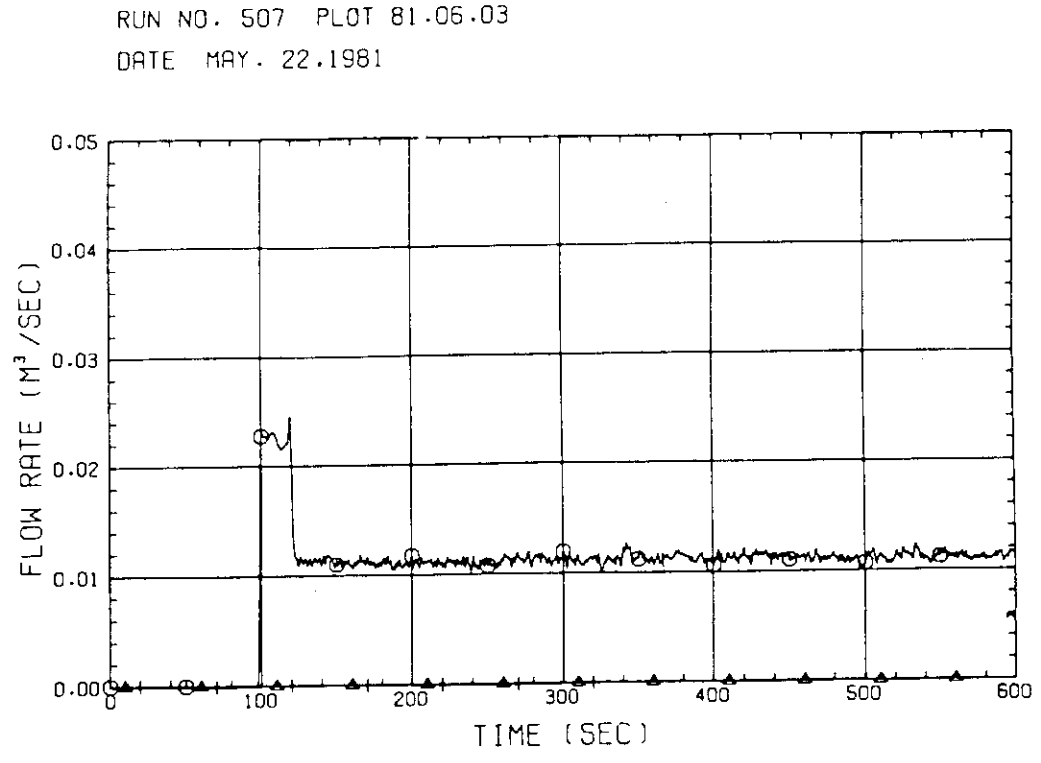

FIG. C-17 ECC Water Injection Rate into Lower Plenum

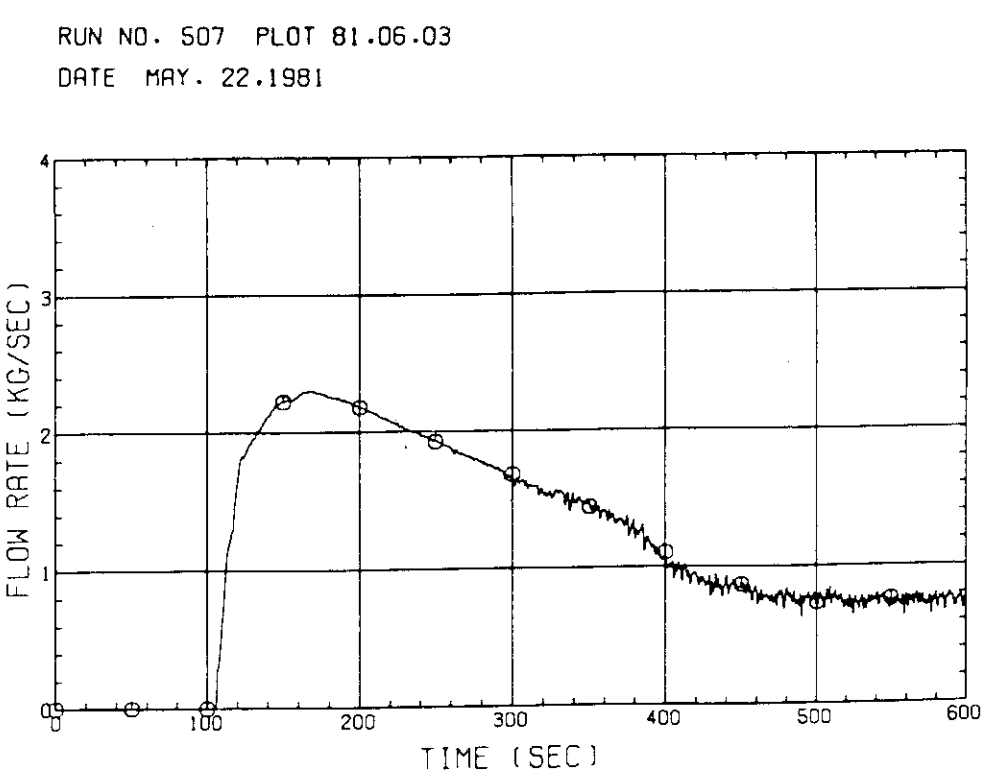

FIG. C-18 Steam Flow Rate at Intact Cold Leg

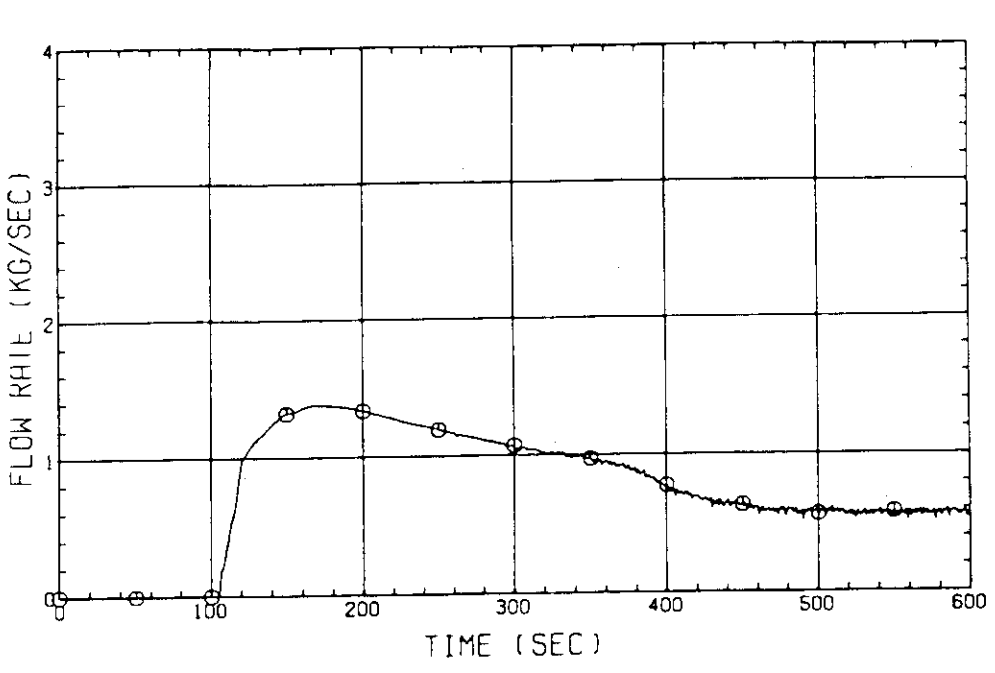

FIG. C-19 Steam Flow Rate at Steam-Water Separator Side Broken Cold Leg

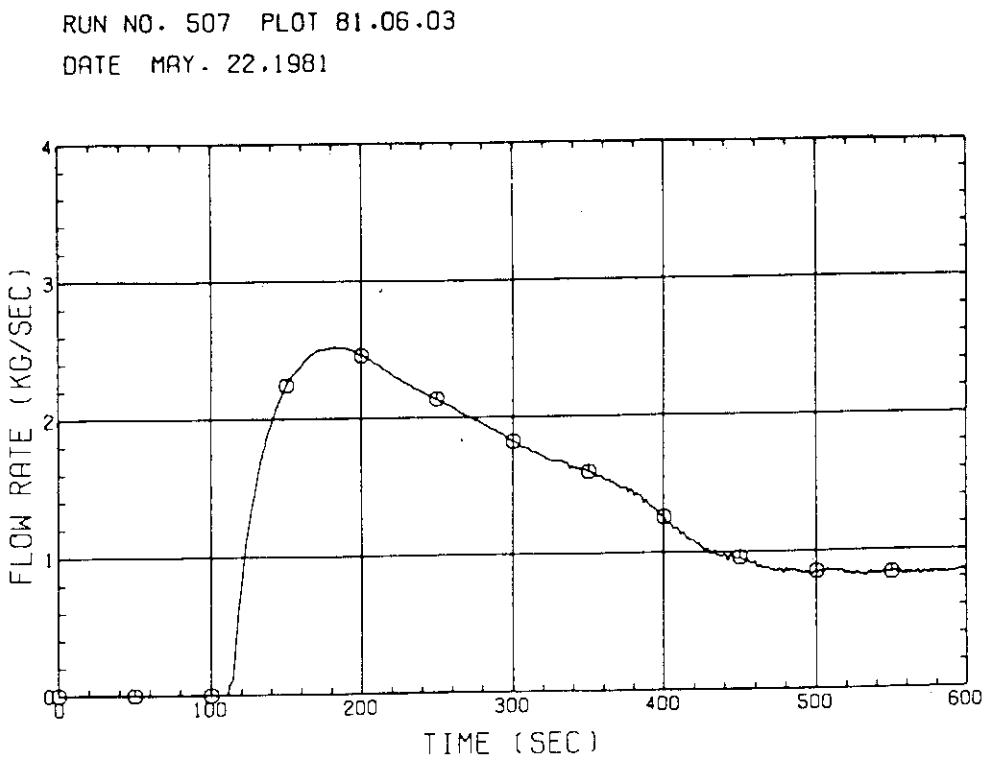

FIG. C-20 Steam Flow Rate between Containment Tanks-I and -II

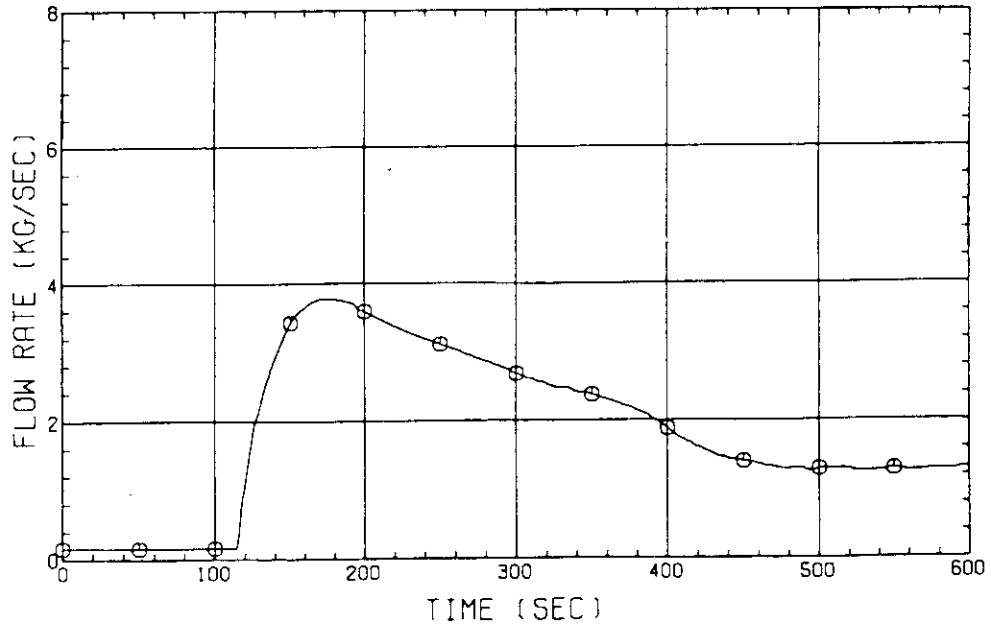

FIG. C-21 Steam Flow Rate at Discharge Line from Containment Tank-II

Appendix D
Selected Data from Test S1-02 (Run 508)

Note:

In Appendix D, selected data from Test S1-02 are introduced. Figure number for each measurement is the same as in Appendix B, except but the test identification character is D instead of B.

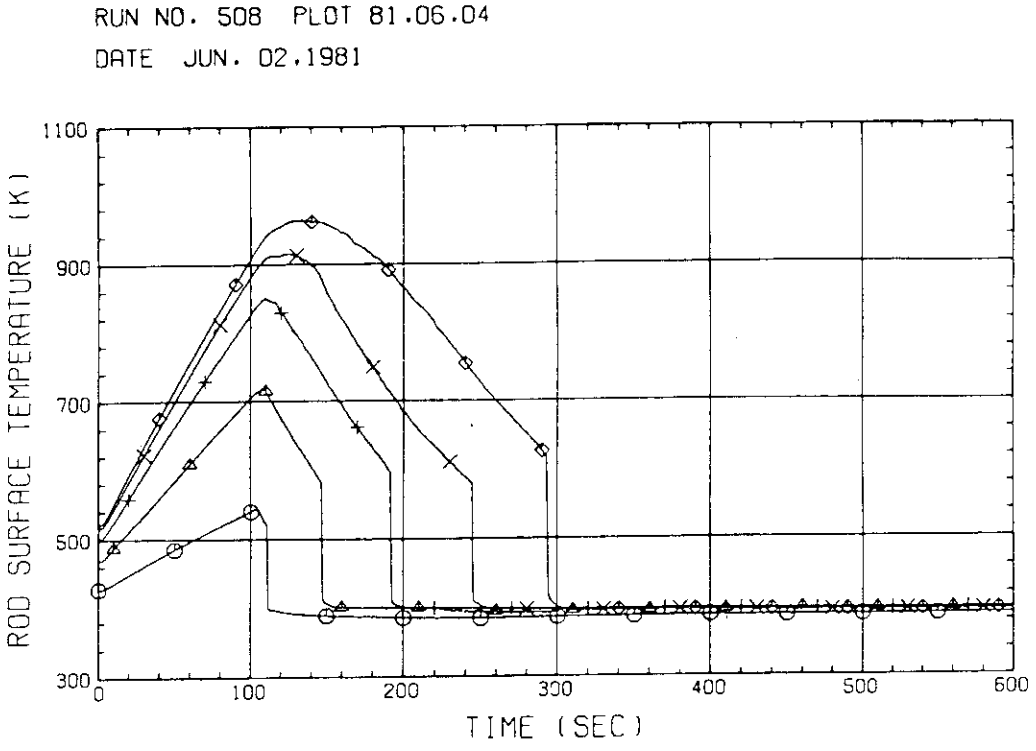

FIG. D-1(1) Heater Rod Temperatures (Lower Half of Bundle 1)

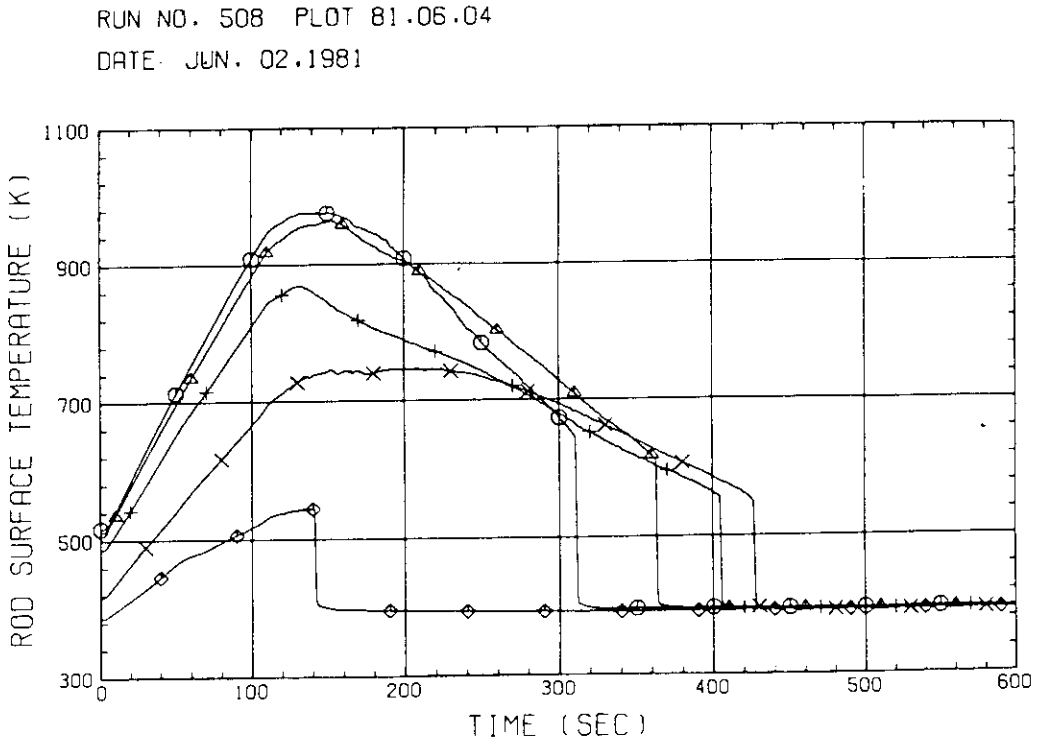

FIG. D-1(2) Heater Rod Temperatures (Upper Half of Bundle 1)

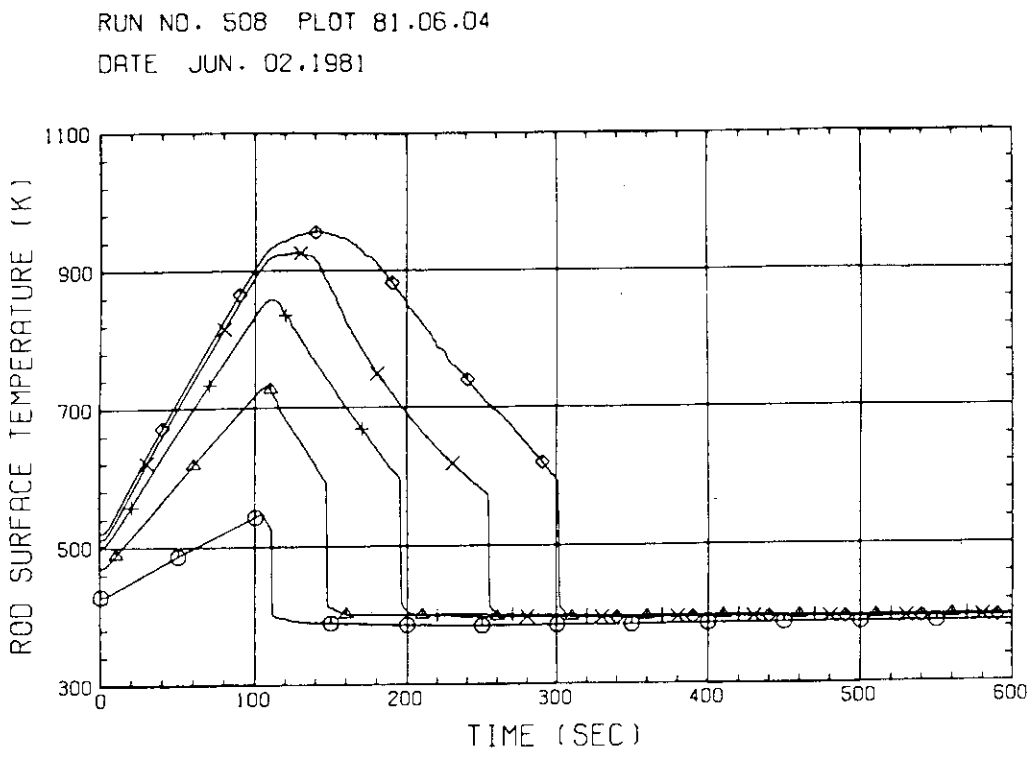

FIG. D-2(1) Heater Rod Temperatures (Lower Half of Bundle 2)

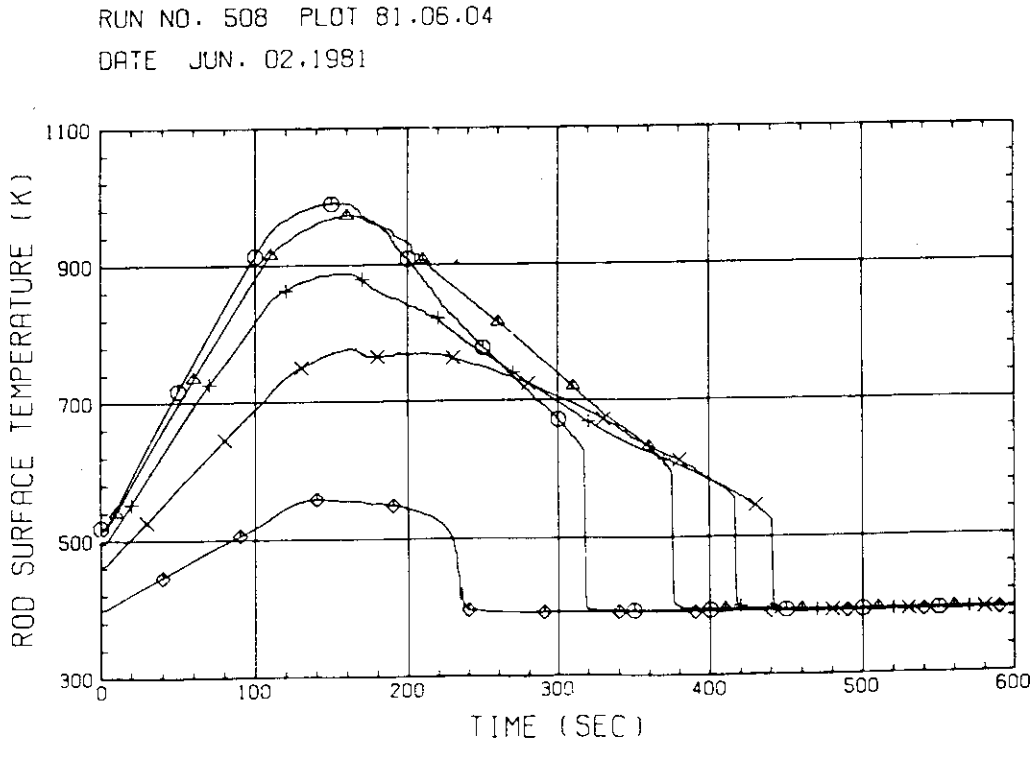

FIG. D-2(2) Heater Rod Temperatures (Upper Half of Bundle 2)

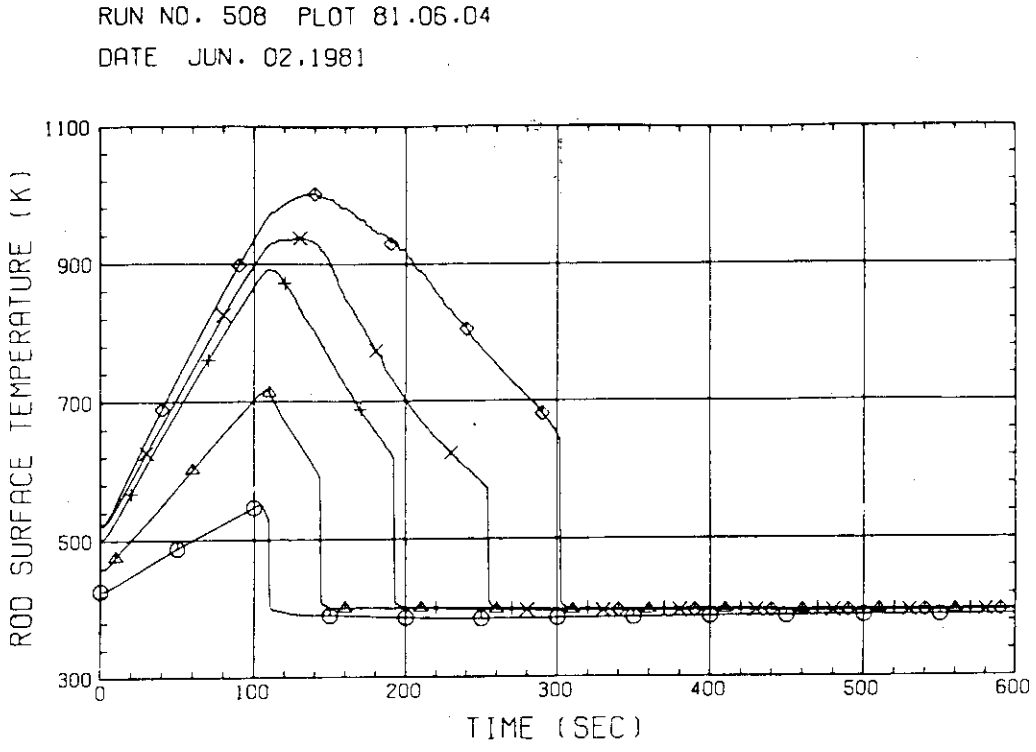

FIG. D-3(1) Heater Rod Temperatures (Lower Half of Bundle 3)

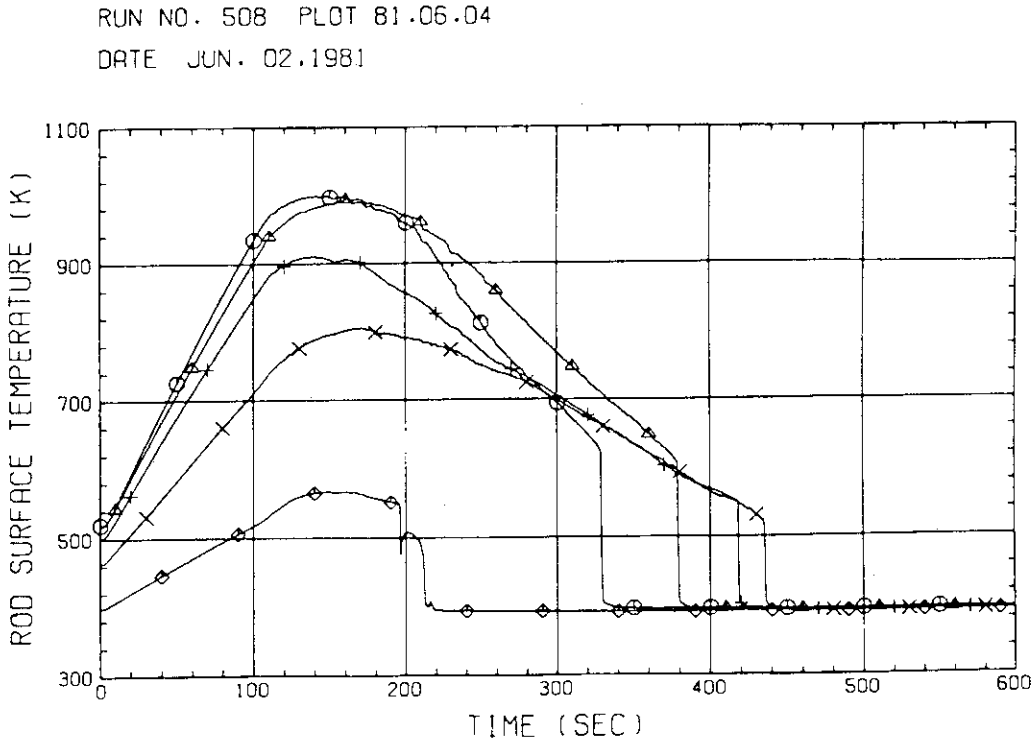

FIG. D-3(2) Heater Rod Temperatures (Upper Half of Bundle 3)

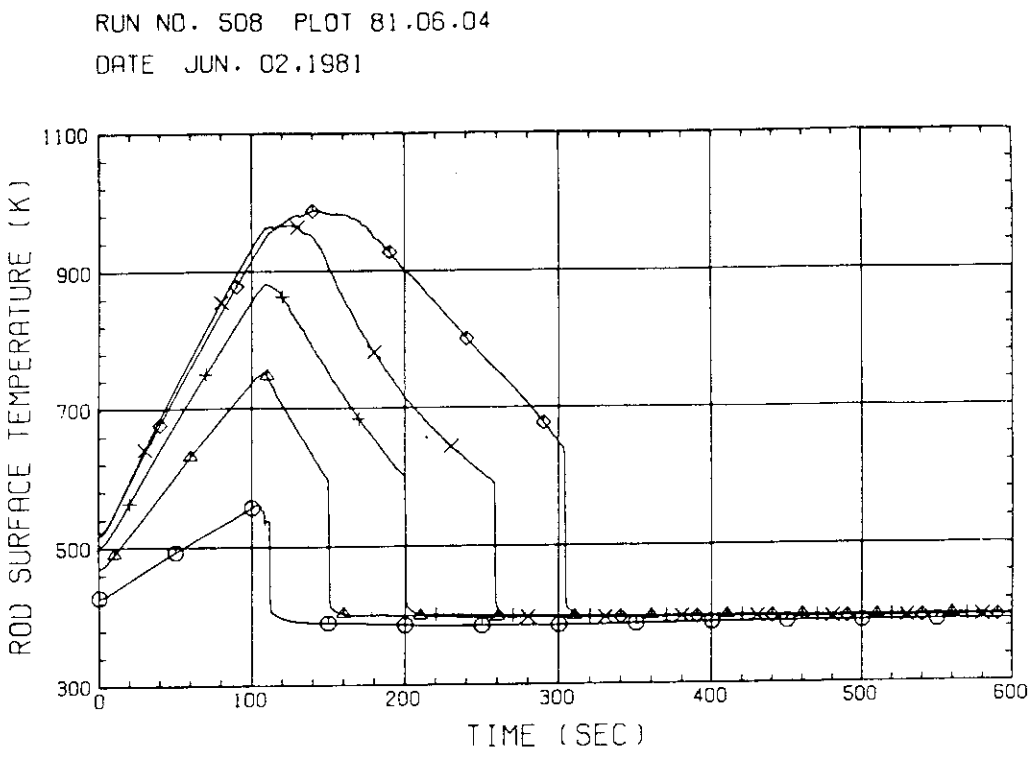

FIG. D-4(1) Heater Rod Temperatures (Lower Half of Bundle 4)

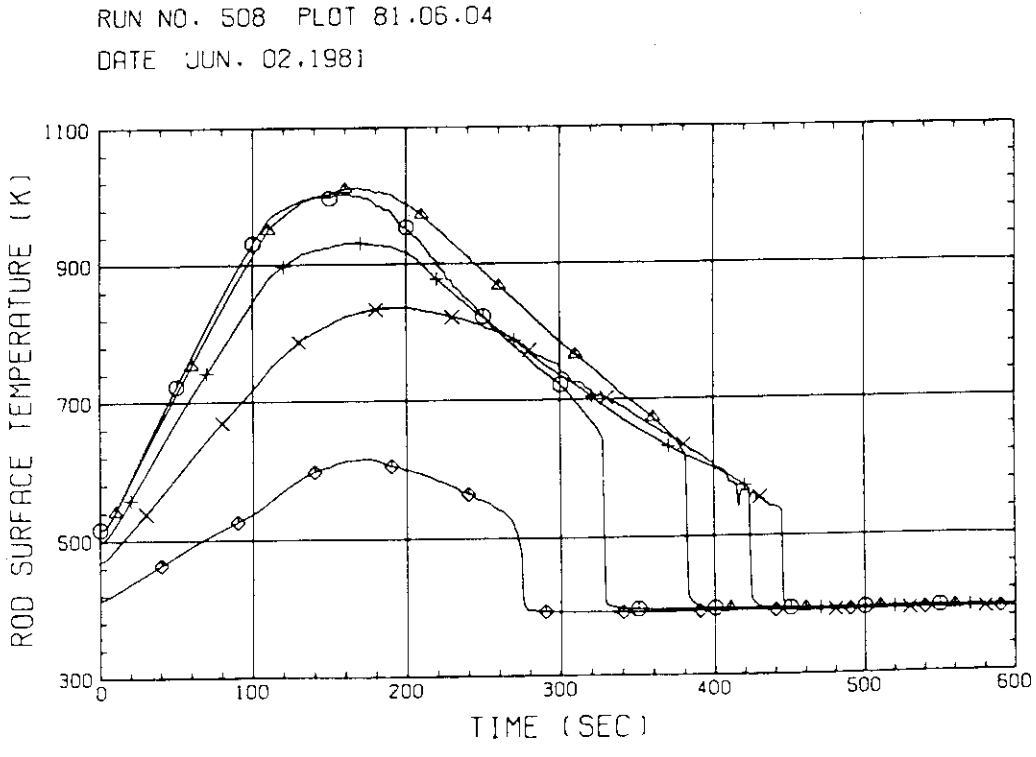

FIG. D-4(2) Heater Rod Temperatures (Upper Half of Bundle 4)

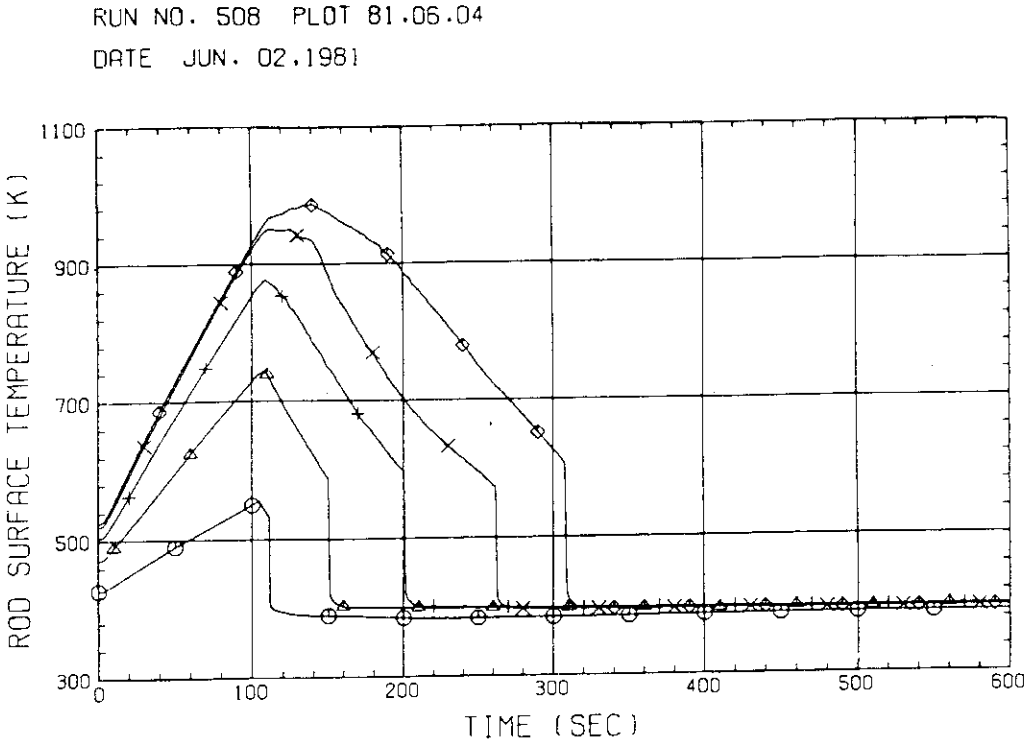

FIG. D-5(1) Heater Rod Temperatures (Lower Half of Bundle 5)

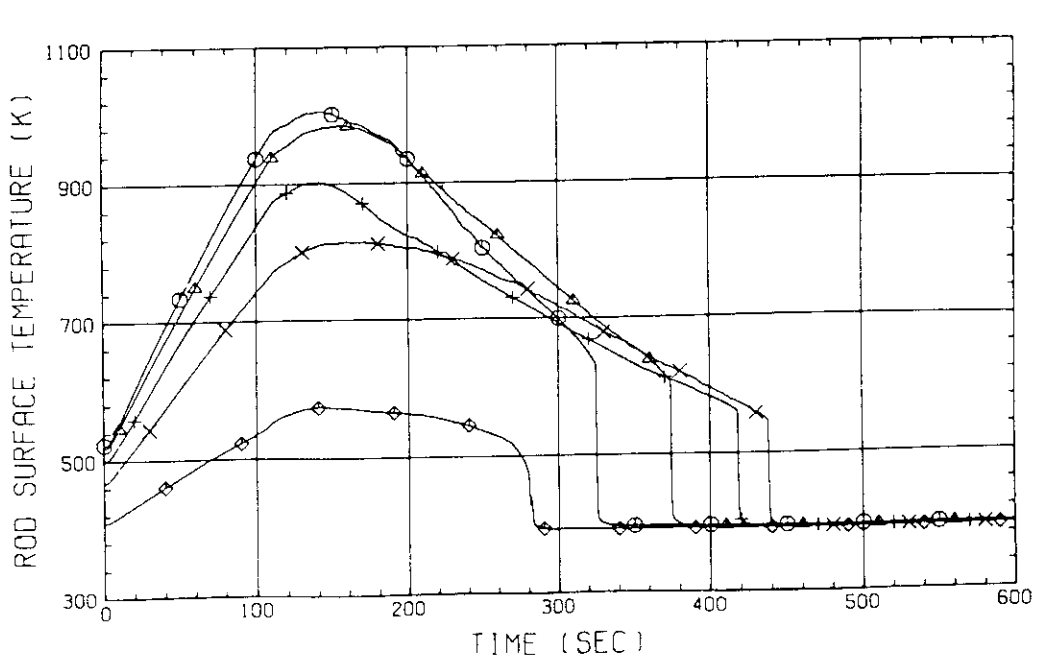

FIG. D-5(2) Heater Rod Temperatures (Upper Half of Bundle 5)

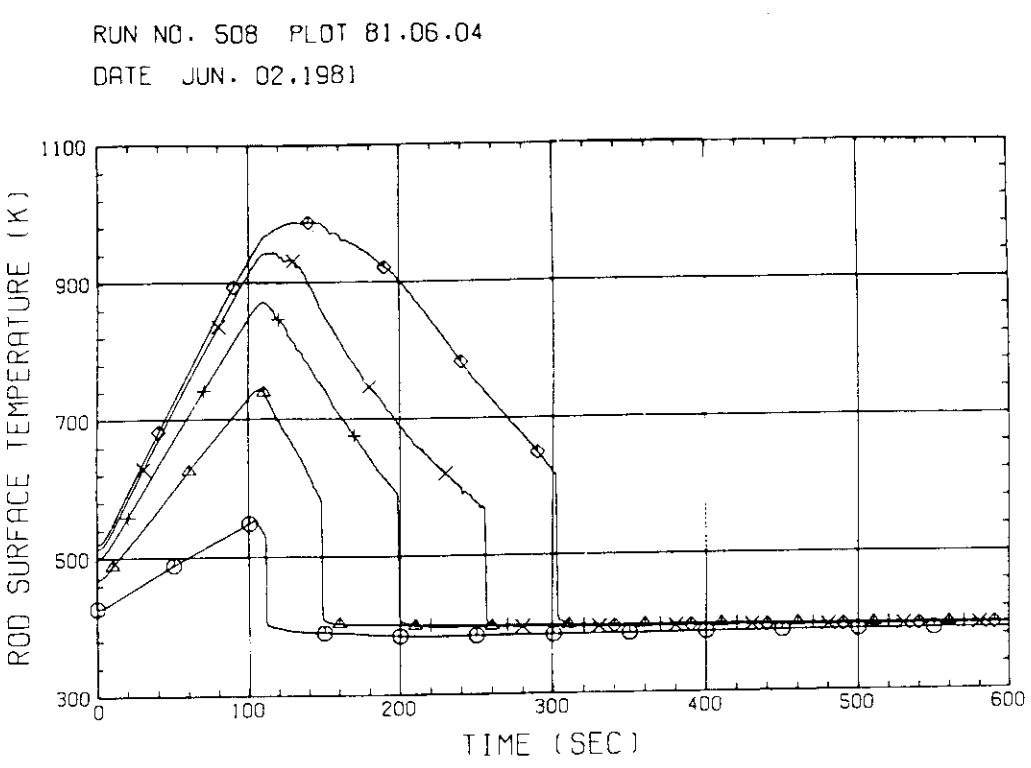

FIG. D-6(1) Heater Rod Temperatures (Lower Half of Bundle 6)

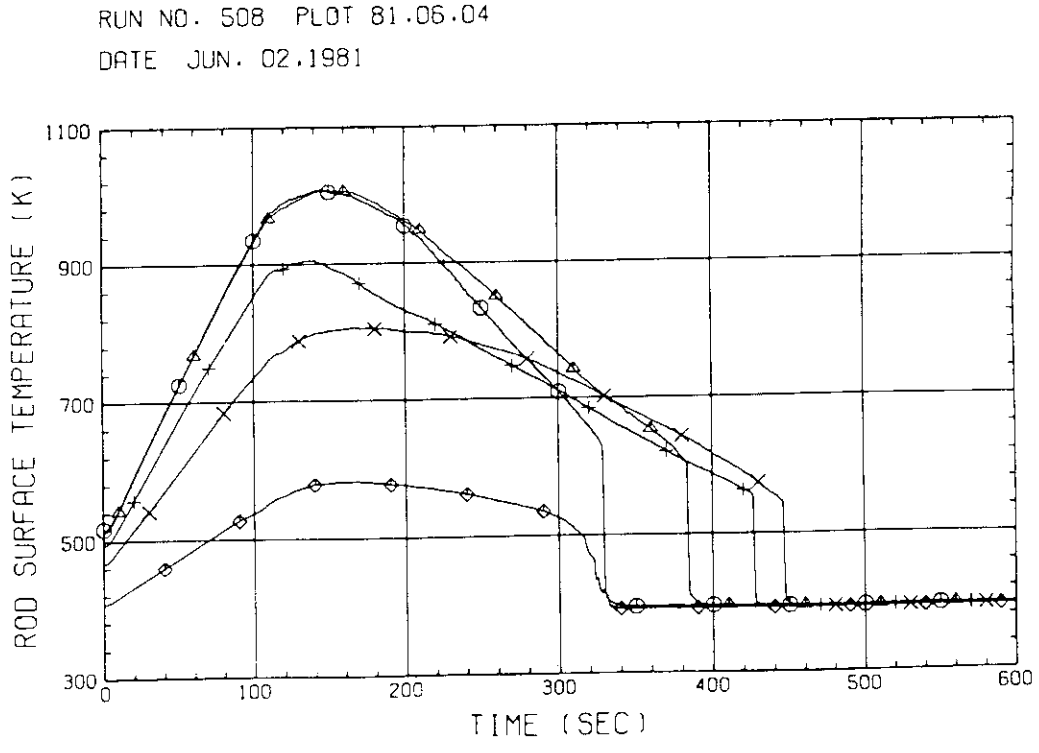

FIG. D-6(2) Heater Rod Temperatures (Upper Half of Bundle 6)

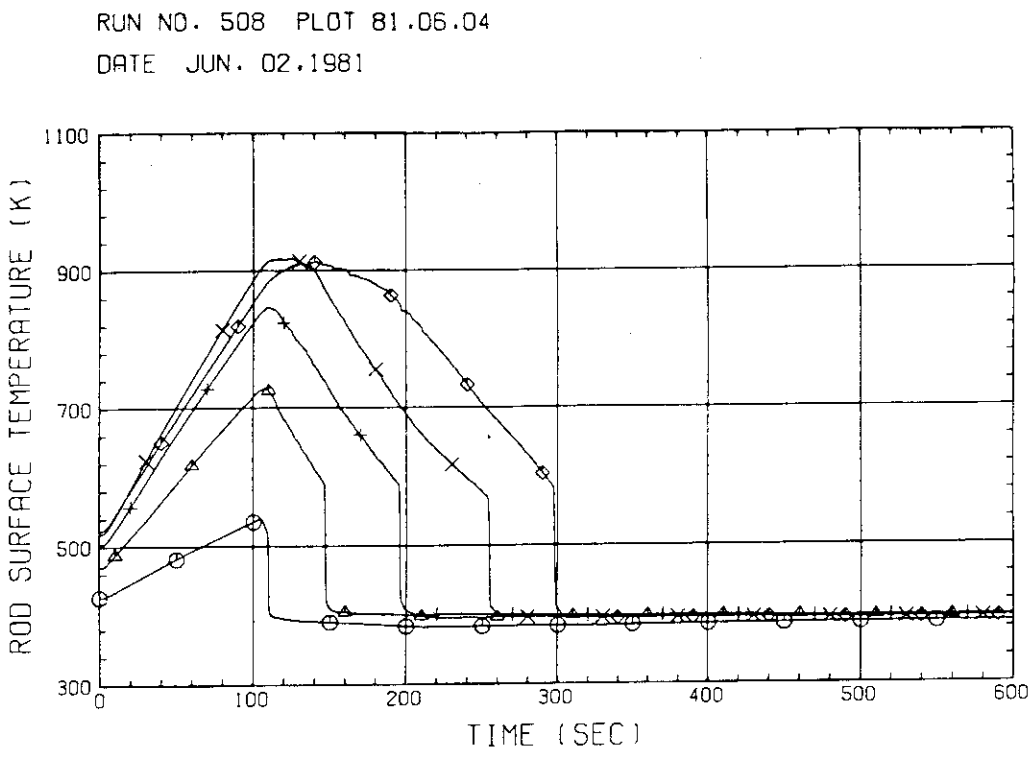

FIG. D-7(1) Heater Rod Temperatures (Lower Half of Bundle 7)

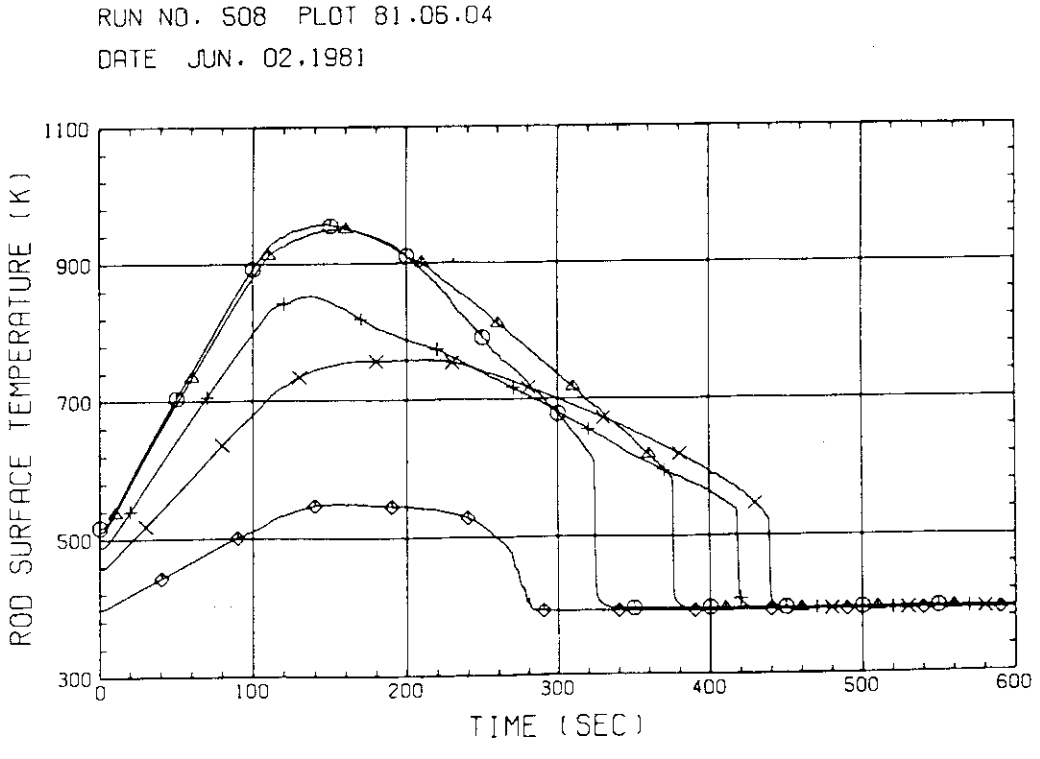

FIG. D-7(2) Heater Rod Temperatures (Upper Half of Bundle 7)

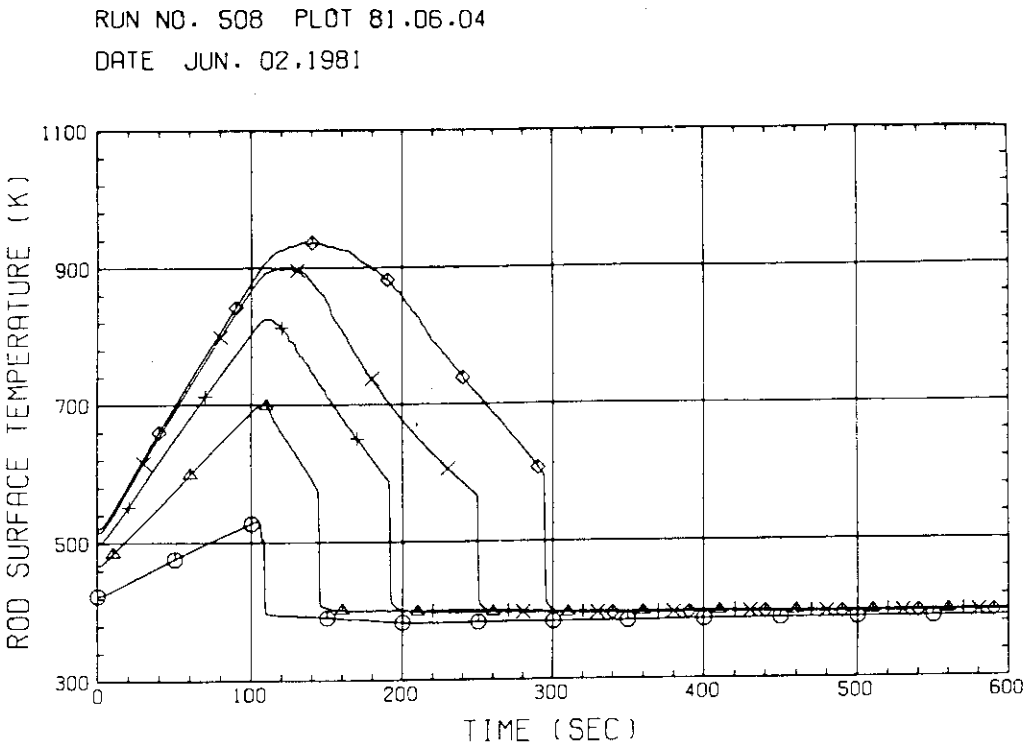

FIG. D-8(1) Heater Rod Temperatures (Lower Half of Bundle 8)

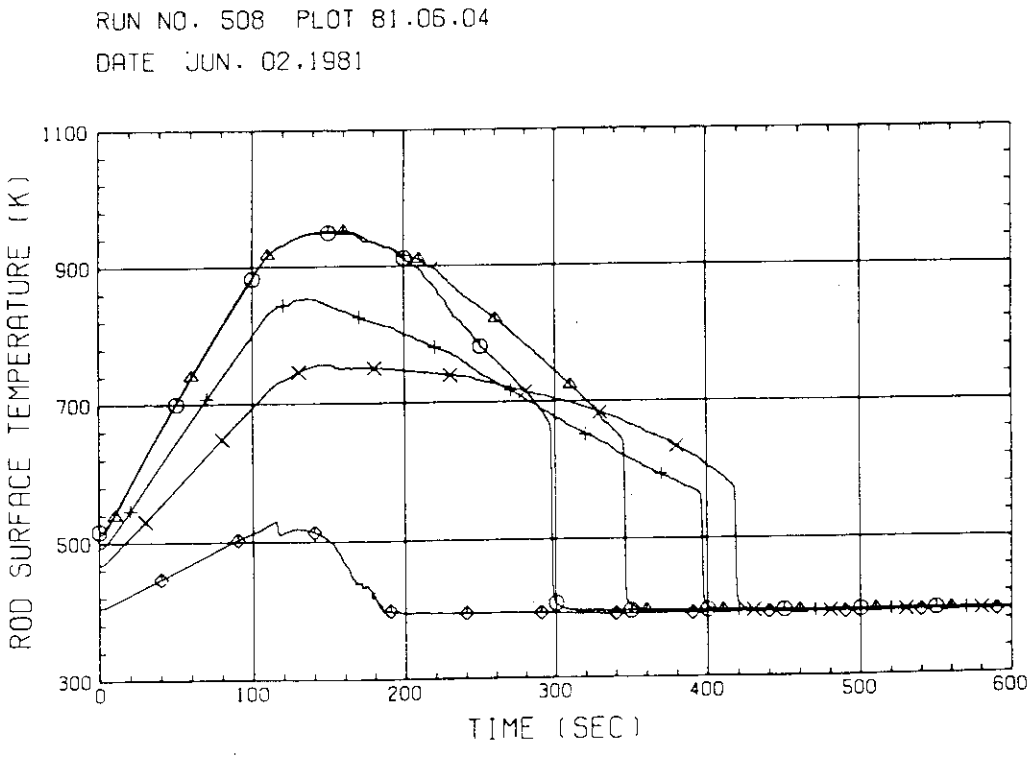

FIG. D-8(2) Heater Rod Temperatures (Upper Half of Bundle 8)

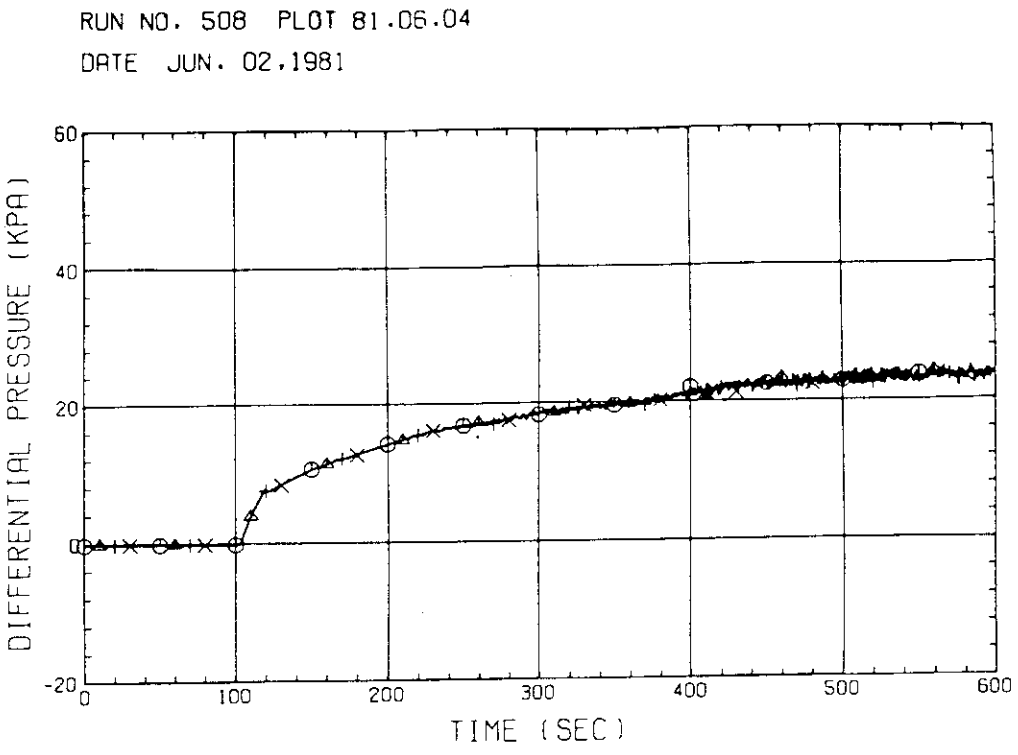

FIG. D-9(1) Differential Pressures across Core Full Height (Bundles 1 through 4)

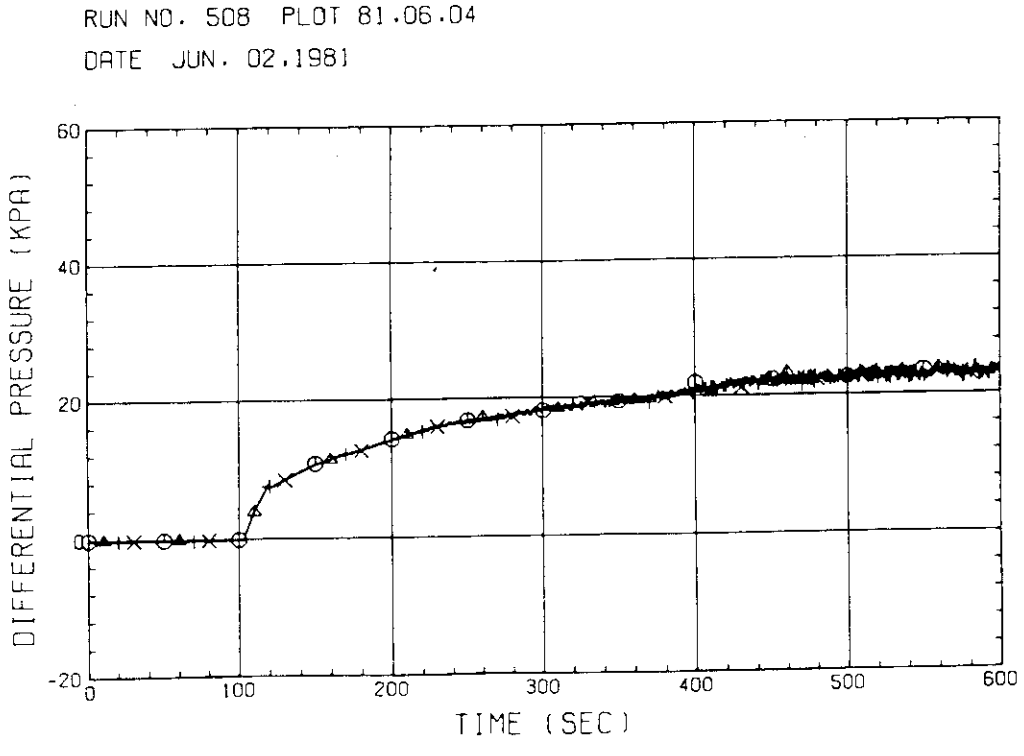

FIG. D-9(2) Differential Pressures across Core Full Height (Bundles 5 through 8)

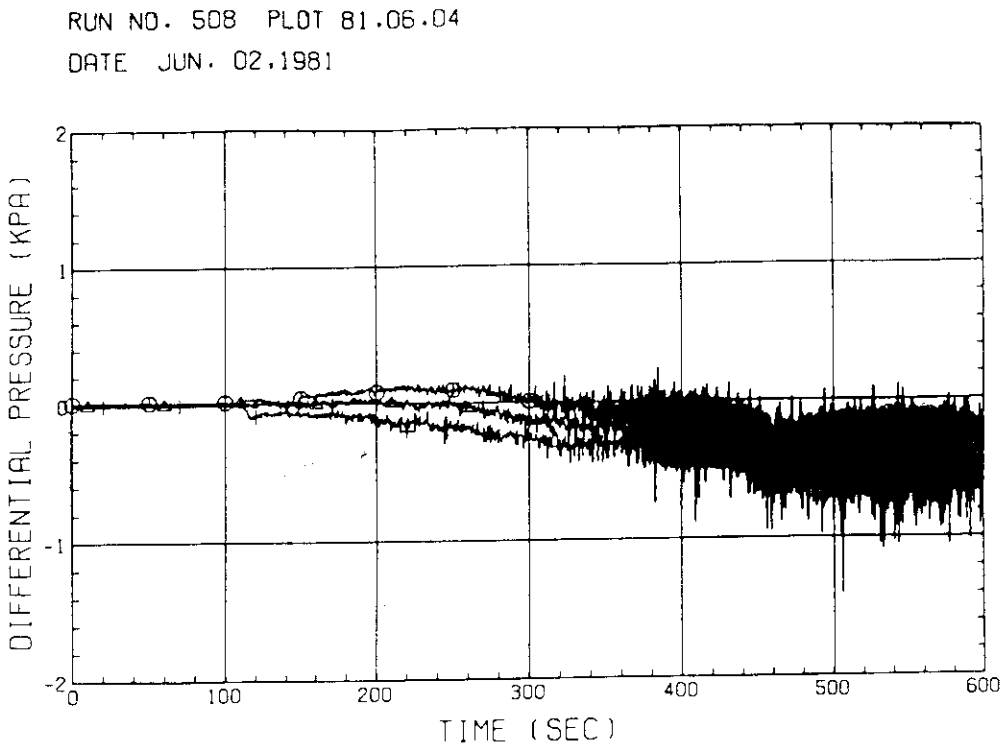

FIG. D-10 Horizontal Differential Pressures in Core (Pressure in Bundle 5 - Pressure in Bundle 8)

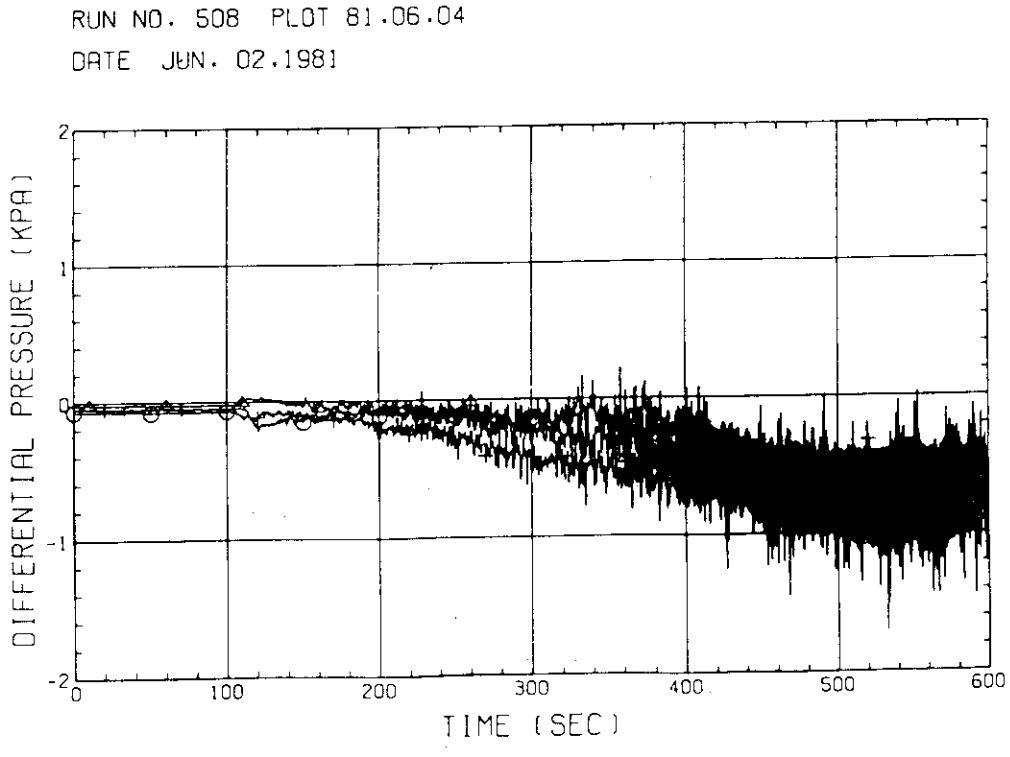

FIG. D-11 Horizontal Differential Pressures in Core (Pressure in Bundle 1 - Pressure in Bundle 4)

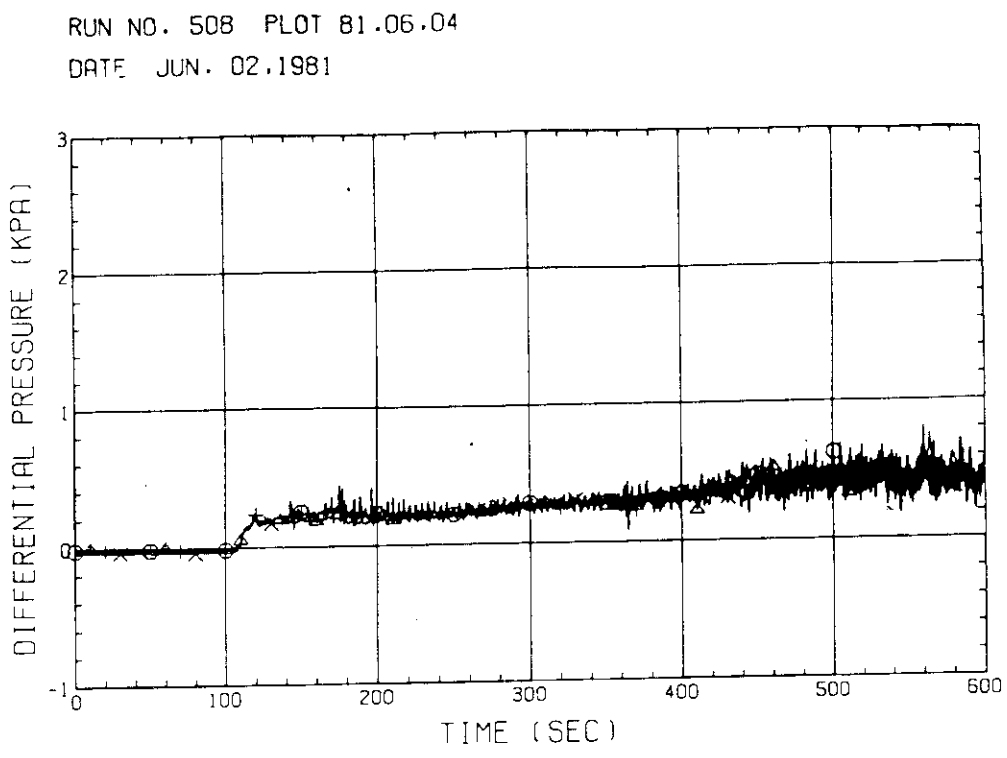

FIG. D-12(1) Differential Pressures across End Box Tie Plates (Bundles 1 through 4)

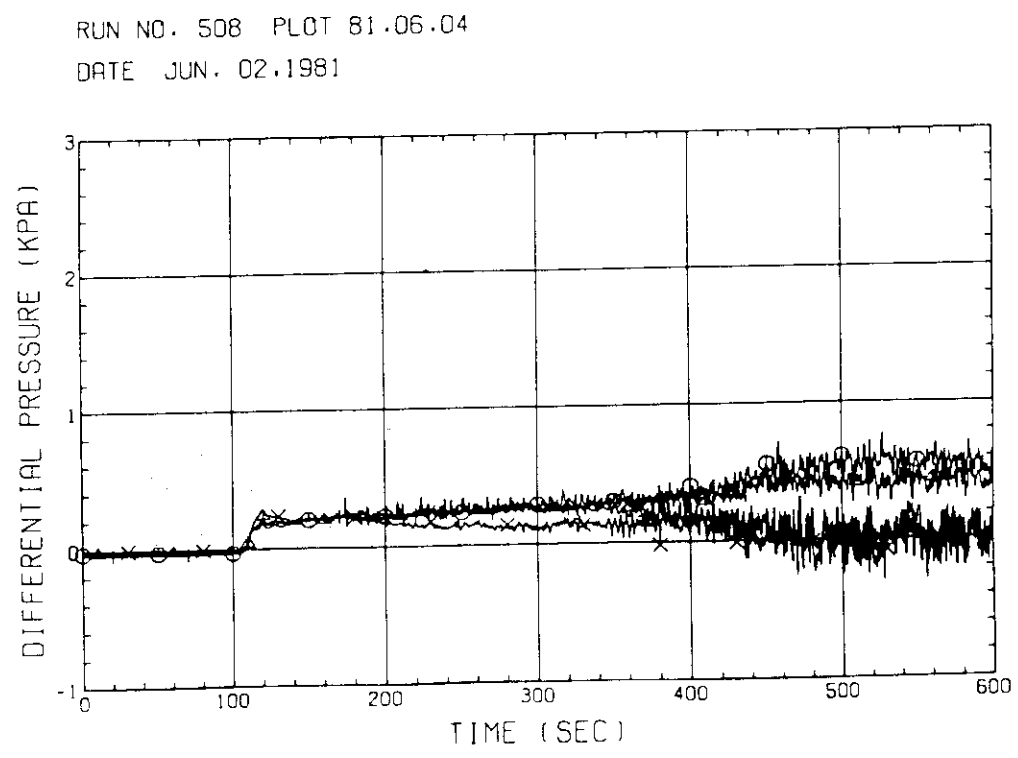

FIG. D-12(2) Differential Pressures across End Box Tie Plates (Bundles 5 through 8)

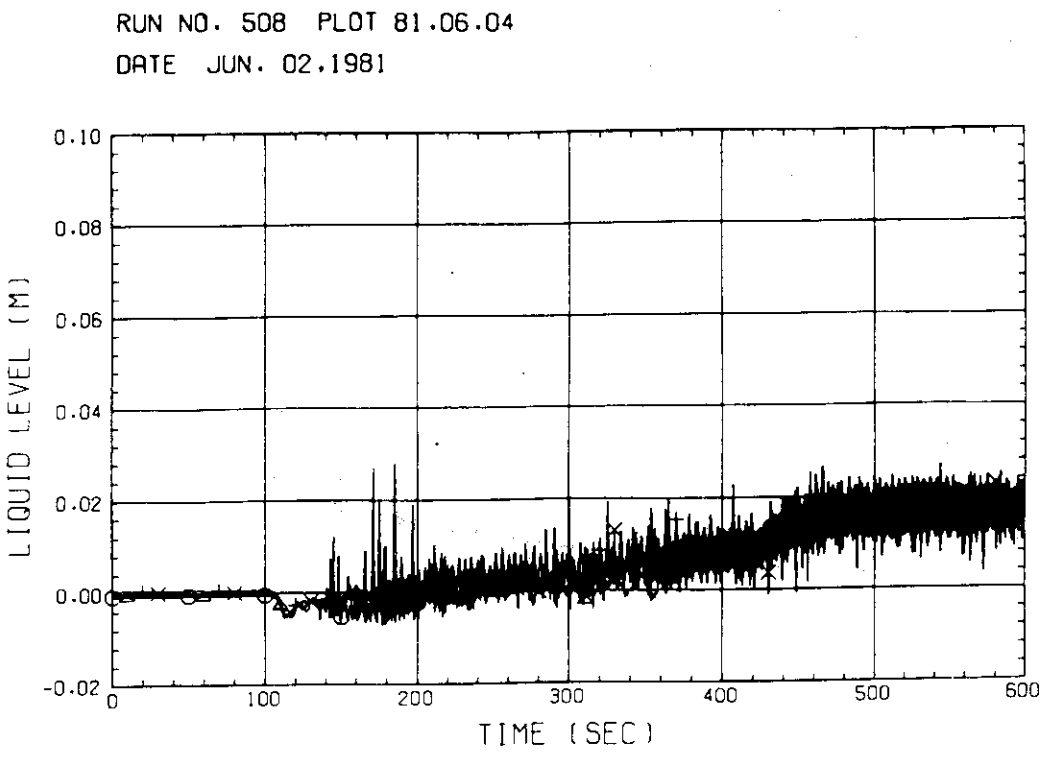

FIG. D-13(1) Collapsed Water Levels in End Boxes (Bundles 1 through 4)

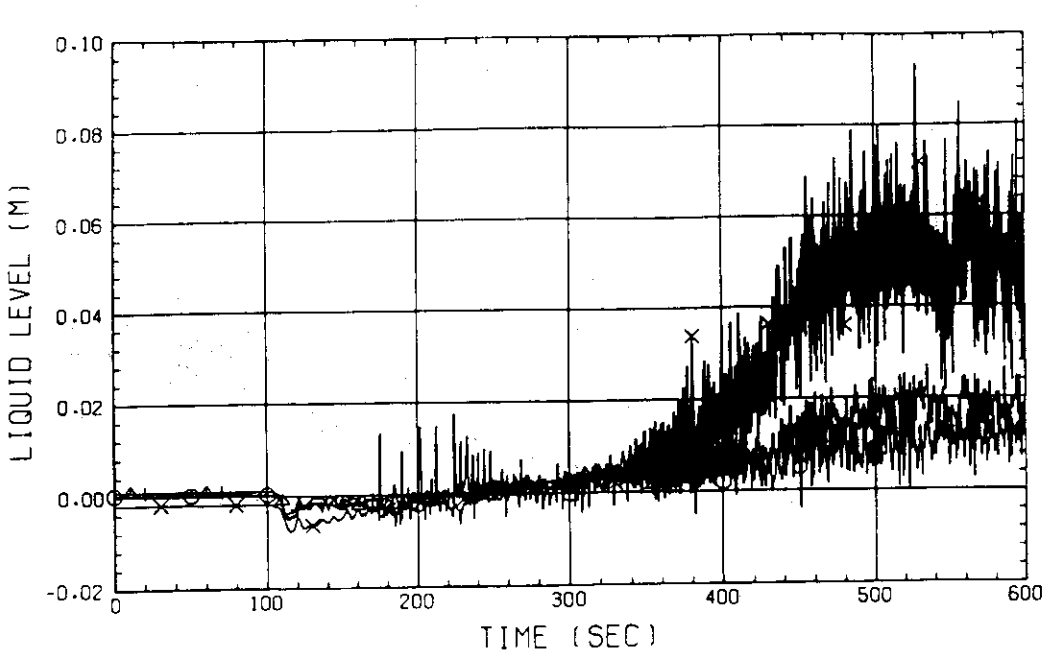

FIG. D-13(2) Collapsed Water Levels in End Boxes (Bundles 5 through 8)

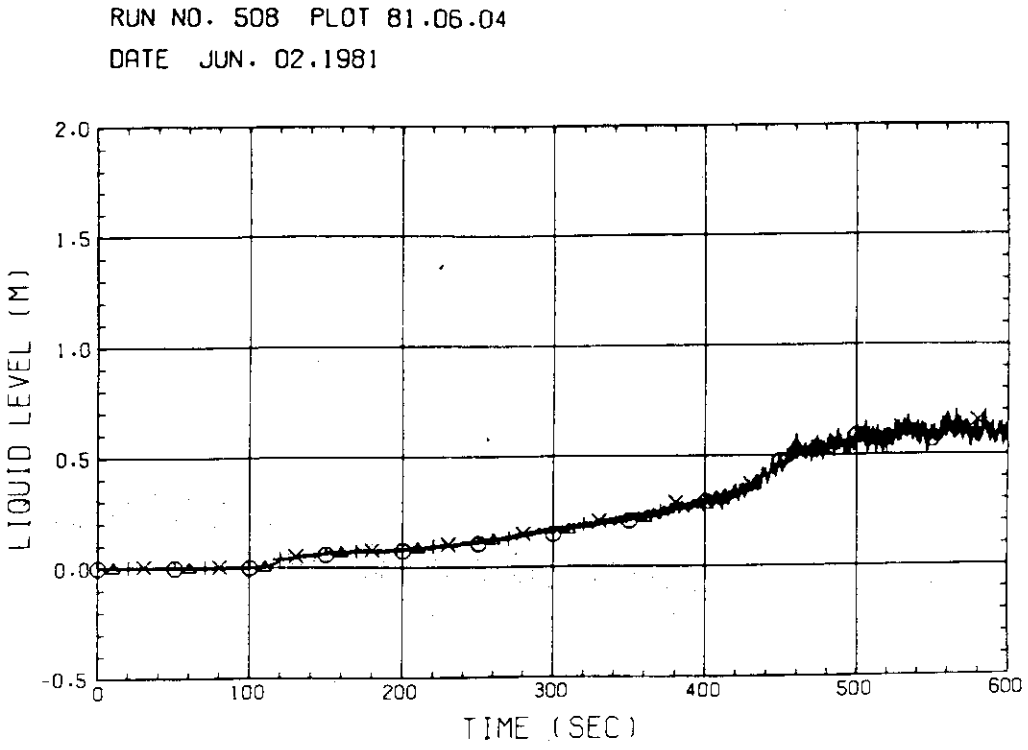

FIG. D-14(1) Collapsed Water Levels above UCSP (Bundles 1 through 4)

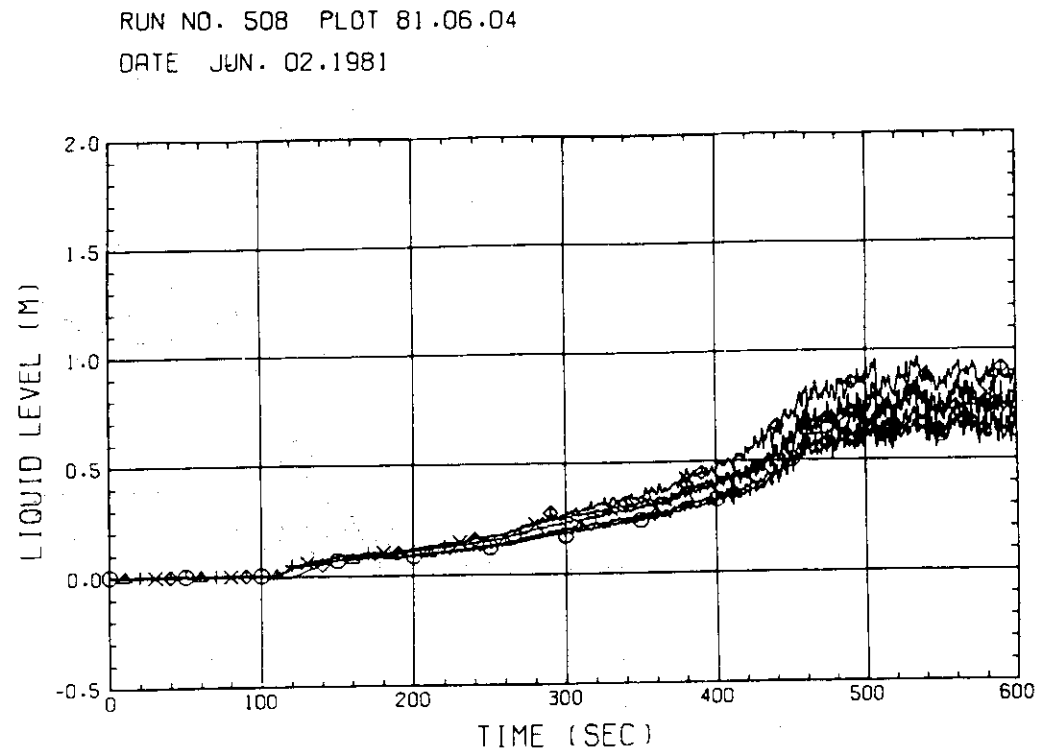

FIG. D-14(2) Collapsed Water Levels above UCSP (Bundles 5 through 8 and Core Baffle)

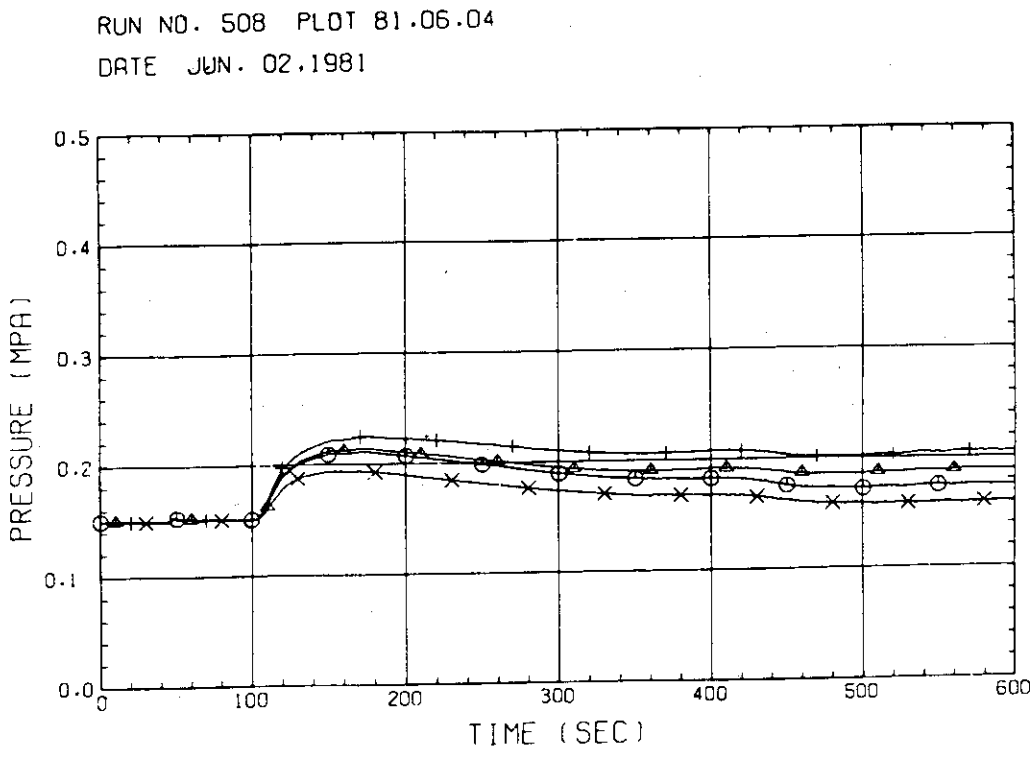

FIG. D-15 System Pressures at Top of Pressure Vessel, Core Center, Core Inlet and Upper Part of Downcomer

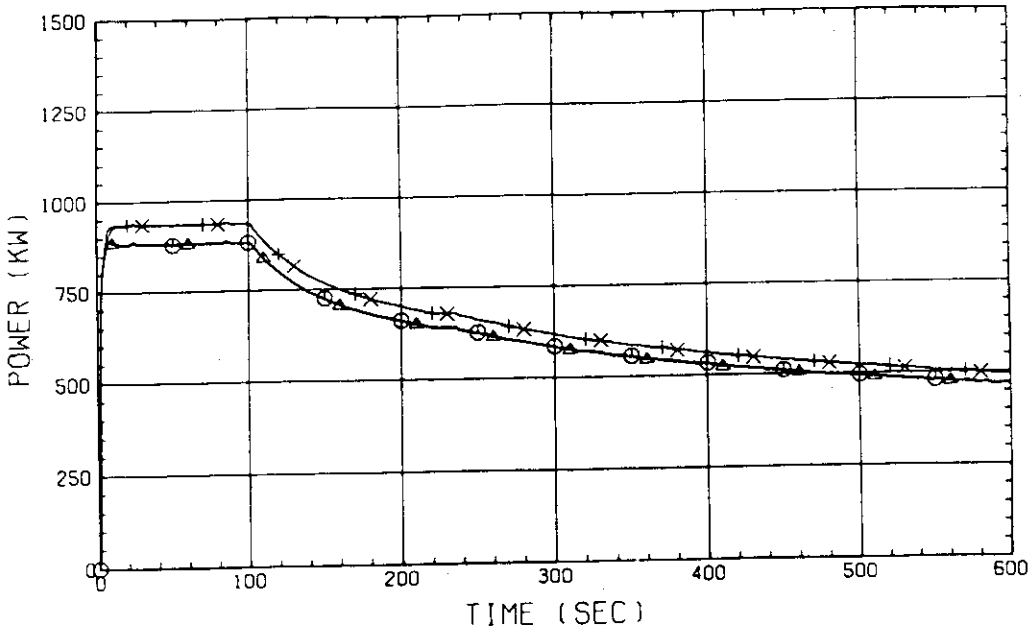

FIG. D-16(1) Heating Powers (Bundles 1 thrgouh 4)

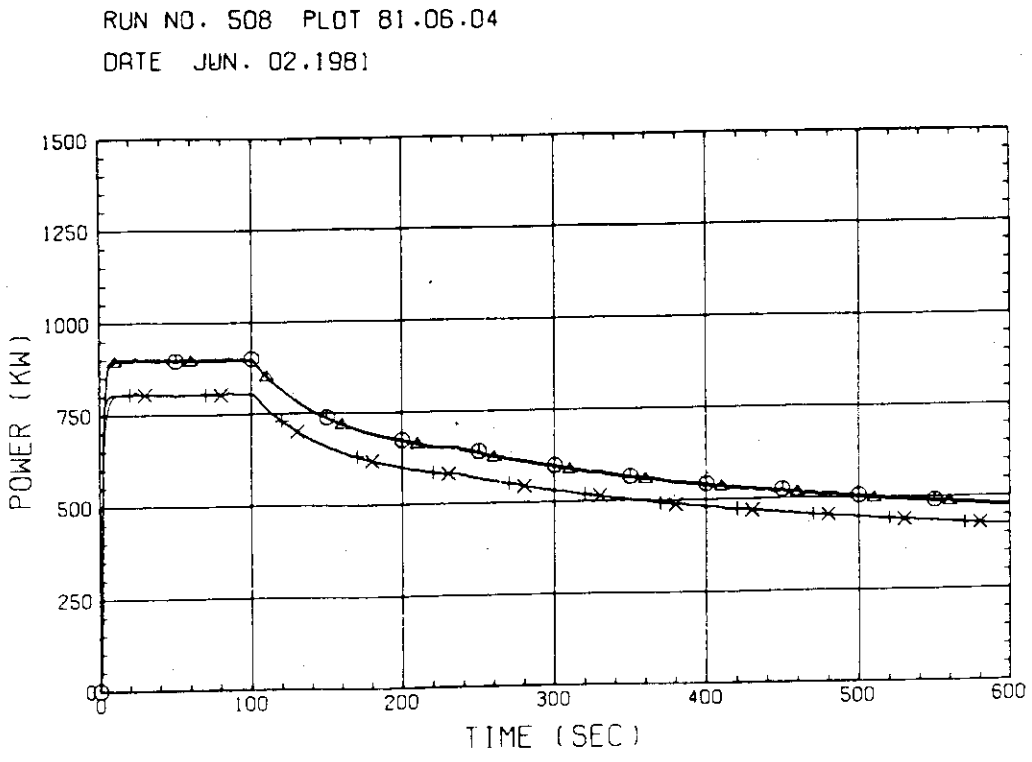

FIG. D-16(2) Heating Powers (Bundles 5 through 8)

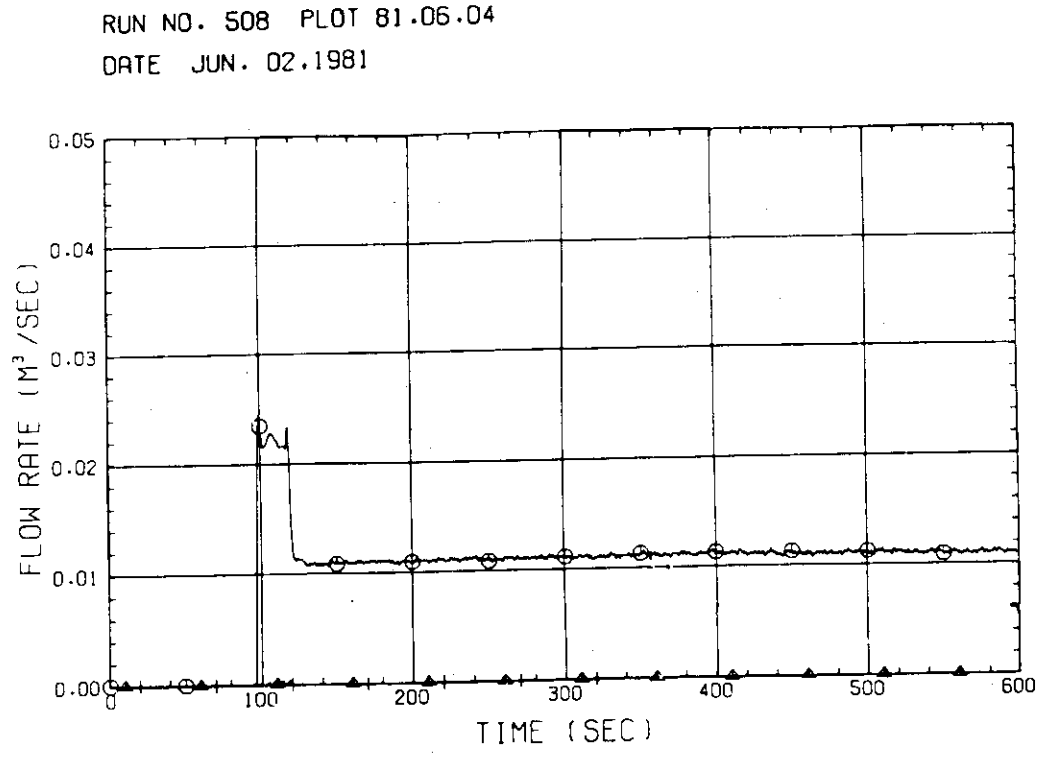

FIG. D-17 ECC Water Injection Rate into Lower Plenum

RUN NO. 508 PLOT 81.06.04
DATE JUN. 02.1981

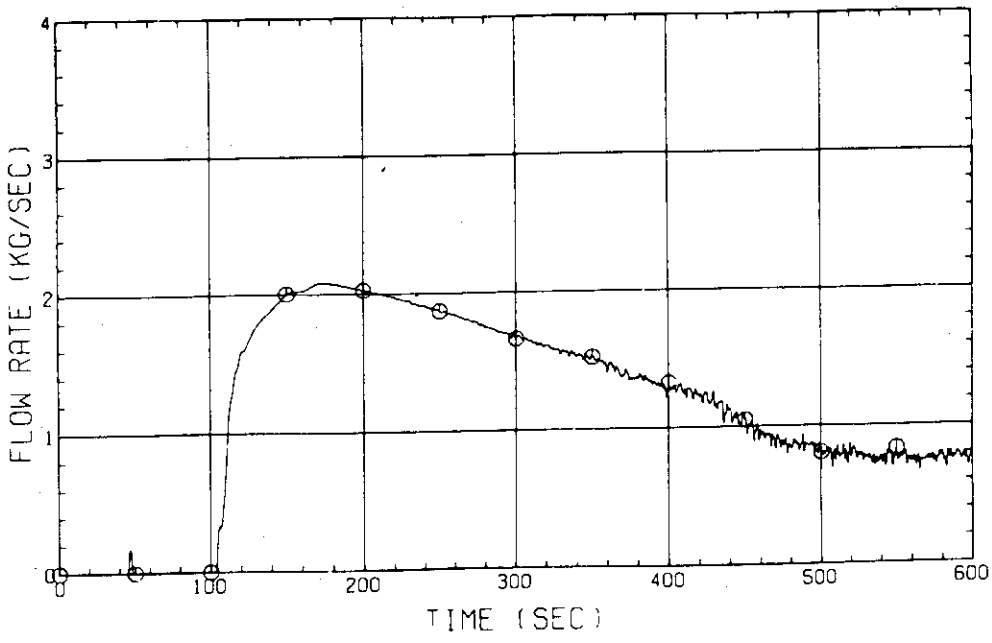

FIG. D-18 Steam Flow Rate at Intact Cold Leg

RUN NO. 508 PLOT 81.06.04
DATE JUN. 02.1981

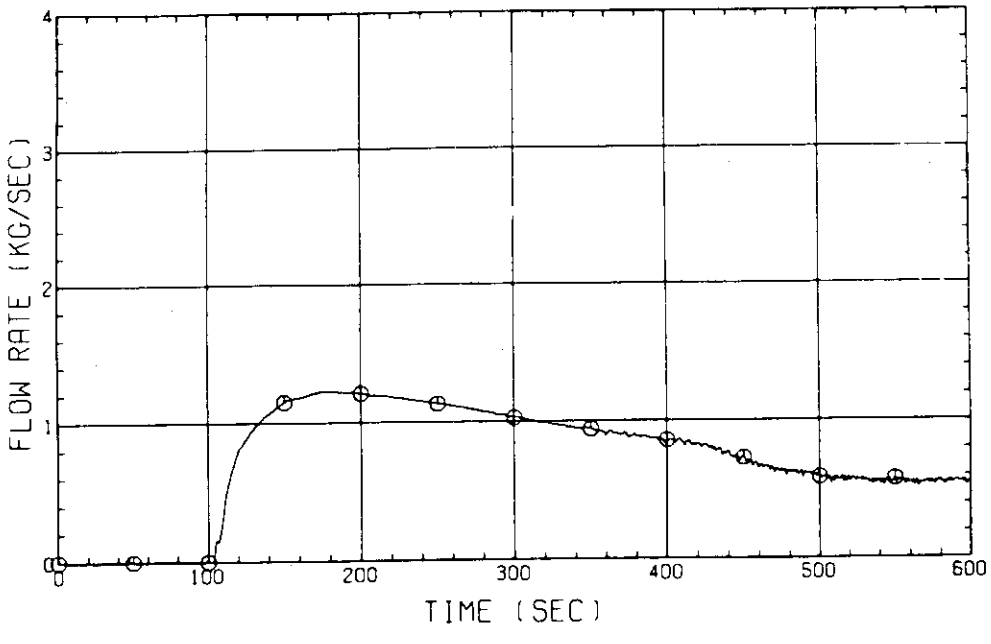

FIG. D-19 Steam Flow Rate at Steam-Water Separator Side Broken Cold Leg

RUN NO. 508 PLOT 81.06.04
DATE JUN. 02.1981

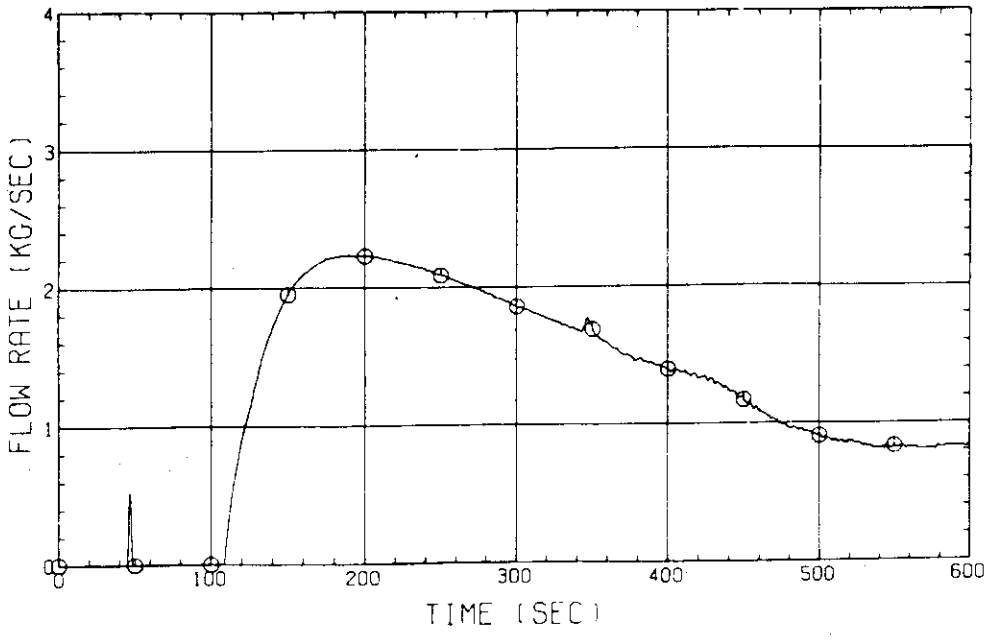

FIG. D-20 Steam Flow Rate between Containment Tanks-I and -II

RUN NO. 508 PLOT 81.06.04
DATE JUN. 02.1981

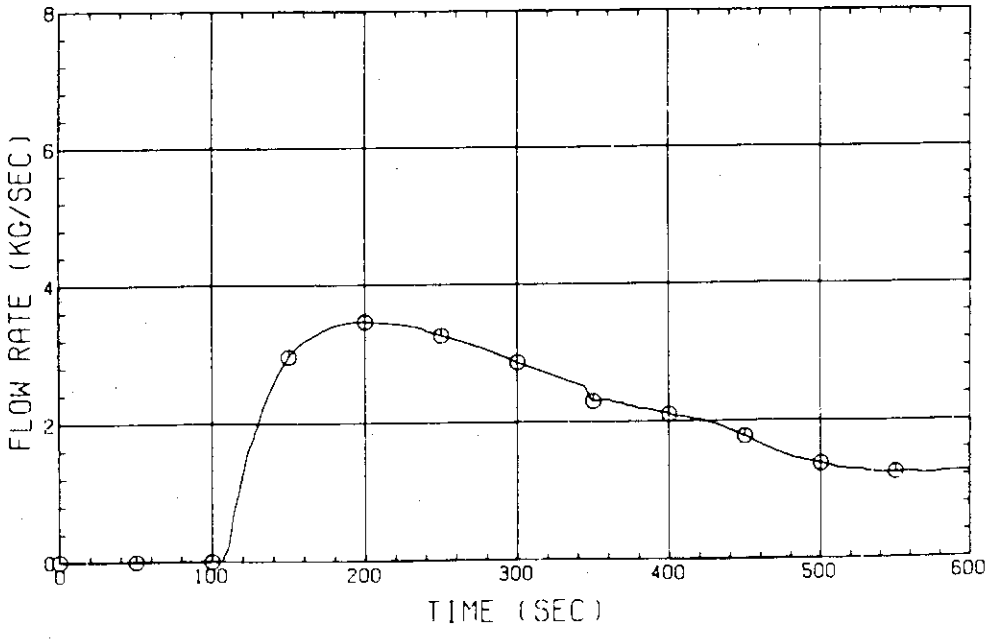

FIG. D-21 Steam Flow Rate at Discharge Line from Containment Tank-II